

CHARACTERIZATION OF THE ANTIVIRAL EFFECTOR IFI6

APPROVED BY SUPERVISORY COMMITTEE

John Schoggins, Ph.D.

Beth Levine, M.D.

Julie Pfeiffer, Ph.D.

Nan Yan, Ph.D.

DEDICATION

I would like to thank my mother for her encouragement, support and most importantly her kindness throughout my studies.

I would like to thank John for his mentorship and guidance and trusting me to embark on an ambitious project and allowing me to openly ask and answer scientific questions as I chose to.

I would like to thank the members of my lab for their assistance in experiments, encouragement, and friendship, and for being a great team of people to work with.

I would like to thank my graduate committee for their invaluable suggestions and support of the project throughout the course of my graduate studies.

I would like to thank my friends for being a source of support, advice, and entertainment when I needed it most.

CHARACTERIZATION OF THE ANTIVIRAL EFFECTOR IFI6

by

RYAN BLAKE RICHARDSON

DISSERTATION

Presented to the Faculty of the Graduate School of Biomedical Sciences

The University of Texas Southwestern Medical Center at Dallas

In Partial Fulfillment of the Requirements

For the Degree of

DOCTOR OF PHILOSOPHY

The University of Texas Southwestern Medical Center at Dallas

Dallas, Texas

December 2018

Copyright

by

Ryan Blake Richardson, 2018

All Rights Reserved

CHARACTERIZATION OF THE ANTIVIRAL EFFECTOR IFI6

Publication No. _____

Ryan Blake Richardson, Ph.D.

The University of Texas Southwestern Medical Center at Dallas, 2019

Supervising Professor: John Schoggins, Ph.D.

The innate immune response is a critical line of host defense against invading pathogens. The production of interferon (IFN) and the subsequent expression of interferon stimulated genes (ISGs) are major contributors to the innate immune response, which establish an antiviral state in the cell. Flaviviruses such as dengue virus, Zika virus, and West Nile virus rely intimately on host pathways for completing a replication cycle, and have developed strategies to overcome the inhibitory effect of the innate immune response. To identify host factors required during an IFN response to flavivirus infection, a genome-wide CRISPR screen was carried out. Two of the top hits from the screen were IFI6, a previously identified ISG long predicted to be antiviral, and BiP, a luminal chaperone in the endoplasmic

reticulum (ER). I questioned whether IFI6 was important for the antiviral response to flaviviruses and sought to investigate its role during infection. I confirmed the results from the CRISPR screen and showed that cells lacking IFI6 were insensitive to IFN, suggesting a key role in the innate immune response to flaviviruses. This was complemented by overexpression studies which showed IFI6 is potentially inhibitory to flavivirus infection. I further demonstrated that BiP is required for an intact IFN response and importantly mediates expression of IFI6, which it binds in a chaperone-dependent manner. I also showed that IFI6 is localized to the ER and is an integral membrane protein. Importantly, IFI6 acts during the flavivirus life cycle to inhibit replication and formation of replication complexes, which are formed by rearrangement of ER membranes. IFI6 specifically inhibits flaviviruses, since other viruses that replicate at the ER such as hepatitis C virus (HCV) are not affected by IFI6. I hypothesize the key to this specificity lies in the orientation of the replication complexes - HCV complexes extend outwards into the cytoplasm while flaviviruses bud inwards into the lumen. Taken together, these data support a model where IFI6 is sensitive to membrane alterations specifically induced by flaviviruses but not other viruses, which provides the innate immune response with a potent and specific ISG to block viral infection.

TABLE OF CONTENTS

DEDICATION	ii
COPYRIGHT.....	iv
CHARACTERIZATION OF THE ANTIVIRAL EFFECTOR IFI6	v
TABLE OF CONTENTS.....	vii
PRIOR PUBLICATIONS	xi
LIST OF FIGURES	xii
LIST OF FIGURES	xiv
CHAPTER ONE: REVIEW OF THE LITERATURE	1
INTERFERON- α -INDUCIBLE PROTEIN 6	1
OVERVIEW	1
EVOLUTIONARY CONSERVATION OF FAM14 PROTEINS	2
PROPERTIES OF THE IFI6 GENE AND PROTEIN	3
LOCALIZATION OF IFI6	4
ROLES IN CANCER AND APOPTOSIS	4
ROLES AS AN ISG	6
<i>FLAVIVIRIDAE</i> REPLICATION STRATEGIES	8
OVERVIEW	8
THE <i>FLAVIVIRIDAE</i> FAMILY	8
<i>FLAVIVIRIDAE</i> LIFE CYCLE.....	10
FLAVIVIRUS REPLICATION COMPLEXES	11
HEPACIVIRUS REPLICATION COMPLEXES	13

CHAPTER TWO: METHODOLOGY	15
VIRUSES AND CELLS	15
PLASMIDS AND MOLECULAR CLONING	17
LENTIVIRAL TRANSDUCTION, VIRUS INFECTIONS AND REPLICON STUDIES	19
CRISPR-CAS9 CLONING, GENE TARGETING AND VIRAL INFECTION STUDIES	20
GENOME-WIDE CRISPR SCREEN	22
NHDF EXPERIMENTS	25
ENDOGENOUS IFI6 GENE TAGGING IN U-2 OS CELLS	27
IMMUNOFLUORESCENCE AND CONFOCAL MICROSCOPY	27
dsRNA	28
SEC1 β M-EMERALD AND PTRIP-MITO GFP	28
U-2 OS HDR CELLS	28
N32-GFP LOCALIZATION	28
DENV NS4B LOCALIZATION	29
ELECTRON MICROSCOPY AND IMMUNOGOLD LABELING	29
RNA AND PROTEIN DETECTION IN CELL CULTURES	30
QUANTITATIVE RT-PCR FOR ISGS	30
RNA SEQUENCING	31
WESTERN BLOT	31
MEMBRANE FLOTATION ASSAY	32

IMMUNOPRECIPITATION ASSAY	32
SECRETION ASSAY	34
PROTEIN CLEAVAGE ASSAYS	35
CHAPTER THREE: A CRISPR SCREEN IDENTIFIES IFI6 AND BIP AS TWO GENES	
IMPORTANT FOR IFN MEDIATED HOST RESPONSE TO YFV INFECTION	36
OVERVIEW	36
A CRISPR SCREEN IDENTIFIES IFI6 AND BIP AS TWO GENES IMPORTANT	
FOR IFN MEDIATED HOST RESPONSE TO YFV INFECTION	37
IFI6 KO CELLS ARE REFRACTORY TO IFN TREATMENT	39
ECTOPIC EXPRESSION OF IFI6 BLOCKS VIRAL INFECTION OF	
FLAVIVIRUSES	42
IFI6 INHIBITS FLAVIVIRUS INFECTION IN NHDF CELLS	44
IFI6 BELONGS TO A UNIQUE FAMILY OF PROTEINS, FAM14	46
IFI6 DOES NOT ALTER THE EXPRESSION OF OTHER ANTIVIRAL GENES ...	48
BIP IS REQUIRED FOR THE IFN RESPONSE AND IFI6 ACTIVITY	
TOWARDS YFV	50
IFI6 INTERACTS WITH BIP IN A CHAPERONE DEPENDENT MANNER	52
CHAPTER FOUR: IFI6 IS AN ER-LOCALIZED PROTEIN THAT INHIBITS	
FLAVIVIRUS REPLICATION.....	57
OVERVIEW	57
IFI6 IS AN ER-LOCALIZED PROTEIN.....	57
IFI6 LOCALIZES TO MEMBRANES AND IS A RESIDENT PROTEIN OF	

THE ER.....	61
IFI6 INHIBITS FLAVIVIRUS REPLICATION.....	64
IFI6 MUST BE EXPRESSED PRIOR TO VIRAL INFECTION AND ACTS PROPHYLACTICALLY	69
IFI6 COLOCALIZES WITH NS4B BUT DOES NOT BIND NS4B	71
IFI6 DOES NOT INHIBIT OTHER RNA VIRUSES	73
MODEL FOR IFI6 ANTIVIRAL ACTIVITY	78
INCONCLUSIVE DATA	78
CHAPTER FIVE: CONCLUSIONS AND RECOMMENDATIONS.....	84
OVERVIEW	84
PREVIOUS HYPOTHESES	85
APOPTOSIS	85
METABOLOMICS AND LIPID METABOLISM	86
HCV PHENOTYPE	88
ANTIVIRAL MECHANISM	89
FUTURE DIRECTIONS	91
BIBLIOGRAPHY	94

PRIOR PUBLICATIONS

Richardson RB, Ohlson MB, Eitson JL, Kumar A, McDougal MB, Boys IN, Mar KB, De la Cruz-Rivera PC, Douglas C, Konopka G, Xing C, Schoggins JW. A CRISPR-screen identifies IFI6 as an ER-resident interferon effector that blocks flavivirus replication. *Nature Microbiology*. 2018 Nov;3(11):1214-1223. DOI: 10.1038/s41564-018-0244-1

Mar KB, Rinkenberger N, Boys IN, Eitson JL, McDougal MB, Richardson RB, Schoggins JW. LY6E mediates an evolutionarily conserved enhancement of virus infection by targeting a late entry step. *Nature Communications*. 2018. DOI: 10.1038/s41467-018-06000-y

Hanners NW, Eitson JL, Usui N, Richardson RB, Wexler EM, Konopka G, Schoggins JW. Western Zika Virus in Human Fetal Neural Progenitors Persists Long Term with Partial Cytopathic and Limited Immunogenic Effects. *Cell Reports*. 2016 Jun 14;15(11):2315-22

Schoggins JW, MacDuff DA, Imanaka N, Gainey MD, Shrestha B, Eitson JL, Mar KB, Richardson RB, Ratushny AV, Litvak V, Dabelic R, Manicassamy B, Aitchison JD, Aderem A, Elliott RM, García-Sastre A, Racaniello V, Snijder EJ, Yokoyama WM, Diamond MS, Virgin HW, Rice CM. Pan-viral specificity of IFN-induced genes reveals new roles for cGAS in innate immunity. *Nature*. 2014 Jan 30; 505(7485): 691-5.

Hunter OV, Sei E, Richardson RB, Conrad NK. Chromatin immunoprecipitation and microarray analysis suggest functional cooperation between Kaposi's Sarcoma-associated Herpesvirus ORF57 and K-bZIP. *Journal of Virology*. 2013 Apr; 87(7): 4005-16.

LIST OF FIGURES

FIGURE 1: IDENTIFICATION OF IFI6 AND BIP AS TOP HITS IN IFN-BASED CRISPR SCREEN	38
FIGURE 2: VALIDATION OF CRISPR PHENOTYPE WITH IFI6-KO CELL LINES .	40
FIGURE 3: ECTOPIC EXPRESSION OF IFI6 INHIBITS FLAVIVIRUS INFECTION .	43
FIGURE 4: IFI6 CONTRIBUTES TO THE ANTIVIRAL RESPONSE IN NHDF PRIMARY CELLS	45
FIGURE 5: IFI6 BELONGS TO THE FAM14 PROTEIN FAMILY AND IS THE ONLY ANTIVIRAL FAMILY MEMBER	47
FIGURE 6: IFI6 DOES NOT MODIFY GLOBAL ANTIVIRAL GENE EXPRESSION	49
FIGURE 7: BIP IS REQUIRED FOR IFN-MEDIATED AND IFI6-MEDIATED INHIBITION OF YFV INFECTION	51
FIGURE 8: IFI6 BINDS BIP WITH OVEREXPRESSION AND ENDOGENOUS EXPRESSION LEVELS	53
FIGURE 9: IFI6 IS DEGRADED IN A PROTEASOME DEPENDENT MANNER AND ITS EXPRESSION DEPENDS ON THE ATPASE ACTIVITY OF BIP	56
FIGURE 10: IFI6 IS ER-LOCALIZED IN MULTIPLE CELL LINES	59
FIGURE 11: IFI6 CONTAINS AN N-TERMINAL SIGNAL PEPTIDE.....	60
FIGURE 12: IFI6 IS AN INTEGRAL MEMBRANE PROTEIN AND IS NOT SECRETED	62
FIGURE 13: IFI6 INHIBITS FLAVIVIRUS REPLICATION	66
FIGURE 14: IFI6 DOES NOT AFFECT VIRAL OR HOST PROTEASE ACTIVITY ...	68

FIGURE 15: IFI6 PROPHYLACTICALLY BLOCKS VIRAL REPLICATION	70
FIGURE 16: IFI6 COLOCALIZES WITH DENV NS4B	72
FIGURE 17: IFI6 DOES NOT BIND NS4B OR NS1	74
FIGURE 18: IFI6 DOES NOT INHIBIT HCV REPLICATION	75
FIGURE 19: IFI6 DOES NOT INHIBIT REPLICATION OF OTHER RNA VIRUSES.	77
FIGURE 20: MODEL OF IFI6 SPECIFIC ANTIVIRAL ACTIVITY	79
FIGURE 21: YFV CANNOT OVERCOME IFI6 INHIBITION WITH A VIRAL MUTANT, AND VIRAL PROTEINS CANNOT SPECIFICALLY ANTAGONIZE IFI6	81

LIST OF DEFINITIONS

BiP - binding immunoglobulin protein

BFA - Brefeldin A

BFP - blue fluorescent protein

BLAST - Basic local alignment search tool

bp - basepairs

Cas9 - Caspase 9

cDNA - complementary DNA

COCV - cocavirus

CM - convoluted membrane

Co-IP - Co-immunoprecipitation

CoV - coronavirus

Ctrl - control

CRISPR - Clustered Randomly Interspersed Short Palindromic Repeats

CVB - Coxsackie virus

DENV - dengue virus

DMV - double-membrane vesicles

dsRNA double-strand RNA

EMCV - encephalomyocarditis virus

ER - endoplasmic reticulum

ESCRT - endosomal sorting complexes required for transport

FACS - fluorescence activated cell sorting (exchangeable with flow cytometry)

FAM14 - Protein superfamily 14

GFP - green fluorescent protein

Gluc - *Gaussia* luciferase

HCV - hepatitis C virus

HIV - human immunodeficiency virus

hNPCs human neuroprogenitor cells

hORF - human open reading frame

IF - immunofluorescence

IFI27 - Interferon alpha inducible protein 27 (other names include ISG12A and FAM14D)

IFI27L1 - Interferon alpha inducible protein 27 like 1 (other names include ISG12C and
FAM14B)

IFI27L2 - Interferon alpha-inducible protein 27 lke 2 (other names include ISG12B and
FAM14A)

IFI27L2A - Interferon alpha-inducible protein 27 like 2A

IFI27L2B - Interferon alpha-inducible protein 27 like 2B

IFI6 - Interferon alpha-inducible protein 6 (other names include IFI6-16, FAM14C and
G1P3)

IFN - Interferon

IFN- α - Interferon alpha

ISG - Interferon-stimulated gene

IRES - internal ribosome entry site

ISRE - Interferon-sensitive response element

ISG12 - interferon stimulated gene 12

JAK - Janus kinase

kb - kilobases

kDa - kiloDalton

KO - knockout

lncRNA - long non-coding RNA

MAMs - mitochondria-associated membranes

MeV - measles virus

MFI - mean fluorescence intensity

MMV - multi-membrane vesicles

MOI - multiplicity of infection

NHDF - normal human dermal fibroblasts

NS - non-structural

NT - non-targeting

OST - oligosaccharyl transferase

PCR - polymerase chain reaction

PFU - plaque forming units

PLA -proximity ligation assay

qRT-PCR - quantitative reverse transcriptase polymerase chain reaction

RC - replication complex

RFP - red fluorescent protein

RLU - relative luciferase units

RLuc - *Renilla* luciferase

RNA - ribonucleic acid

RNA-seq - RNA sequencing

RT-PCR - reverse transcriptase polymerase chain reaction

SFV - Semliki Forest virus

SINV - Sindbis virus

SMV - single membrane vesicles

ssRNA - single-strand RNA

STAT - Signal Transducer and Activator of Transcription

TEM - transmission electron microscopy

UTSW - University of Texas Southwestern Medical Center

VSV - vesicular stomatitis virus

WNV - West Nile virus

WT -wild type

YFV - yellow fever virus

ZIKV - Zika virus

CHAPTER ONE

Review of the Literature

INTERFERON- α -INDUCIBLE PROTEIN 6

Overview

Interferon- α -inducible protein 6 (IFI6, IFI6-16, FAM14C, G1P3), was one of the earliest identified interferon-stimulated genes (ISGs) when it was shown to be highly induced in a cDNA screen for genes induced with interferon-alpha (IFN- α) (Friedman et al., 1984). Since its identification as an ISG, IFI6 has been used as a tool to characterize important details of Type I ISGs, such as the interferon stimulated response element (ISRE) present in many Type I ISGs (Friedman et al., 1984; Porter et al., 1988). Recently IFI6 has been grouped into a protein family with family members that contain a core domain that has been evolutionarily conserved across a diverse range of species (Parker and Porter, 2004). Research in the cancer field has suggested IFI6 is a mitochondria-localized protein with anti-apoptotic properties, but mechanistic details have not been uncovered (Cheriyath et al., 2007; Cheriyath et al., 2018; Cheriyath et al., 2012; Tahara et al., 2005). Additionally, because of its IFN-inducibility, IFI6 has long been speculated to have antiviral properties. Research investigating this predicted antiviral activity reported IFI6 to have modest antiviral activity against several medically relevant viruses such as hepatitis C virus (Fusco et al., 2013; Liu et al., 2018; Metz et al., 2012; Meyer et al., 2015; Qi et al., 2017; Zhao et al., 2012), with stronger antiviral effects shown for flaviviruses like yellow fever virus and dengue virus (Li et al., 2013; Schoggins et al., 2012; Schoggins et al., 2011).

Evolutionary conservation of FAM14 proteins

IFI6 belongs to a recently identified protein family, FAM14 (Parker and Porter, 2004). In humans there are 4 family members: IFI27 (ISG12A, FAM14D), IFI27L1 (ISG12C, FAM14B), IFI27L2 (ISG12B, FAM14A) and IFI6. The sequences of these human proteins were used to identify similar protein sequences in a BLAST search. The alignment of these sequences led to the discovery of a consensus sequence present in all FAM14 members called the ISG12 motif (Parker and Porter, 2004). This motif is approximately 80 amino acids in length and all members of the FAM14 family contain one of these motifs. One exception is the IFI27L2B protein in mice, which contains two motifs. The ISG12 motif is usually found in the middle of the protein sequence. Despite good conservation of this motif, sequences on the N and C terminus of the FAM14 proteins are divergent. Generally, members of the FAM14 family are predicted to be hydrophobic and associated with membranes based on amino acid analysis (Parker and Porter, 2004). Members of this protein family have been identified in over 25 animal species, with proteins containing the ISG12 motif in many high-order mammals such as primates and ungulates (hooved livestock); notably, proteins containing this motif have been found in birds, reptiles, fish and the amoeba *Dictostelium discoideum* (Parker and Porter, 2004).

Since *D. discoideum* contains a single protein with an ISG12 motif but mammals contain several proteins with this motif, it is speculated that this gene has undergone several duplication events through evolution (Parker and Porter, 2004). Importantly, while many homologs of IFI27 and IFI27-like genes can be identified in several divergent species, IFI6 is only found in high-order mammals and ungulates, suggesting that it emerged from a separate

gene duplication event that occurred after the initial gene duplication events that gave rise to the IFI27-like genes. IFI6 and IFI27 are known to be interferon-stimulated genes (ISGs) in many species; however early animals like *D. discoideum* lack an interferon system, suggesting that FAM14 proteins may have evolved for a separate purpose, such as sensing environmental stress, and were later incorporated into the IFN system of more evolved organisms (Parker and Porter, 2004).

Properties of the IFI6 gene and protein

In humans, IFI6 is located on chromosome 1p35 and spans a 6 kb region (Itzhaki et al., 1992). IFI6 is made up of 5 exons, which produce a RNA transcript of approximately 836 bp. There are several interesting features of the *IFI6* gene locus. One feature is a minisatellite repeat of 12 nucleotides repeated 26 times (Turri et al., 1995). This sequence occurs in the intragenic region between exons 2 and 3. The minisatellite sequence is similar to a mammalian splice site sequence, and can lead to alternative splicing. When alternative splicing occurs exon 2 is lengthened by 12 or 24 nucleotides, resulting in 4 or 8 additional amino acids in the mature polypeptide. The role of this minisatellite is not clear, but its repetitive nature is suggestive of a regulatory role. In addition to a minisatellite, IFI6 also contains a CpG island and generally has a high GC content. These and other regulatory elements including a repeat of 5 Alu elements have yet to be investigated (Turri et al., 1995).

IFI6 is a relatively small protein, with an observed molecular weight of 12-13 kDa (Cheriyath et al., 2011). Sequence analysis predicts IFI6 has a signal peptide in approximately the first 20-25 amino acids, followed by a relatively long stretch of hydrophobic residues (Kelly et al., 1986). Based on these properties IFI6 has been predicted

to associate with membranes. Surface probability analysis by Emini's method predicts the probability that a given protein region lies on the surface of a protein (Emini et al., 1985). Using this analysis, an amphipathic helix is predicted near the C-terminus of IFI6 followed by a hydrophilic sequence, suggesting some regions of IFI6 may protrude from membranes to allow for interaction with other proteins (Cheriyath et al., 2018; Cheriyath et al., 2011).

Localization of IFI6

Previous studies have reported IFI6 to be a mitochondria-localized protein (Cheriyath et al., 2007; Cheriyath et al., 2018; Tahara et al., 2005). Based on its amino acid sequence and the putative signal peptide, IFI6 is thought to be localized to mitochondria with a signal peptide where it is thought to associate with mitochondrial membranes. However, it is worth noting that these experiments were not well controlled for contamination of other membranes and were limited in their characterization of IFI6 localization. Therefore, it cannot be ruled out that IFI6 localizes on a contaminating membrane that co-fractionates with mitochondria in cell fractionation experiments.

Roles in cancer and apoptosis

In addition to characterization as an ISG, IFI6 has been reported to play a role in apoptosis signaling pathways. Initial experiments in TMK-1 cells, a gastric cancer cell line, demonstrated IFI6 was able to repress apoptosis induced by agents such as 5-fluoruracil or cyclohexamide, suggesting IFI6 has antiapoptotic properties (Tahara et al., 2005). In the same study IFI6 was also shown to impede cytochrome c release and inhibit mitochondria

membrane depolarization, two processes strongly associated with induction of apoptosis. Subsequent experiments demonstrated that treatment with Type I IFN had initial antiapoptotic effects at early time points after treatment, but at later time points elicited proapoptotic effects (Cheriyath et al., 2007). This observation led to the assumption that specific ISGs must regulate this transition from an anti- to pro-apoptotic state. Based on results from high throughput gene expression analysis and experimental validation, IFI6 was identified as a mediator of this IFN-dependent effect. Similar to earlier studies IFI6 was shown to localize to mitochondria and establish an antiapoptotic state upon overexpression. This observation was made in both malignant and nonmalignant cells, suggesting IFI6 may play an important role in the progression of cancers if malignant cells could establish an antiapoptotic or pro-survival state. Importantly, several cancer therapies induced the expression of IFI6 suggesting IFI6 may play a role in therapeutic resistance of certain cancers.

Recently, the antiapoptotic role of IFI6 has been more extensively characterized in breast cancer cells. IFI6 has been shown to be upregulated by estrogen in breast cancer cells (Cheriyath et al., 2012). Additionally, IFI6 has also been shown to prevent cell death due to cell detachment, a type of apoptosis known as anoikis (Cheriyath et al., 2012). Mechanistic studies suggested IFI6 increases the production of mitochondrial reactive oxygen species which enhances cell migration, a prerequisite for metastasis (Cheriyath et al., 2018).

Roles as an ISG

IFI6 was first identified in a cDNA screen designed to identify genes induced by IFN- α in neuroblastoma cells (Friedman et al., 1984). IFI6 was one of the most highly induced genes, accounting for approximately 0.1% of total cellular RNA. Numerous other reports have identified IFI6 as interferon-inducible across a variety of cell lines and tissues (Cheriyath et al., 2007; Kelly et al., 1986; Tahara et al., 2005). Because of its high inducibility, IFI6 was used in several studies as a tool to characterize the ISRE element found in the promoter region of many Type I ISGs, as well as in the identification of STATs and JAKs involved in IFN signaling (Friedman et al., 1984). Therefore, because of the long-standing knowledge of the high level of IFN-inducibility of IFI6, it has been speculated to play a role in the IFN antiviral response.

Initial experiments with viral infections demonstrated viruses such as VSV, HCV and HIV could act as stimuli to induce the expression of IFI6 (Martensen and Justesen, 2004). Other viruses such as EMCV, SFV, and COV were assayed for their plaque production in IFI6 knockout cells and no difference in the amount of plaques were observed (Yanez and Porter, 2002).

The most extensive amount of literature regarding IFI6 and its antiviral activity focuses on the antiviral activity of IFI6 towards HCV. Several reports have identified IFI6 as an ISG that inhibits HCV replication (Fusco et al., 2013; Itsui et al., 2006; Liu et al., 2018; Manns and Rambusch, 1999; Marukian et al., 2008; Metz et al., 2012; Meyer et al., 2015; Qi et al., 2017; Zhao et al., 2012). One proposed mechanism suggests that IFI6 inhibits the interaction of HCV receptors CD81 and CLDN1, thereby inhibiting downstream activation of

EGFR (Meyer et al., 2015). Another paper also suggests that IFI6 inhibits HCV during the replication phase by interacting with the HCV p7 protein thought to be an important factor for immune evasion during infection. Consistent with previous reports of the ability of IFI6 to stabilize mitochondrial membrane potential, p7 was found to antagonize depolarization of mitochondrial membranes, suggesting these two proteins may play opposing roles during infection (Qi et al., 2017). Recently, a RNAseq screen identified a lncRNA, named lncRNA-IFI6, in the IFI6 gene shown to be important for regulation of IFI6 expression during IFN treatment (Liu et al., 2018). Importantly, lncRNA-IFI6 is a negative regulator of IFI6 expression and upon knockdown of this lncRNA using CRISPR-Cas9 technology IFI6 expression was increased and suppressed HCV infection more effectively.

Other reports of the antiviral activity of IFI6 suggest the most potent effects are not seen with HCV, but rather with flaviviruses. A high throughput screen designed to identify novel ISGs with antiviral activity demonstrated IFI6 is a potentially antiviral ISG against flaviviruses like yellow fever virus (YFV) and dengue virus (DENV) (Schoggins et al., 2011). Further work with a DENV reporter virus demonstrated that IFI6 was inhibitory to DENV during the replication phase of the life cycle (Schoggins et al., 2012). Another report also demonstrated that West Nile virus (WNV), a flavivirus like DENV and YFV, replicated more efficiently in the absence of IFI6 (Li et al., 2013). Importantly, the magnitude of the antiviral effects seen with flaviviruses is significantly greater when compared to the antiviral effects of other viruses such as HCV.

Together, this literature suggests IFI6 is a highly inducible ISG that belongs to a unique family of proteins, FAM14. All family members contain an ISG12 motif but have

differing N and C termini. The function of IFI6 is not clear, but it is highly speculated to have antiviral activity, and has been reported to have antiviral activity against flaviviruses. Other reports suggest IFI6 is antiapoptotic and may promote cell survival, which may promote tumor growth in the context of cancer cells.

***FLAVIVIRIDAE* REPLICATION STRATEGIES**

Overview

Flaviviridae is a diverse family of viruses that causes a range of diseases in a wide range of hosts. Many viruses in the family are medically relevant, and viruses in this family continue to emerge as new pathogens and cause outbreaks worldwide (Wikan and Smith, 2016). Despite continuing research, many flaviviruses do not have available vaccines or antivirals (Hadinegoro et al., 2015). While these viruses cause a range of diseases, the viruses generally utilize similar replication strategies (Neufeldt et al., 2018; Paul and Bartenschlager, 2015). All *Flaviviridae* members are (+)-ssRNA viruses that replicate on ER membranes. They generate so-called “replication complexes” as a hallmark of their replication. These structures feature single-membrane vesicle-like compartments that bud inwards into the lumen of the ER, while HCV forms double-membrane replication complexes that extend outwards into the cytoplasm.

The *Flaviviridae* family

The *Flaviviridae* family represents many diverse viruses with a wide range of host tropism and disease (Stanaway et al., 2016). Members of *Flaviviridae* are positive-sense

single-stranded RNA (+ssRNA) viruses. Many of these viruses are arboviruses, viruses transmitted between reservoirs and host through an arthropod vector such as mosquitoes or ticks. There are four genera in the family, Flavivirus, Hepacivirus, Pestivirus and Pegivirus (Neufeldt et al., 2018). Several viruses in the Flavivirus and Hepacivirus genera are causative agents of medically relevant diseases including dengue virus (DENV), West Nile virus (WNV), Zika virus (ZIKV), and hepatitis C virus (HCV). Several of these viruses cause disease with global impact such as DENV, which infects approximately 100 million people annually (Stanaway et al., 2016). Symptoms caused during DENV infection can range from asymptomatic or mild flu-like symptoms to severe hemorrhagic fever or dengue shock syndrome. Despite ongoing research efforts, many viruses in the Flavivirus genus have no direct acting antivirals or vaccines available. Recently, a vaccine for DENV has been licensed but its efficacy is uncertain (Hadinegoro et al., 2015). However, for HCV there has been significant progress made in the development of therapy in patients with chronic infection (Manns et al., 2017).

Viruses in the *Flaviviridae* family have significant impacts on health worldwide with outbreaks occurring frequently (Wikan and Smith, 2016). ZIKV, a virus that until recently was poorly characterized and not thought to cause severe disease in adult humans, is now known to be a cause of Guillain-Barre syndrome and microcephaly in infants in a recent South American outbreak (Wikan and Smith, 2016). This change in pathogenicity is thought to be caused by an emerging lineage of ZIKV that has traversed the globe and caused only small outbreaks in isolated locations, until its emergence in South America.

***Flaviviridae* Life Cycle**

Although the members of *Flaviviridae* are diverse in tropism and disease severity, these viruses all utilize similar replication strategies with differences that will be described later in this chapter. Viruses are obligate intracellular pathogens and therefore depend on host machinery and pathways to replicate their viral genome and produce new viral particles. Most (+)-RNA viruses are dependent on interactions with host membranes to complete a viral life cycle. Additionally, the genomic organization of flaviviruses and hepaciviruses are similar. Both genera have several genes encoding structural proteins near the 5' end of their genome followed by several genes encoding non-structural proteins involved in replication and assembly near the 3' end of the genome (Neufeldt et al., 2018).

Viral attachment and binding vary between the two genera and will be discussed below. Once internalized, flaviviruses and hepaciviruses utilize the membranes of the endocytic pathway similarly, requiring acidification of endosomes to initiate viral fusion and release of their respective genomes into the cytosol for translation. Genomes of both genera encode a polyprotein that, when translated, generates a large protein which spans the ER membrane numerous times and requires protease activity of host and viral proteins to produce mature viral proteins. Once cleaved, nonstructural viral proteins dramatically rearrange membranes of the ER to generate organelle-like structures called replication complexes. While both genera use these membranes the molecular details vary greatly and will be discussed below. However, the function of these organelles is similar - to establish an environment for viral genomic replication where nucleic acids will not be recognized by innate immune sensors. It is not clear how viral assembly is initiated, but after a significant

increase in viral genomes and proteins occurs, assembly occurs in association with ER membranes. Once viral particles have been assembled, they transit through the secretory pathway to the cell surface, where maturation of structural proteins occurs, and are eventually secreted from the cell for the life cycle to begin again (Neufeldt et al., 2018).

Flavivirus replication complexes

While the life cycle of flaviviruses and hepaciviruses are generally similar, there are several steps that are different between the two genera. HCV has clearly defined receptors required for viral entry, while the entry of flaviviruses is less clearly understood. Receptors used may be cell-type dependent, and a variety of receptors (TIM, TAM, DC-SIGN, the mannose receptor, heparin sulfate glycoproteins) have been reported as involved in flavivirus entry (Neufeldt et al., 2018). Another difference is found in the translation mechanism of the viruses. While flaviviruses utilize cap-dependent translation, hepaciviruses use an internal ribosome entry site (IRES) for translation.

The most striking difference between flaviviruses and hepaciviruses is in the architecture of their replication complex (RC). Flaviviruses generate invaginated, spherule replication complexes that bud inwards into the lumen of the ER (Cortese et al., 2017; Junjhon et al., 2014; Paul and Bartenschlager, 2015; Welsch et al., 2009). These RCs utilize the membranes of rough ER. The size of these RCs is approximately 90nm, but can vary depending on cell type (Cortese et al., 2017). The small size of these complexes is thought to help coordinate the replication step of the viral life cycle by spatially partitioning the replication machinery into distinct compartments. Both dsRNA and nonstructural proteins

can be detected in these complexes. The RCs have a small pore that opens to the cytoplasm and is approximately 10 nm in diameter. This small opening is presumably used to transfer small metabolites and nucleic acids in and out of the complex, while protecting the viral replication machinery from recognition by innate immune sensors. In addition to generating RCs, some flaviviruses like DENV and ZIKV generate structures called convoluted membranes (CMs) (Cortese et al., 2017; Welsch et al., 2009). These membranes are thought to be made from smooth ER and appear as dense, web-like structures by electron microscopy. The role of CMs during flavivirus replication is not clear. There is no apparent accumulation of dsRNA inside the CMs, but non-structural viral proteins are found in these membranes (Miller et al., 2006). One hypothesis suggests these CMs sequester host lipids and metabolites required for efficient replication and act as a supply of these resources during replication. Additionally, CMs can be found near mitochondria and ER contact sites, or MAMs, suggesting they may sequester factors important for innate immune signalling (Chatel-Chaix et al., 2016). Interestingly, DENV does not form CMs in mosquito cells, and ZIKV does not form CMs in human neural progenitor cells, suggesting these membranes may play a cell-specific role, since both viruses can generate CMs in hepatocytes (Cortese et al., 2017; Junjhon et al., 2014).

While the architecture of the RCs is well defined, less is known about the mechanism of how the complexes are assembled. Several reports suggest a role for NS4A and NS4B, two small hydrophobic proteins with several transmembrane domains (Miller et al., 2007; Miller et al., 2006). The topology of these proteins suggests they may be able to bend the membrane and induce the negative curvature observed in the RCs. Additionally these

proteins have been shown to form hetero-oligomers and homo-oligomers, which may increase their membrane remodeling activity (Zou et al., 2014). Importantly, when expressed alone these proteins are not sufficient to create the architecture seen with a complete viral genome (Miller et al., 2006). This implies that other viral or host components are required. Some reports suggest a role for viral NS1, which can bind NS4A and NS4B and has been shown to bind lipids, or NS2A, which also has transmembrane domains and has been reported to alter membrane permeability (Scaturro et al., 2015). Other host factors such as the ESCRT machinery or OST complex may also play a role in the formation of the replication complex (Marceau et al., 2016; Tabata et al., 2016).

Hepacivirus replication complexes

The architecture of HCV replication complexes is well described and distinct from that of flaviviruses. Hepaciviruses like HCV form RCs that are single, double or multimembrane vesicles (SMV, DMV, MMV) that extend outwards from the ER membrane into the cytoplasm (Romero-Brey et al., 2012). The complexes are slightly larger than those of flaviviruses with an average size of 150nm. These vesicles form clusters referred to as a membranous web (Egger et al., 2002). Unlike flaviviruses a minimal set of nonstructural proteins, NS3-NS5B, is known to generate the formation of these complexes independent of viral replication (Romero-Brey et al., 2012). Additionally, DMVs are thought to be the site of HCV RNA replication, while roles for SMV and MMV are less clear. It is thought that MMV may be formed later in the life cycle as a stress response (Esser-Nobis et al., 2013).

The assembly of the HCV replication complexes is known to require the activity of NS4B and NS5A (Paul and Bartenschlager, 2015). Similar to the NS4A and NS4B proteins of flaviviruses, the HCV NS4B protein contains transmembrane and amphipathic helices and can oligomerize, an activity thought to be important for inducing membrane curvature. The NS5A protein is capable of producing DMVs independently of other viral proteins, and can also recruit several host factors required for formation of the RCs.

CHAPTER TWO METHODOLOGY

Viruses and cells

Huh7.5, U-2 OS, A549, 293T (from C. Rice, The Rockefeller University), 293T (from N. Conrad, UT Southwestern Medical Center) and COS-7 (from N. Alto, UT Southwestern Medical Center) cells and all derivatives were maintained in ‘complete’ DMEM (Gibco) supplemented with 10% FBS (Gibco) and 1× non-essential amino acids (NEAA; Gibco). Human STAT1^{-/-} fibroblasts (from J.-L. Casanova, The Rockefeller University) were maintained in RPMI supplemented with 10% FBS (Gibco) and 1× NEAA (Gibco). BHK21-J (from C. Rice) were grown in MEM (Gibco) supplemented with 10% FBS and 1× NEAA. Stable cells expressing antibiotic resistance genes were grown in complete media supplemented with puromycin (Sigma) at 4 µg ml⁻¹ or blasticidin (Gibco) at 15 µg ml⁻¹. Normal human dermal fibroblasts (NHDFs) were purchased from Lonza and cultured in fibroblast basal media (American Type Culture Collection (ATCC) or Lonza) as recommended by the supplier. Human fetal neural progenitors were cultured as previously described (Hanners et al., 2016). Cell lines were routinely tested for mycoplasma using a PCR-based assay (Vendor GeM Mycoplasma Detection Kit, MP0025-1KT, Sigma). When applicable, cell lines were authenticated with short tandem repeat (STR) analysis using the ATCC Cell Line Authentication service.

The generation and propagation of the following viruses or replicons have been previously described (Schoggins et al., 2014; Schoggins et al., 2011): YFV strain 17D

expressing Venus GFP (YFV-Venus), HCV genotype 2a intragenotypic chimera expressing Ypet GFP (HCV-Ypet), CVB-GFP, Sindbis virus AR86 expressing GFP (SINV-GFP), WNV-GFP, measles virus Edmonston lineage expressing GFP, HCV replicon expressing Gaussia luciferase (Bi-Gluc-JFH-SG) and ZIKV strain PRVABC59 (Hanners et al., 2016). Infectious HCV-Gluc was generated from the infectious clone Jc1FLAG(p7-nsGluc2A) as previously described (Marukian et al., 2008). An infectious clone of non-reporter WNV (strain TX02) was kindly provided by I. Frolov (University of Alabama Birmingham) and the virus was propagated as described above for WNV-GFP. DENV-Fluc with a L52F mutation in the gene encoding NS4B was derived from pDENV2-IC30P-A and propagated as previously described (Schoggins et al., 2012). A ZIKV MR766-GFP infectious clone (kindly provided by M. Evans, Icahn School of Medicine at Mount Sinai) was used to generate the virus as described (Schwarz et al., 2016). The infectious clone pACNR-FLYF-17Dx (kindly provided by C. Rice) was used to generate non-reporter YFV-17D. Briefly, the plasmid was linearized with XhoI and the purified DNA was used as a template for transcription with the mMessage mMachine SP6 Transcription kit (Thermo Fisher). RNA was purified with the RNeasy Mini Kit (Qiagen) and electroporated into BHK21-J cells. Virus-containing supernatants were collected, clarified by centrifugation and stored at -80°C . Human coronavirus OC43 (ATCC strain VR-1558) was propagated in HCT-8 cells as specified by the ATCC. Viral titers were determined by antibody staining (MAB9012, Millipore) and flow cytometry (Grigorov et al., 2011).

Plasmids and molecular cloning

To generate a C-terminal 3×FLAG-tagged IFI6 variant, pENTR221.IFI6 from the ISG library previously described (Schoggins et al., 2011) was digested with PstI and XhoI (NEB). Full-length IFI6 containing a glycine-serine linker was PCR amplified from pENTR221.IFI6. A 3×FLAG epitope was PCR amplified from pcDNA4/TO/GFP-3×FLAG (kindly provided by I. D'Orso). The three fragments were combined with the Gibson Assembly Cloning Kit (New England Biolabs) according to the manufacturer's instructions, to yield the final pENTR221.IFI6-3×FLAG construct. A similar HA-tagged construct was generated by replacing the 3×FLAG epitope with annealed oligos encoding the HA epitope, to generate pENTR221.IFI6-HA. To generate a GFP expressing the putative IFI6 signal peptide at its N terminus, full-length enhanced GFP (eGFP) was PCR amplified with primers containing SacI or XhoI sites and directionally cloned into a SacI/XhoI-digested pENTR221.IFI6 vector. The resulting plasmid was named pENTR221.IFI6(N32)-eGFP.

To generate CCL2 with a 1×FLAG tag on the C terminus, pENTR221.CCL2 from the ISG library previously described (Schoggins et al., 2011) was modified as follows. A DNA fragment containing a 1×FLAG coding sequence flanked by CCL2 homology arms was synthesized and inserted into pENTR221.CCL2 with the Gibson Assembly Cloning Kit (New England Biolabs) according to the manufacturer's instructions.

To generate DENV-2K-NS4B-HA, the 2K-NS4B region from pDENV2-IC30P-A was PCR amplified and cloned into a lentiviral expression plasmid, pTRIP.XKB-GFP (gift from C. Rice), replacing the GFP sequence. A similar construct expressing DENV C-prM was generated by PCR.

The Gateway-compatible lentiviral SCRPSY-DEST plasmid co-expressing TagRFP and a puromycin resistance cassette has been previously described (Schoggins et al., 2012). A derivative of this plasmid in which TagRFP was replaced with a nuclear-localized TagBFP (Evrogen) was generated and named SCRPSY-DEST-nlsBFP. A second derivative of SCRPSY-DEST, named SCRBBL-DEST, was generated by removing the TagRFP-2A-PuroR cassette and subcloning a PCR-amplified blasticidin resistance gene in its place. The previously described pTRIP.CMV.IVSB.ires.TagRFP-DEST vector (Schoggins et al., 2011) was modified to remove the IRES-TagRFP cassette, generating a non-reporter Gateway-compatible lentiviral vector named pTRIP.CMV.IVSB-DEST. Lentiviral expression constructs were generated by combining ENTR and DEST vectors in the recombination reaction using LR Clonase II (Invitrogen) according to the manufacturer's instructions. All pENTR constructs were propagated in DH5- α cells, whereas lentiviral vectors were grown in DH5- α or MDS42RecA cells (Scarab Genomics). To complement cells that had genomic BiP edited by CRISPR, an overexpression construct of BiP containing six silent mutations in the region targeted by BiP CRISPR guide 3 was generated. A synthetic gene fragment of BiP containing silent mutations was cloned into pENTR221-BiP (kindly provided by N. Alto) after digestion with AflII and PmlI restriction enzymes, using Gibson Assembly Cloning Kit (New England Biolabs) according to the manufacturer's instructions. Constructs expressing catalytic mutant versions of guide 3 CRISPR-resistant BiP (T37G, E201G and T229G) were generated using site-directed mutagenesis and verified by sequencing.

Lentiviral transduction, virus infections and replicon studies

Lentiviral production and transductions were performed as previously described (Schoggins et al., 2011). Viral infections for GFP-expressing reporter viruses and for ZIKV were carried out as previously described (Hanners et al., 2016; Schoggins et al., 2014; Schoggins et al., 2011). For the non-reporter YFV-17D growth curve, cells were infected with a multiplicity of infection (MOI) of 2 in DMEM supplemented with 1% FBS for 1 h. Media were aspirated and cells were washed with serum-free DMEM four times and replaced with 500 μ l complete DMEM. Virus yields in supernatants were quantified by plaque assay titration on BHK-21J cells. Studies using the HCV subgenomic replicon (Bi-Gluc-JFH[SG]) were carried out as previously described (Schoggins et al., 2011). The YFV-17D subgenomic replicon YFRP-Rluc (kindly provided by R. Kuhn) was propagated and used to generate viral RNA as previously described (Jones et al., 2005). Assays to detect YFV-Rluc replicon activity were conducted similar to HCV replicon studies, with the detection of intracellular Rluc using the Renilla Luciferase Assay System (Promega). For IFN-mediated inhibition studies, cells were treated with the indicated dose of human IFN- α 2a (11100-1, PBL Assay Science) for 4 h or 16 h prior to infection. Infections proceeded for approximately one round of viral replication and cells were collected for analysis by flow cytometry. For studies in human fetal neural progenitors, approximately 100,000 cells per well were plated onto 24-well plates. Two or three days later, cells were transduced with SCRPSY-Empty or SCRPSY-IFI6 lentivirus for 2 days in 1 ml human fetal neural progenitor proliferation media. Two days post-transduction, cells were infected with approximately 0.5 MOI ZIKV (PRVABC59) for 1–2 h. Cells were washed three times with media and supernatants were

collected at 24, 48 and 72 h. Supernatants were titered by limiting dilution on STAT1^{-/-} fibroblasts, using 4G2 (D1-4G2-4-15, ATCC) staining as the readout (Grigorov et al., 2011).

CRISPR–Cas9 cloning, gene targeting and viral infection studies

Oligos encoding sgRNAs for generating knockout cells using CRISPR–Cas9 were cloned into the lentiCRISPRv2 plasmid (a gift from F. Zhang, Addgene plasmid 52961) as previously described (Sanjana et al., 2014; Shalem et al., 2014). LentiCRISPRv2 clones containing guide sequences were sequenced, purified and used for lentiviral production as described above. For generating heterogeneous knockout cell populations, Huh7.5, A549 or U-2 OS cells were infected with the lentiCRISPRv2-derived lentivirus for 48 h, then reseeded into complete DMEM containing 1–4 $\mu\text{g ml}^{-1}$ puromycin for 3 days to select for transduced cells.

Single-cell clones of Huh7.5 cells targeted for IFI6 knockout via CRISPR could not be propagated. To overcome this limitation, CRISPR-targeted Huh7.5 cells (using sgRNA ‘BR2’) were diluted with parental Huh7.5 cells at a ratio of 1/2,000. Mixed cells were plated at 100 cells per well in 96-well plates. Once confluent, cells were passaged to a 48-well format in the presence of 4 $\mu\text{g ml}^{-1}$ puromycin to kill non-targeted cells. Surviving populations derived in this manner were propagated and expanded for 6 weeks before cryopreserving stock cultures. Using this strategy, an IFI6-targeted knockout cell line was generated and named ‘IFI6-KO1’. In another strategy, two distinct guides targeting IFI6 (‘g1g2’) were co-expressed, one by lentiCRISPRv2 (blasticidin selectable) and the other by

lentiCRISPRv2 (puromycin selectable). Double drug selection led to bulk populations of cells, with each cell receiving two independent CRISPR guides targeting IFI6. These were named 'IFI6-KO2' cells.

The following methods were used for cells targeted via the IFI6-KO1 strategy. The day before IFN treatment and infection, 70,000–150,000 cells were plated onto 24-well plates. Cells were pre-treated with serial dilutions of IFN- α 4 h before infection. The IFN-containing media were removed and cells were incubated with 0.5–1.0 MOI virus (CVB-GFP, SINV-GFP, YFV-Venus or WNV-GFP) for 1–2 h before being brought to volume with complete DMEM. After approximately one viral life cycle, cells were harvested and analyzed by flow cytometry.

The following methods were used for cells targeted via the IFI6-KO2 strategy. For YFV-Venus infections: 100,000 cells were plated in 24-well plates. Cells were treated with 1,000 U ml⁻¹ IFN- α overnight at time of plating. The next day, cells were infected with 7 MOI of YFV-Venus for 2 h at 37 °C. Cells were harvested 24 h later for flow cytometry analysis. For HCV infection: 80,000 cells were plated in 24-well plates. Cells were treated with 100 U ml⁻¹ IFN- α overnight at time of plating. The next day, cells were infected with 1 MOI of HCV (BiYPetJC1Flag2) for 1 h at 37 °C. Cells were harvested for flow cytometry analysis 48 h later. For WNV infections: 100,000 cells were plated in 24-well plates. Cells were treated with 1,000 U ml⁻¹ IFN- α overnight at time of plating. The next day, cells were infected with 0.01 MOI of WNV for 2 h at 37 °C. Cells were washed four times with DMEM/3% FBS media. Supernatant was collected at 24, 48 and 72 h and titered by plaque assay on BHK cells.

Genome-wide CRISPR screen

The human “Brunello” CRISPR knockout pooled library was purchased (#73179, addgene.org) and amplified according to instructions. The amplified pooled plasmid library was used to make infectious lentivirus from 293T cells. The day before transfection, 293T cells were seeded into twenty polylysine-coated 15 cm plates at a density of 6×10^6 cells per plate. The day of transfection, the culture media was exchanged for 15 mL DMEM supplemented with 3% FBS, 1X NEAA, and Pen-Strep, and pooled library plasmid was then co-transfected with lentiviral packaging plasmids expressing Gag-Pol and VSV-g at a ratio of 5:4:1 using X-tremeGENE 9 reagent (Roche) in transfection reactions containing 30 total μg of DNA per plate. Six h post-transfection, transfection complex-containing media was removed and replaced with 23 mL DMEM supplemented with 3% FBS, 1X NEAA, and Pen-Strep. Culture supernatant containing lentiviral particles was collected at 48 and 72 h post-transfection, pooled, and HEPES and polybrene was added to a final concentration of 20 mM and 4 $\mu\text{g}/\text{mL}$, respectively. To eliminate plasmid DNA carryover into NextGen sequencing reactions for subsequent screens (Sack et al., 2016), pooled library lentiviral supernatant was treated with Benzonase (Sigma) by adding 20X Benzonase buffer (1 M Tris-HCl pH 8.0, 20 mM MgCl_2 , 2 mg/mL BSA) to a final concentration of 1X, and 50 U/mL Benzonase was added and the supernatant was incubated for 30 min at 37°C. Treated lentiviral supernatant was filtered through a 0.45 micron filter and aliquots were stored at -80°C. Lentiviral transduction efficiency was determined by transducing Huh7.5 cells with volumes of lentiviral supernatant ranging from 500 μl to 10 μl in 6w plates for 48 h, and the ratio

(X100%) of puromycin-resistant to puromycin-sensitive cells following 3 days of incubation after splitting equal numbers of transduced cells into media with and without 4 $\mu\text{g}/\text{ml}$ puromycin was determined using CellTiter-Glo reagent (Promega). The volume of lentivirus that produced 30% transduction efficiency was used for all subsequent transductions in order to minimize the likelihood that any single cell would be infected with more than one lentivirus at a time during library screening (Fusco et al., 2013). To perform the IFN- α CRISPR screen, Huh7.5 cells were seeded into ten 6-well plates at a density of 4×10^5 cells per well and transduced the next day with library lentiviral supernatant in 1ml per well of DMEM supplemented with 3%FBS, 1X NEAA, 20 mM HEPES, and 4 $\mu\text{g}/\text{mL}$ polybrene for 1 h, after which 2 mL per well of DMEM complete media was added. After 48 h, transduced cells from all wells were trypsinized, pooled, and re-plated into nine 15 cm plates containing DMEM supplemented with 10% FBS, 1x NEAA, and 4 $\mu\text{g}/\text{ml}$ puromycin and incubated for 3 days to select for transduction. Puromycin selected cells were harvested with trypsin, pooled, counted, and reseeded into eight 15 cm plates at a density of 6.5×10^6 cells per plate, corresponding to 675X library coverage. Cells were allowed to adhere to plates for 3 h, then were treated overnight with DMEM supplemented with 10% FBS, 1X NEAA and 100 U/ml IFN- α . The next day, each plate was infected with 0.8 mL YFV-17D-venus (MOI = 1) in 16 ml of DMEM supplemented with 1% FBS and 1X NEAA for 3 h, then an additional 16 ml of DMEM complete media was added and the cells were incubated overnight. Twenty-four h post-infection the cells were trypsinized, pooled, pelleted and resuspended in FACS buffer (PBS, 2% FBS, 0.5 mM EDTA). Cells were filtered with a 100-micron cell strainer, stored on ice, then sorted at the Children's Medical Center Research Institute Flow Cytometry

Facility by a FACSAria II (Becton Dickenson) flow cytometer while kept at 4°C. GFP-positive gated cells were collected in cell collection buffer (PBS, 50% FBS, 50 mM HEPES), and pelleted. Genomic DNA (gDNA) was extracted from isolated cell pellets following lysis in 500 µl of tissue lysis buffer, containing 460 µl of STE buffer (1 mM EDTA (pH 8.0), 10 mM TrisHCl (pH 8.0), 100 mM NaCl) supplemented with 10µl of 0.5 M EDTA, 10 µl of proteinase K (10 mg/ml in 10 mM Tris-HCl (pH 8.0) and 1 mM EDTA), and 20 µl of 10% SDS. Lysates were incubated overnight at 55°C while shaking at 550 rpm on a Thermomixer (Eppendorf). The following day, 5 µl of 2 mg/ml RNase A was added to each tube and incubated at 37°C for 1 h while shaking at 550rpm. Extractions were collected after mixing samples with an equal volume of phenol:chloroform:isoamyl alcohol (25:24:1) twice, followed once by chloroform; each extraction was separated using MaXtract high density phase lock tubes (Qiagen). Twenty micrograms of glycoblu (Roche) and 1 mL of 100% ethanol were added to each sample and DNA was precipitated at -20°C for 1h followed by centrifugation at 18,000g for 10 minutes at 4°C. Pellets were washed with 1 mL of 75% ethanol, dried, and resuspended in 50 µL of water by incubating at 4°C overnight. Uninfected cell pellets of transduced cells were lysed and gDNA was extracted for controls. To amplify sgRNA sequences for Next Gen Sequencing, four parallel 100 µl PCR reactions were run for each condition, and pooled. Each 100 µl PCR reaction contained 6-10 µg of gDNA, Ex Taq polymerase, pooled P5 and barcoded P7 primers as previously described (Doench et al., 2016). DNA was purified for sequencing using AMPure XP beads (Agencourt) by mixing 300 µl of pooled PCR with 150 µl beads and incubated for 5 minutes to pre-clear genomic DNA. Magnetic separation was used to collect the supernatant. The supernatant was then

mixed with 540 μ l of AMPure XP beads and incubated for 5 minutes to bind the PCR products. The supernatant was collected and discarded. Beads were washed twice with 1 mL 70% ethanol and then dried for approximately 5 minutes. Bound DNA was eluted from the beads using 300 μ l sterile water. Before sequencing, all PCR DNA libraries were analyzed using a Bioanalyzer High Sensitivity DNA Analysis Kit (Agilent). Library concentration was determined by qPCR using a KAPA Library Quantification Kit for Illumina platforms. The samples were sequenced using Illumina NextSeq 500 with the read configuration as 75bp, single end. Each sample was subjected to approximately 10 million to 15 million reads. An in-house script was used to trim the adapter sequences from raw de-multiplexed FASTQ files and unique 20bp sgRNA sequences were processed for further downstream analysis. The reference sgRNA sequences for the human Brunello library were downloaded from Addgene (<https://www.addgene.org/pooled-library/>). Identical sgRNAs targeting the same protein coding genes were removed from the reference library. Software MAGeCK (v0.5.1) was used for data analysis (Li et al., 2014). Sample reads were mapped to the reference sgRNA library with mismatch option as 0. Median normalization was performed to adjust for library sizes and read counts. Positively and negatively selected sgRNA and genes were identified with default parameters.

NHDF experiments

For lentiviral transductions, NHDFs were plated at approximately 100,000 cells per well onto 6-well plates. The next day, cells were transduced via spinoculation with lentiCRISPRv2 (expressing non-targeting sgRNAs or sgRNAs targeting IFI6) in 2 ml

fibroblast basal media at 37 °C for at 800g. Two days post-transduction, cells were pooled and placed under selection with 4 µg ml⁻¹ puromycin and 15 µg ml⁻¹ blasticidin. Three days after selection, cells were plated for experiments or passaged once before plating for experiments. For DENV infections, 100,000 cells per well were plated onto 6-well plates. The next day, cells were infected with DENV at an MOI of 2 for 2 h in 1 ml fibroblast basal media. The supernatant was aspirated and cells were washed four times with 500 µl media and 1.5 ml media was added back. Forty-eight h post-infection, supernatants were collected and titered by limiting dilution on STAT1^{-/-} fibroblasts as described above. Cell lysates were collected for western blot to detect IFI6 expression. For WNV infections, 40,000–80,000 cells per well were plated onto 6-well plates. The next day, cells were infected with WNV at an MOI of 0.01 for 1 h in 1 ml fibroblast basal media. The supernatant was aspirated and cells were washed four times with 500 µl media and a final volume of 1 ml was placed on the cells. Supernatant was collected at 24, 48 and 72 h for titering by plaque assay on BHK cells. To detect IFI6 induction by IFN in NHDFs, 100,000 cells per well were plated onto 6-well plates (for RNA isolation) or 200,000 cells were plated onto 6-cm dishes (for protein isolation). Cells were treated with IFN at indicated doses for 4 h or 24 h. Cells collected for RNA were processed using the Qiagen RNeasy protocol and IFI6 mRNA was detected by quantitative RT-PCR as described above. For protein detection, cells were collected, resuspended in lysis buffer and mixed with 1× SDS loading buffer lacking β-mercaptoethanol (BME). Samples were sonicated but not boiled, and loaded onto Tris-tricine low-molecular-weight gels and analysed for IFI6 expression as described above.

Endogenous IFI6 gene tagging in U-2 OS cells

Oligos encoding an sgRNA near the C-terminal coding region of IFI6 were cloned into LentiCRISPRV2 as described above. An IFI6-based donor vector containing homology arms flanking the protospacer adjacent motif site by 800 bp in both directions and a 3×FLAG sequence was synthesized in a pUC57 backbone (Genewiz). The protospacer adjacent motif site codons were altered to avoid re-targeting of the site once DNA repair had occurred. For transfections, 200,000 U-2 OS cells were seeded onto 6-well plates in complete DMEM containing 0.1 μM SCR-7, a DNA ligase IV inhibitor (Tocris). The donor vector and the LentiCRISPRv2 vector were transfected with X-tremeGENE 9 (Roche) into U-2 OS cells at a ratio of 2/1 with a final DNA amount of 2 μg per well. Two days post-transfection, cells were re-plated in complete DMEM with 1 $\mu\text{g ml}^{-1}$ puromycin and 0.1 μM SCR-7 for 24 h, then replaced with complete DMEM with 0.1 μM SCR-7 and no puromycin. Cells were maintained for at least 1 week before use in experiments.

Immunofluorescence and confocal microscopy

Cells were fixed in 4% paraformaldehyde in PBS for 15 min, permeabilized with 0.2% Triton-X 100 in PBS for 5 min and blocked with 10% BSA, 5% goat serum and 50 mM glycine in PBS for 30 min. Primary antibody incubation for 2 h at room temperature was followed by secondary incubation with an Alexa Fluor-conjugated secondary antibody (AF-488 for green channels and AF-555 for red channels, Life Technologies). Cells were

mounted with ProLong Diamond with DAPI (Life Technologies) and imaged with a Zeiss Axiovert 200 microscope or Zeiss Observer Z.1 microscope, unless otherwise indicated.

dsRNA

Approximately 20,000 Huh7.5 cells stably expressing IFI6 or an empty vector were plated into 8-well chamber slides. Cells were infected with 1.5 MOI YFV-17D for 1 h. Cells were incubated for 48 h and, following the protocol described above, were stained with J2 dsRNA antibody (1:200, Scicons) and Hoechst stain (1:12,000, Thermo Fisher) and mounted with ProLong Gold (Life Technologies).

Sec61 β -mEmerald and pTRIP.Mito-GFP

mEmerald-Sec61-C-18 was a gift from M. Davidson (Addgene plasmid 54249). COS-7 or Huh7.5 stably expressing IFI6 3 \times FLAG were plated at 5,000 cells per well into 8-well chamber slides. The next day, cells were transfected with 75 ng per well (Huh7.5) or 20 ng per well (COS-7) of mEmerald-Sec61 β or 75 ng per well of pTRIP.Mito.eGFP (kindly provided by C. Rice). Cells were stained as described above with anti-GFP antibody (1:4,000, 6556, Abcam) and FLAG-M2 (1:1,000, 3165, Sigma).

U-2 OS HDR cells

U-2 OS cells were plated at 5,000 cells per well onto 8-well chamber slides. The next day, cells were transfected with 75 ng per well of mEmerald-Sec61 β and 6 h post-transfection treated with 1,000 U ml⁻¹ IFN- α . Cells were stained with antibodies against FLAG and GFP as described above.

N32-GFP localization

COS-7 cells were plated at 5,000 cells per well onto 8-well chamber slides. The next day, cells were transfected with 75 ng per well of SCRPSY.IFI6(N32)GFP-nlsBFP. Twenty-four hours post-transfection, cells were stained with antibodies against FLAG and the ER retention KDEL sequence (1:250, ADI-SPA-827, Enzo).

DENV NS4B localization

IFI6-3×F-expressing Huh7.5 cells were plated at 5,000 cells per well into 8-well chamber slides. Cells were infected with DENV at a MOI of 2 for 2 h. Cells were incubated for 48 h and stained with antibodies targeting DENV NS4B (1:200, Thermo Fisher) and FLAG (1:1,000, Sigma). Images were acquired using a Zeiss 880 laser scanning confocal microscope with Airyscan for super-resolution capability. Images were deconvolved using AutoQuant X3. Deconvolved images were analysed for colocalization using Imaris 7.7.2, where a background subtraction was performed and a threshold for pixel intensity was automatically determined by the software. The Pearson values shown indicate the overlap in the automatically determined region of interest.

Electron microscopy and immunogold labelling

Approximately 2×10^6 Huh7.5 cells stably transduced with SCRPSY.empty or SCRPSY.IFI6 lentivirus were seeded into 10-cm tissue culture dishes. The next day, cells were mock infected or infected with YFV-17D at 1 MOI. Cells were processed 24 h post-infection for electron microscopy as previously described (Hanners et al., 2016). For immunogold labelling, COS-7 cells stably expressing SCRPSY.IFI6-HA were fixed for 30 min at room temperature with 4% paraformaldehyde and 0.1% glutaraldehyde in 0.1 M

sodium phosphate buffer (pH 7.4). Cells were permeabilized with 0.25% saponin in phosphate buffer for 30 min and blocked with 5% goat serum in 0.01% saponin in phosphate buffer for 1 h. Cells were then incubated with anti-HA antibody (1:1,000 dilution, 901501, BioLegend) overnight at 4 °C. The next day, cells were washed four times with phosphate buffer, followed by incubation with 1.4-nm gold-conjugated fragment antigen-binding goat antibodies to mouse IgG (1:100, 7202, Nanoprobes) for 2 h at room temperature. After washing five times with phosphate buffer, cells were further fixed with 1% glutaraldehyde and washed three times with phosphate buffer. After rinsing with water, the immunogold-labeled samples were gold enhanced for 2.5 min using the gold enhancement kit (Nanoprobes) and washed again with water and 0.1 M sodium cacodylate buffer. Cells were then post-fixed in 1% osmium tetroxide and 0.8% K₃[Fe(CN)₆] in 0.1 M sodium cacodylate buffer for 1 h at room temperature and en bloc stained with 2% aqueous uranyl acetate. Samples were then dehydrated with increasing concentrations of ethanol, infiltrated with Embed-812 resin and polymerized in a 60 °C oven overnight. Blocks were sectioned with a diamond knife (Diatome) on a Leica Ultracut UCT (7) ultramicrotome (Leica Microsystems) and collected onto copper grids. Images were acquired on a Tecnai G2 spirit transmission electron microscope (FEI) equipped with a LaB6 source using a voltage of 120 kV.

RNA and protein detection in cell cultures

Quantitative RT-PCR for ISGs

For gene expression assays, total RNA was isolated from cells stably expressing IFI6 or, alternatively, after treatment with 0 or 100 U ml⁻¹ IFN- α . RNA was isolated using a

RNeasy Mini Kit (Qiagen). Total RNA (50 ng) was analysed by quantitative RT–PCR using the QuantiFast SYBR Green RT–PCR kit (Qiagen). Commercially available QuantiTect primers specific for IFI27, IFI27L1, IFI27L2, IRF1, IFITM3, RSAD2, IFIT1, HSPA5 and the housekeeping control gene RPS11 (Qiagen) were used according to the manufacturer’s instructions. Reactions were run on an ABI7500 Fast Real Time PCR System and gene expression was calculated using the $\Delta\Delta\text{CT}$ method.

RNA sequencing

Gene expression analysis by RNA sequencing was performed as previously described (Perelman et al., 2016). The RNA sequencing data have been deposited to the NCBI Gene Expression Omnibus with the accession number GSE105771.

Western blot

For protein expression assays, cells were lysed in RIPA buffer (25 mM Tris (pH 7.5), 150 mM NaCl, 0.1% SDS, 0.5% sodium deoxycholate, 1% Triton X-100 and 1× Complete Protease Inhibitor Cocktail (Roche)) or NP-40 lysis buffer (50 mM Tris (pH 7.5), 150 mM NaCl, 1 mM EDTA, 1% NP-40 and 1× Complete Protease Inhibitor Cocktail) to obtain a post-nuclear lysate. The protein concentration of cell lysates was determined by Bradford Assay (Pierce). Alternatively, cell pellets were directly boiled in 2× SDS–PAGE sample buffer (100 mM Tris (pH 6.8), 20% glycerol, 4% SDS, 2% BME and 0.1% Bromophenol blue) or 2× Tricine sample buffer (200 mM Tris-HCl (pH 6.8), 40% glycerol, 2% SDS and 0.04% Coomassie blue). Lysates were separated on 12% polyacrylamide gels using the

Laemmli method. For endogenous IFI6 detection, 10% Tris-Tricine gels were used. Proteins were blotted to PVDF (polyvinylidene difluoride) membranes (Bio-Rad) and processed for western blotting. Blots were blocked overnight in 3% or 5% milk in TBST (50 mM Tris-Cl (pH 7.5), 150 mM NaCl and 0.05% Tween-20), followed by incubation with primary and secondary antibodies for 1 h and 30 min, respectively. Proteins were visualized by incubating blots with enhanced chemiluminescent substrate (ECL, Pierce) and exposing blots to autoradiography film (Denville Scientific). The antibodies used in the study include: anti-FLAG M2 (F3165, Sigma), anti-FLAG polyclonal (F7425, Sigma), anti- β -actin (ab6276, Abcam), anti-BiP (PA5-34941, Thermo Fisher), anti-calnexin (ADI-SPA-860-D, Enzo Life Sciences), anti-KDEL (ADI-SPA-827D, Enzo Life Science), anti-RFP (AB233, Evrogen), anti-DENV NS4A (GTX132069, GeneTex), anti-NS1 (gift from M. Diamond), rabbit IgG control (ab27478, Abcam), mouse IgG control (ab81032, Abcam), goat anti-rabbit horseradish peroxidase and goat anti-mouse horseradish peroxidase (Pierce). For the detection of endogenous IFI6, a rabbit polyclonal antibody was custom generated by ProSci, Inc. The antigen consisted of a peptide corresponding to the C terminus of IFI6 (LMGYATHKYLDSEED) and containing an N-terminal cysteine to assist in conjugation to the carrier protein. Antibody was further isolated by immunoaffinity purification of the serum.

Membrane flotation assay

Huh7.5 cells stably expressing IFI6-3 \times FLAG were collected from confluent 15-cm tissue culture dishes and resuspended in 2 ml cold 0.25 M sucrose. Cells were lysed in a

2-ml tight-fitting Dounce homogenizer with 200 strokes on ice to yield approximately 90% lysis. The lysate was centrifuged at 2,500g for 10 min at 4 °C to pellet debris. The supernatant was transferred to a new tube and pelleted at 20,000 g for 10 min at 4 °C to pellet membranes. Pellets were resuspended in 2 ml PBS, PBS with 1 M NaCl, PBS with 0.1 M Na₂CO₃ (pH 11.5) or PBS with 0.5% Triton X-100 and incubated on ice for 30 min. The samples were mixed with 2 ml cold 60% Histodenz (Sigma) and transferred to an ultracentrifuge tube (Beckman Coulter Ultra-Clear, 14 × 95 mm). To avoid mixing, the sample was overlaid with gentle pipetting of 4 ml cold 20% Histodenz in PBS/sucrose and finally with 4 ml cold 10% Histodenz in PBS/sucrose. An additional 10% Histodenz in PBS/sucrose was used to bring the tube volume to ~1 mm from the rim of the tube. Alternatively, in some experiments, samples were loaded onto an iodixanol (Sigma) gradient. Samples were centrifuged at 35,000 r.p.m. (~209,000g) in a SW40Ti rotor for 16 h. Samples were collected in 1-ml fractions from the top of the tube and mixed with 1 ml 2× SDS–PAGE sample loading buffer. Aliquots (20 µl) were analysed by western blot with anti-FLAG, anti-calnexin or anti-RFP antibodies as described above.

Immunoprecipitation assay

Approximately 1.5×10^6 Huh7.5 cells stably expressing IFI6-3×FLAG were collected for each condition and pelleted. Cells were resuspended and lysed gently at 4 °C with nutation for 15 min in 250 µl of a buffer containing 20 mM Tris-HCl (pH 7.5), 1.5 mM MgCl₂, 150 mM NaCl, 1% NP-40, 5% glycerol and 1 protease inhibitor pellet (Roche) per 10 ml of solution. When used, ATP was included at a final concentration of 2 mM (A6559,

Sigma). Cells were then pelleted at 16,000g for 8 min at 4 °C. An affinity gel containing 4% agarose beads with FLAG-M2 antibody covalently bound (F2426, Sigma) was equilibrated in washing buffer (20 mM Tris-HCl (pH 7.5), 250 mM NaCl, 0.2% NP-40, 1.5 mM MgCl₂ and 5% glycerol). Cleared lysate (5–10%) was collected as inputs and stored at –80 °C. The remaining lysate was added to the beads and incubated overnight at 4 °C on a rotator. The next morning, the supernatant was collected and beads were washed four times with washing buffer. A 3×FLAG peptide (4799, Sigma) was used to elute the bound products off of the column at 4 °C with constant vortexing for 1 h. Input samples and eluted products were run on a SDS–PAGE gel and transferred to a PVDF membrane, which was probed with antibodies against BiP or FLAG (rabbit polyclonal).

Secretion assay

293T cells plated at 400,000 cells per well in 6-well plates were transfected with pTRIP.CMV.IVSB-CCL2-1×FLAG or pTRIP.CMV.IVSB-IFI6-3×FLAG plasmids using XtremeGENE 9 (Roche). The next day, media were removed and 1 ml Optimem (Gibco) with or without 1 µg ml⁻¹Brefeldin A was added to cells. After 5 h, supernatants were removed and proteins were precipitated with trichloroacetic acid. Cells were harvested with Accumax and post-nuclear cell lysates were analysed by western blot with anti-FLAG or anti-actin antibodies as described above.

Protein cleavage assays

293T, 293T control sgRNA or 293T SPCS1-KO cells (the latter two kindly provided by M. Diamond) were plated at 400,000 cells per well in 6-well plates. As indicated, cells were transfected with pTRIP.XKB-2K-NS4B-HA, pTRIP.XKB-C-prM-HA, pTRIP.CMV.IVSB-IFI6-3×FLAG, pTRIP.CMV.IVSB-GFP-1×FLAG, pQCXIP-DENV-NS2B-NS3 (wild type or S135A; gifts from M. Gack) and MRX-HA-STING (gift from N. Yan) plasmids using X-tremeGENE 9 (Roche). The next day, cells were harvested with Accumax and post-nuclear cell lysates were analysed by western blot with anti-FLAG, anti-HA or anti-actin antibodies as described above.

CHAPTER THREE

Results

A CRISPR SCREEN IDENTIFIES IFI6 AND BiP AS TWO GENES IMPORTANT FOR IFN-MEDIATED HOST RESPONSE TO YFV INFECTION

Overview

The interferon response and the subsequent production of ISGs represent a critical line of host defense against invading pathogens. Flaviviruses have evolved mechanisms to counteract IFN signaling, suggesting that ISGs exist to suppress these viruses (Grant et al., 2016; Szretter et al., 2011). In vivo data shows that the IFN response is required to protect the host from flavivirus infection, since mice lacking components of the IFN signaling pathway are more susceptible to flavivirus infection (Lazear et al., 2011; Samuel and Diamond, 2005). This directly shows evidence that ISGs are involved in controlling viral infection. To identify which ISGs and host factors were required to efficiently inhibit viral replication, a genome-wide CRISPR screen was used in the context of infection with a flavivirus, yellow fever virus (YFV). The CRISPR screen identified several ISGs, but only one ISG not directly involved in the IFN pathway itself, IFI6, as well as BiP, a host factor with chaperone activity. Here, I show that IFI6 is a potently antiviral ISG against flaviviruses and is required for the IFN response to YFV infection. I also show that BiP is required for the IFN response, and interacts with IFI6 in a chaperone-dependent manner.

A CRISPR screen identifies IFI6 and BiP as two genes important for IFN-mediated host response to YFV infection

Recently published CRISPR screens identified host factors important for flavivirus replication in host cells (Marceau et al., 2016; Zhang et al., 2016). Another member of my lab, Maikke Ohlson, and the McDermott Bioinformatics Core members, Chao Xing and Ashwani Kumar, performed a CRISPR screen. This screen used the same Brunello library used in previous CRISPR screens but with a different goal (Figure 1a). The CRISPR screen was designed to identify host factors and potentially ISGs that were required for IFN signaling during infection with a prototypic flavivirus, YFV-Venus. The screen used Huh7.5 cells, which have the unique ability to respond to IFN, but do not naturally produce IFN due to a mutation in the RIG-I gene, providing efficient control of IFN signaling (Blight et al., 2002). Normally, Huh7.5 cells are highly permissive to YFV infection such that nearly all cells can be infected with a single viral life cycle (Figure 1a). However, pre-treatment before infection with IFN- α can inhibit nearly all infection. In the case of a cell population that has been transduced with the Brunello CRISPR lentiviral library, followed by IFN pre-treatment and YFV infection there is a slight increase in the amount of cells infected, despite being treated with IFN. The experiment was performed and after one round of viral infection, cells were collected via fluorescence-activated cell sorting (FACS). Genomic DNA was isolated from these cells. The barcoded sgRNA guides were amplified by PCR and purified via magnetic bead separation and sent for sequencing at the McDermott Core.

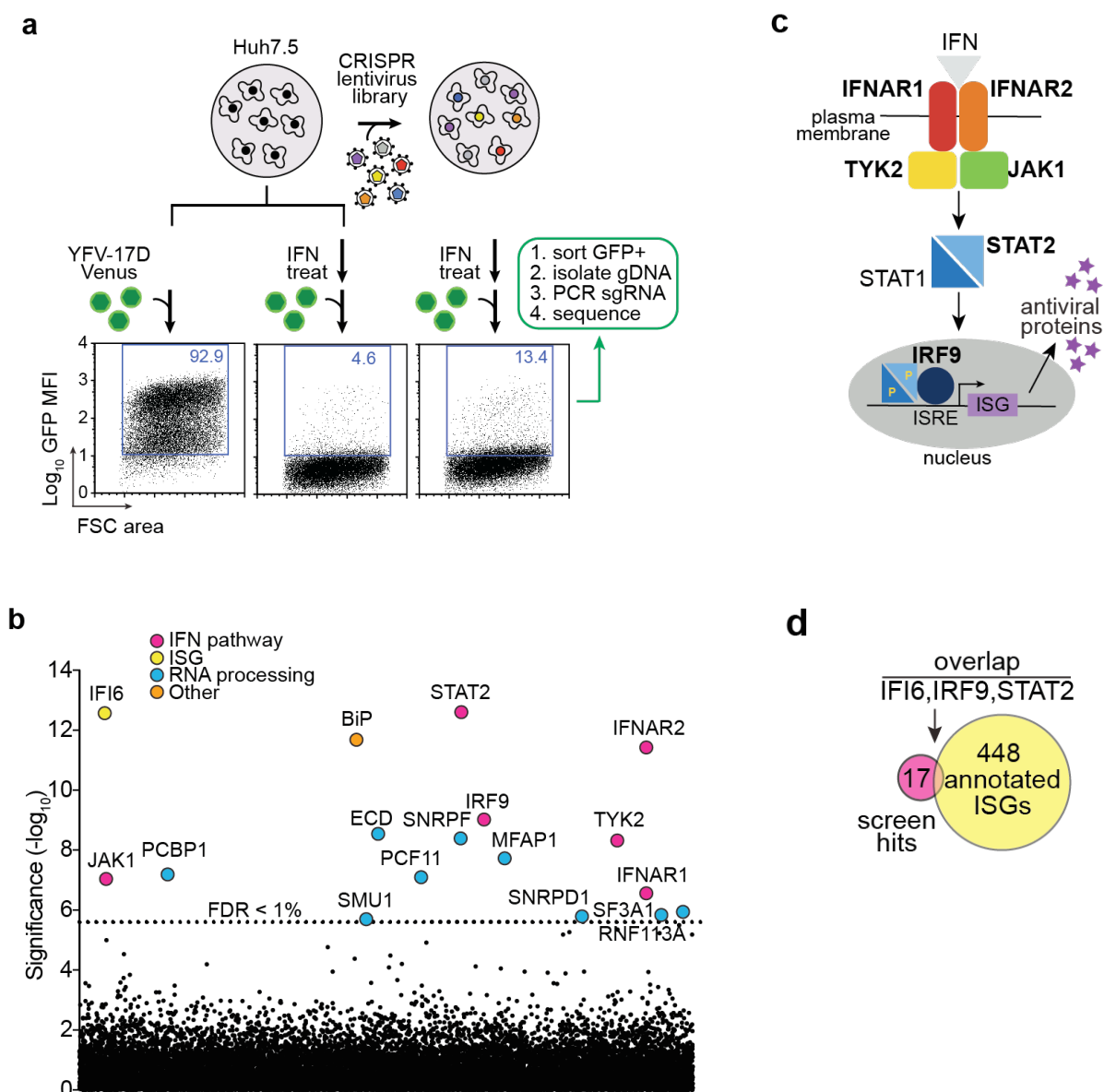


Figure 1: Identification of IFI6 and BiP as top hits in IFN-based CRISPR screen.

a, Schematic of genome-wide CRISPR screen to identify genes required for the IFN- α - induced antiviral response to YFV. **b**, Manhattan dot plot of genome-wide CRISPR screen results with significance of enrichment calculated by the MAGeCK method. Genes with an FDR < 0.01 (dotted line) are coloured. The numbers in blue represent the percentage of GFP-positive cells. **c**, IFN signalling pathway with CRISPR hits in bold. ISRE, interferon stimulated response element. **d**, Overlap of CRISPR screening hits with common ISGs.

Bioinformatics analysis revealed several interesting groups of hits (Figure 1b). Several genes involved in RNA processing were significantly enriched, which may broadly impact the transcription of ISGs. Another group of genes that emerged were genes involved in the IFN signaling pathway. Every gene with the exception of STAT1 was recovered, which is expected since the IFN pathway must be intact in order for a cell to respond to IFN treatment (Figure 1c). The final two hits observed in the screen were the most surprising. IFI6 and the ER chaperone BiP were recovered as two of the top three significant hits in the screen. Importantly, when the list of hits from the screen was compared to a list of known ISGs only three ISGs were found to overlap (Figure 1d). The three genes were IRF9, STAT2, and IFI6. IRF9 and STAT2 are involved in the IFN-signaling pathway directly, which leaves IFI6 as the only downstream ISG identified in the screen. This result implies a significant role for IFI6 during the context of a YFV infection.

IFI6 KO cells are refractory to IFN treatment

Subsequent validation of the CRISPR screen began by generating a Huh7.5 CRISPR knockout cell line lacking expression of IFI6. With help from Jennifer Eitson, I confirmed the IFN-induction of IFI6 in wild type Huh7.5 cells in a timecourse experiment, and showed that the Huh7.5 knockout cells did not express IFI6 (Figure 2a). I also observed that peak levels of IFI6 protein expression occurred at 24 hours post IFN treatment. Once the knock out of IFI6 was confirmed, I tested the knockout cells for sensitivity to IFN treatment followed by infection with a panel of RNA viruses (Figure 2b). I tested IFN concentrations

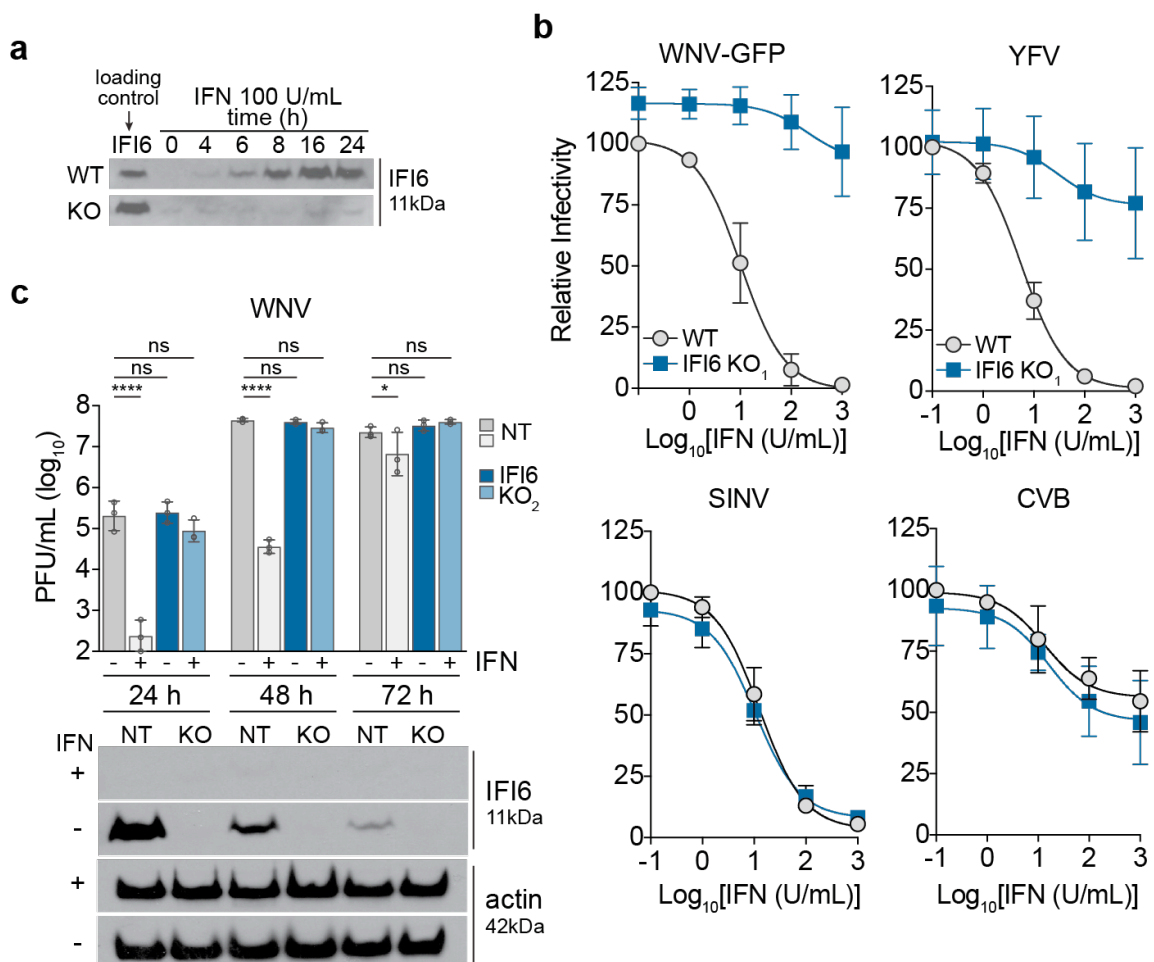


Figure 2: Validation of CRISPR phenotype with IFI6-KO cell lines

a, Western blot of Huh7.5 or Huh7.5-IFI6-KO1 cells treated with IFN. **b**, IFN- α dose response curves in Huh7.5 or Huh7.5-IFI6-KO₁ cells challenged with WNV-GFP, YFV-Venus, SINV-GFP or CVB-eGFP. **c**, Time course of WNV production in Huh7.5-NT or Huh7.5-IFI6-KO₂ cells with or without a single dose of IFN- α . Western blots corresponding to the WNV time course (bottom).

ranging from 1000 U/mL to 0.1 U/mL and pretreated KO and WT cells for 4 hours. The cells were infected with a panel of RNA viruses: YFV-Venus, WNV-GFP, SINV-GFP and CVB-eGFP. After one round of viral replication, cells were collected and analyzed by flow cytometry to measure infectivity. I found that WT cells were responsive to the IFN treatment for infection with most viruses, since infection was inhibited in a dose-dependent manner with IFN treatment. CVB was less sensitive to IFN treatment, however there was still an observable change in the amount of infection in the WT cells. In the KO cells I observed no difference in infectivity with CVB or SINV relative to the WT cells, suggesting IFI6 is not required for the IFN response to these viruses. However, in the YFV and WNV infections the KO cells were highly permissive to infection at all IFN concentrations, suggesting IFI6 plays a critical role in the IFN response to flaviviruses.

In a similar experiment performed by Jennifer Eitson, the plaque production of WNV in the context of IFN treatment in WT and KO cells was measured over time (Figure 2c). A second but analogous Huh7.5 KO cell line lacking IFI6 was generated and used with a CRISPR NT control. Cells were pretreated with 1000 U/mL of IFN followed by WNV infection. At 24 h the untreated NT and KO cells produced the same titer of WNV. When cells were treated with IFN, the NT cells produced low titers of WNV, while IFI6 KO cells treated with IFN produced nearly the same titer as untreated cells. At 48 h WNV titers were increased but a similar trend to the titers produced at 24 h was observed. At 72 h the NT IFN treated cells had nearly the same titers as all other cell lines. Since the NT cells treated with IFN eventually produced viral titers equivalent to non-treated cells, I speculated that the effect of IFN had diminished at later timepoints. An increase in viral titers correlated with a

decrease of IFI6 expression in NT cells treated with IFN, suggesting a loss of ISG expression over time, allowing for increased viral titers.

Ectopic expression of IFI6 blocks viral infection of flaviviruses

Complementary to CRISPR knockout experiments, I performed experiments where IFI6 was ectopically overexpressed. Using lentiviral transduction I transduced Huh7.5 cells with the SCRPSY lentivirus overexpressing IFI6 or an empty sequence. These cells were infected with YFV-Venus or DENV-GFP and cells were collected at intervals over the course of several viral life cycles (Figure 3a). Cells were analyzed by flow cytometry. I found that at early time points of infection IFI6 cells were inhibitory to infection with both YFV and DENV. As the virus spread, the control cells eventually all became infected, and at these same time points the IFI6 cells remained relatively uninfected. I also tested a non-reporter virus YFV-17D (Figure 3b). I infected Huh7.5 cells with an MOI of 2 and supernatants were collected at early timepoints in the viral life cycle and at later timepoints, which reflect multiple rounds of replication. I performed the supernatants and observed an approximate 2-3 \log_{10} difference between control and IFI6-expressing cells, suggesting the inhibitory effects I see with IFI6 overexpression are not due to attenuation of a reporter virus. When I infected the IFI6 Huh7.5 cells with MR-766 ZIKV-GFP or with ZIKV PRVABC59 I observed a similar trend to that of YFV and DENV (Figure 3c). Interestingly, both strains of ZIKV were inhibited by IFI6 but to a lesser degree, which suggests ZIKV may have strategies for overcoming the IFI6 inhibition. When neural progenitor cells overexpressing IFI6 were infected with PRVABC59, a similar result was observed,

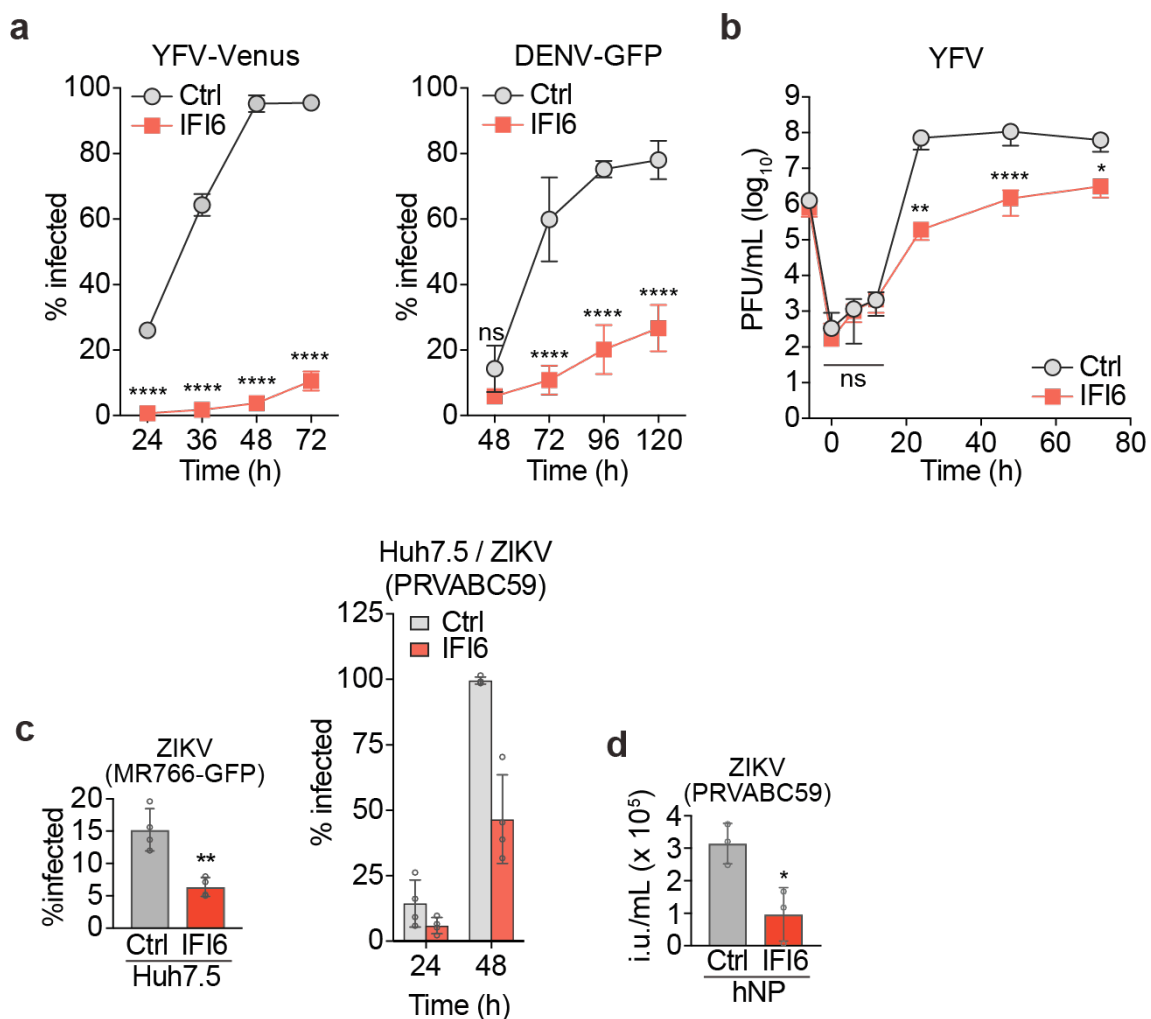


Figure 3: Ectopic expression of IFI6 inhibits flavivirus infection.

Huh7.5 cells transduced with lentivirus expressing IFI6 or an empty (Ctrl) vector were infected with viruses at 0.5–2.0 MOI as follows: **a**, Time courses of YFV-Venus and DENV-GFP. **b**, Single-step growth curve of YFV-17D. **c**, Infectivity of ZIKV-GFP (MR766) and PRVABC59 in Huh7.5. **d**, hNP cells transduced with lentivirus expressing IFI6 or an empty (Ctrl) vector were infected with PRVABC59 and the titer was quantified.

ranging from 1000 U/mL to 0.1 U/mL and pretreated KO and WT cells for 4 hours. The cells were suggesting the IFI6 inhibitory effect is conserved across several cell lines (Figure 3d).

IFI6 inhibits flavivirus infection in NHDF cells

To determine if the IFI6 phenotype is relevant in primary cells I characterized the antiviral effect of IFI6 in normal human dermal fibroblasts (NHDF). I treated these cells with IFN and observed an induction of IFI6 by RNA and protein levels similar to kinetics observed in Huh7.5 cells (Figure 4a, 4b). Additionally when I infected the NHDF with DENV-WT-NS4B, a mouse-adapted DENV that had been passaged once in cell culture to high titers, I saw that viral infection also induced expression of IFI6 (Figure 4c). I generated CRISPR KO cells lacking IFI6 and observed that these cells did not produce IFI6 with viral infection (Figure 4c). I collected supernatants from the DENV infected cells and quantified virus production by titrating supernatants on STAT1^{-/-} fibroblasts (Figure 4d). Since the primary fibroblasts are IFN competent I chose a cell line that was not responsive to IFN to avoid unwanted effects of IFN in the supernatant. The STAT1^{-/-} fibroblasts were stained with a 4G2 antibody that recognizes the envelope protein of DENV, and infectivity was analyzed by flow cytometry. I observed a less dramatic, but consistent increase in the virus production of the primary fibroblasts when IFI6 was knocked out, suggesting that IFI6 is important in primary cells for mediating virus infection. In a similar experiment Jennifer Eitson used IFI6 KO cells with WNV and quantified plaque production (Figure 4e). She observed that IFI6 KO cells produced approximately ten-fold more virus than NT cells, further suggesting IFI6 plays an important antiviral role in primary cells.

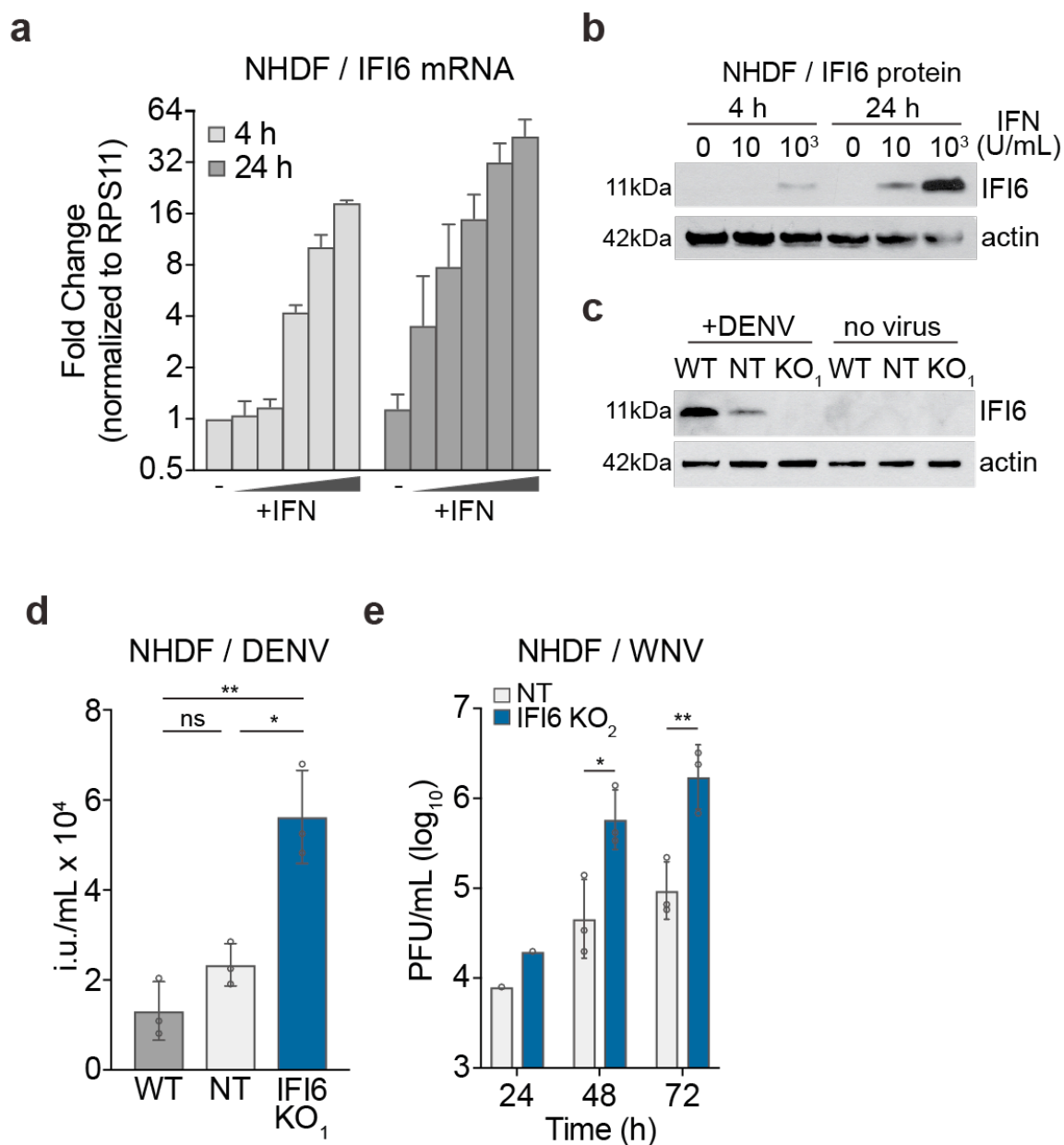


Figure 4: IFI6 contributes to the antiviral response in NHDF primary cells.

a, RT-PCR quantification of IFI6 mRNA levels with an IFN dose response at 4h and 24h post IFN treatment of NHDF cells. **b**, Western blot analysis of IFI6 induction by IFN in NHDF cells at 4h and 24h post IFN treatment. **c**, Induction of IFI6 by DENV in WT NHDF or NHDF transduced with LentiCRISPR-NT or LentiCRISPR-IFI6 KO₁. **d**, Titers of DENV in WT NHDF or NHDF transduced with LentiCRISPR-NT or LentiCRISPR-IFI6 KO₁. **e**, Titers of WNV in WT NHDF or NHDF transduced with LentiCRISPR-NT or LentiCRISPR-IFI6 KO₂.

IFI6 belongs to a unique family of proteins, FAM14

Previous literature reports IFI6 belongs to the FAM14 protein family, which is reviewed in Chapter 1. In humans, there are four members of this protein family: IFI6, IFI27, IFI27L1 and IFI27L2 (Figure 5a). The interferon-inducibility of each family member was tested in three cell lines, Huh7.5, U-2 OS, and A549. Only IFI6 and IFI27 were inducible with IFN, while IFI27L1 and IFI27L2 were not (Figure 5b). Previous screening data also suggested that while IFI6 and IFI27 are both IFN-inducible, IFI6 was the only antiviral ISG when tested against flaviviruses (Schoggins et al., 2011). I confirmed this result with YFV infection (Figure 5c).

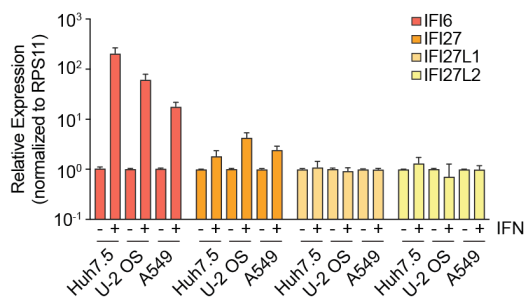
The FAM14 families in humans and mice have four and three members respectively, but several of the proteins have multiple transcript variants. I tested all transcript variants of these protein families for their antiviral activity (Figure 5d). I transduced these lentiviruses into STAT1^{-/-} fibroblasts. I challenged these cells with YFV-Venus and DENV-GFP. Among the human genes, I found that consistent with previous reports, only IFI6 was inhibitory, while IFI27, IFI27L1 and IFI27L2 or any of their transcript variants were not. Interestingly, all three transcript variants of IFI6 were inhibitory. As previously mentioned in Chapter 1, these transcript variants differ by 4 amino acids each. While these constructs were all inhibitory, with the addition of 4 or 8 amino acids, the antiviral activity decreased slightly in a stepwise fashion. This suggests these amino acids may alter IFI6 in a manner that negatively impacts its antiviral function. In mice, I found that none of the five IFI27

a

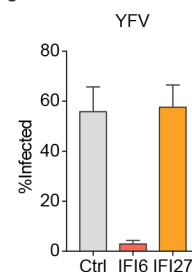
IFI6	1	MRQKAVSLFLCYLLLFTCSGVEAGKKKCSSESSDSGSGFWKALTF-----MAVGGGLAVAG	55
IFI27	1	-----MEASALTSsavtSVAKVVRVASGSAVVLPLARIATVVIGGVVAMAA	46
IFI27L1	1	-----MGKESGWDSGRAAVA-----AVVGGVVAVGT	26
IFI27L2	1	-----MM-----KRAAA-----AAVGGALAVGA	18
IFI6	56	LP----ALGFTGAGIAANSVAA SLM SWSA ILNNGGGVPAGGLVATLQSLGAGG----SSVV	107
IFI27	47	VPMVLSAMGFTAAGIASSIAAKMMSAAA IANGGGVAGSLVATLQSLGATGLSGLTKFI	106
IFI27L1	27	VLVALSAMGFTSVGIAASSIAAKMMSAAA IANGGGVAGSLVA I LQSVGAAGLSTSKVI	86
IFI27L2	19	VPVVLSAMGFTGAGIAASSIAAKMMSAAA IANGGGVSAGSLVATLQSVGAAGLSTSSNIL	78
IFI6	108	IGNIGALMGYATHKYLDSEEDEE-----	130
IFI27	107	LGSIGSAAIAAVIARFY-----	122
IFI27L1	87	GGFAGTALGAWLGSPSS-----	104
IFI27L2	79	LASVGSVLGACLGNSSSLLPAEP EAK EDEAR ENVPQGEPPKPLKSEKHEE	130

Aliphatic/hydrophobic	I L V A M
Aromatic	F W Y
Positive	K R H
Negative	D E
Hydrophilic	S T N Q
Conformationally special	P G
Cysteine	C

b



c



d

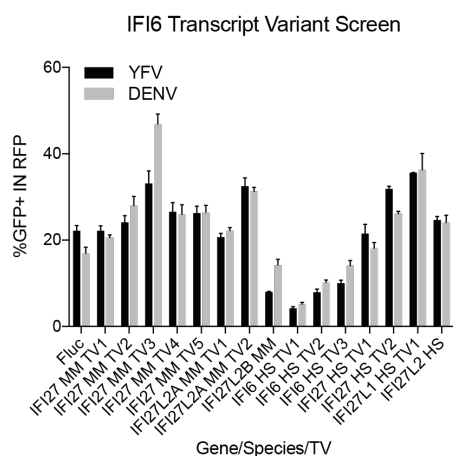


Figure 5: IFI6 belongs to the FAM14 protein family and is the only antiviral family member.

a, Amino acid alignment of the human FAM14 protein family. **b**, IFN inducibility of FAM14 family members in Huh7.5, U-2 OS and A549 cells. **c**, Huh7.5 cells transduced with lentivirus expressing empty (Ctrl), IFI6 or IFI27 were infected with YFV-Venus. **d**, STAT1^{-/-} fibroblasts transduced with lentivirus expressing a human or mouse transcript variant of a FAM14 family member were infected with YFV-Venus or DENV-GFP.

transcripts or the two IFI27L2A transcripts were inhibitory, but that the IFI27L2B transcript, which uniquely contains two ISG12 motifs, was inhibitory to YFV. Taken together, these data suggest IFI6 and its transcript variants retain their antiviral activity and imply that IFI27L2B, despite having low sequence homology with human IFI6, may be an antiviral paralog in mice. A previous publication identified IFI27L2A as the functional paralog of IFI6 in mice; however I was unable to observe an antiviral phenotype with this gene. (Lucas et al., 2015).

IFI6 does not alter the expression of other antiviral genes

Because the phenotype I observed with IFI6 was so potent, I wanted to confirm that there was no impact to IFN signaling, such as positive feedback or in induction of other ISGs. Jennifer Eitson overexpressed IFI6 in STAT1^{-/-} fibroblasts and looked for ISG induction with IFI6 overexpression. STAT1^{-/-} fibroblasts do not respond to IFN which allowed her to observe the effects of IFI6 overexpression alone. She checked expression of several ISGs known to be readily induced to high levels with IFN treatment: IRF1, IFIT1, IFITM3, OAS2, and RSAD2 and found that compared to a control cell line these genes were not expressed at higher levels when IFI6 was overexpressed (Figure 6a). However, in a positive control cell line overexpressing IRF1, a known positive regulator of IFN-signaling, she saw elevated levels of expression. These data suggest IFI6 is not involved in the induction of other ISGs.

Additionally, in another experiment Katrina Mar performed RNA-seq on STAT1^{-/-}

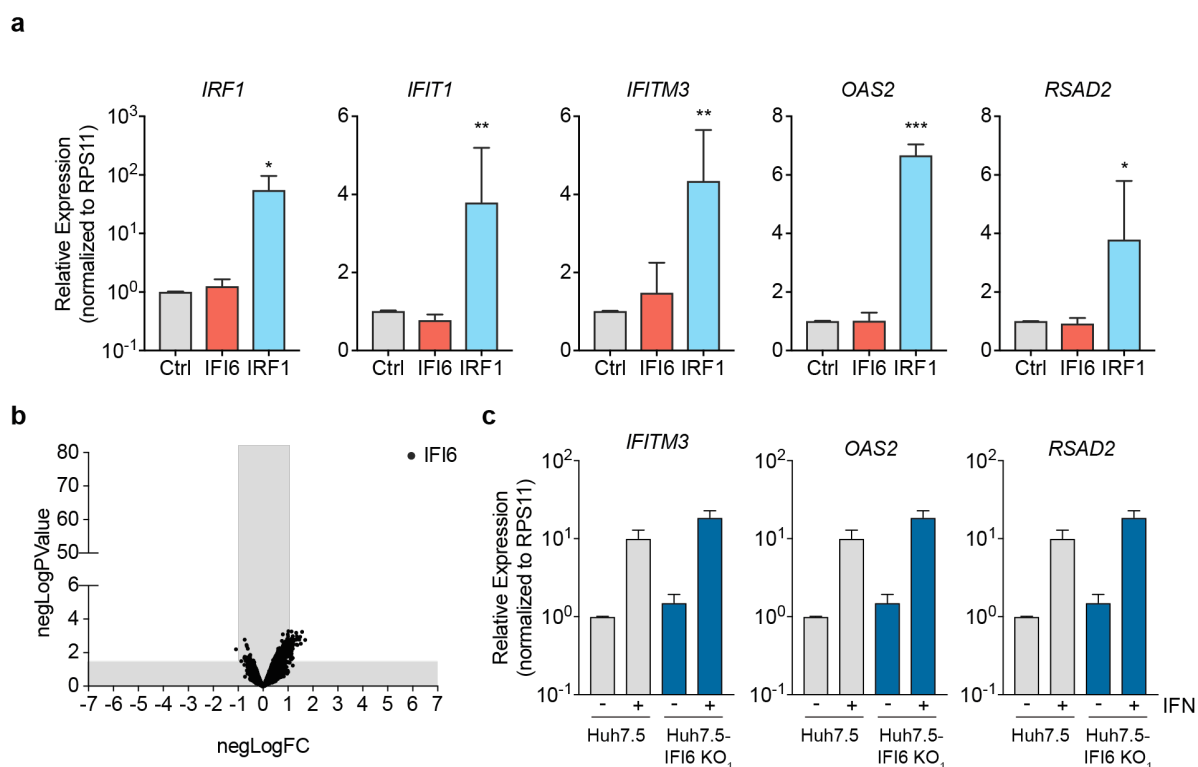


Figure 6: IFI6 does not modify global antiviral gene expression.

a, RT-qPCR analysis of IRF1, IFIT1, IFITM3, OAS2, and RSAD2 mRNA expression in STAT1^{-/-} fibroblasts transiently transduced with lentivirus expressing IFI6, an empty vector, or the antiviral transcription factor IRF1. **b**, RNA-Seq analysis of global differential gene expression in STAT1^{-/-} fibroblasts transiently transduced with lentivirus expressing IFI6 or Fluc as a control. **c**, RT-PCR analysis of IFITM3, OAS2, and RSAD2 mRNA expression in Huh7.5 or Huh7.5-IFI6-KO cells treated for 6 h with 100 U/mL IFN α .

fibroblasts overexpressing IFI6 and found that the only significant change in gene expression was in the expression of IFI6 itself, further suggesting IFI6 does not regulate gene expression of other ISGs or any other host gene (Figure 6b).

In a complementary experiment, Jennifer used a Huh7.5 KO cell line lacking IFI6 and a control cell line (Figure 6c). When these cells were treated with IFN to induce ISG expression, Jennifer found that the ISGs in IFI6 KO cells were able to express to equal levels, suggesting that IFI6 is not required in IFN-signaling. Taken together, these data suggest IFI6 displays a potent antiviral phenotype that is not caused by feedback or dysregulation of IFN signaling.

BiP is required for the IFN response and IFI6 activity towards YFV

The other outstanding hit from the CRISPR screen was BiP (HSPA5, GRP78) (Munro and Pelham, 1986; Wang et al., 2017). With the help of Maikke Ohlson and Jennifer Eitson, BiP was validated for its antiviral effects. Jennifer demonstrated that only IFI6 and not BiP was interferon-inducible since levels of BiP mRNA and protein remained constant over time, while IFI6 mRNA and protein levels increased (Figure 7a). Maikke generated a CRISPR KO cell line lacking BiP expression and validated the results of the CRISPR screen. Maikke showed that BiP KO cells were more permissive to infection in the presence of interferon compared to NT cells, while in the absence of interferon BiP KO cells were more inhibitory to infection (Figure 7b). This phenotype suggests BiP plays both pro- and anti-viral roles as a chaperone to host factors that are required for or inhibitory to

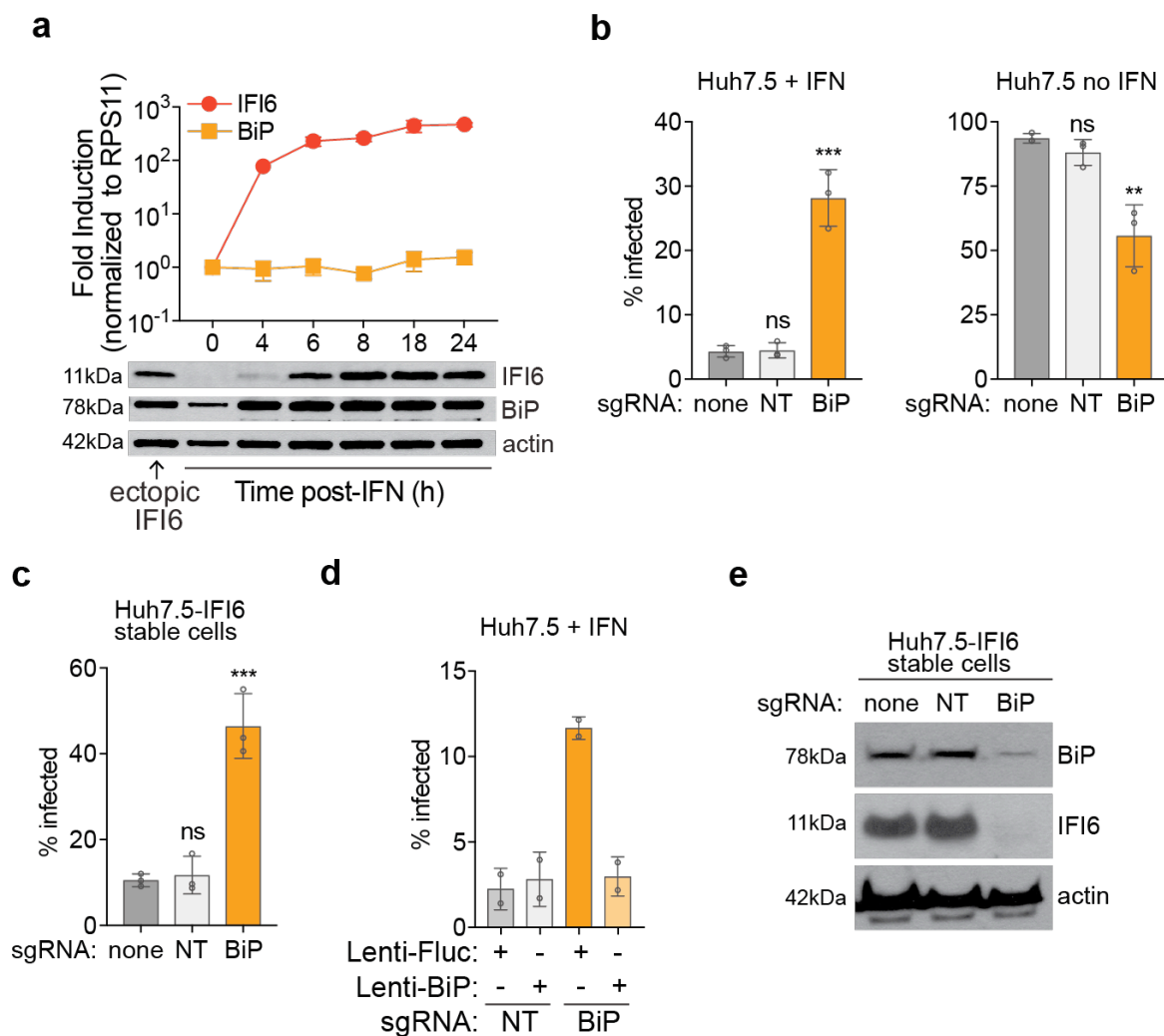


Figure 7: BiP is required for IFN-mediated and IFI6-mediated inhibition of YFV infection.

a, RT-PCR analysis of mRNA expression (top) and western blot analysis (bottom) of IFI6 and BiP in Huh7.5 cells treated with IFN over time. **b**, The effect of BiP knockout on YFV infection with (left) or without (right) IFN- α (100 U ml⁻¹) pre-treatment. **c**, The effect of BiP knockout on YFV infection in cells ectopically expressing IFI6. **d**, Restoration of IFN activity by BiP add back. **e**, Western blots correlating the loss of BiP expression by CRISPR targeting with the loss of ectopically expressed IFI6 in Huh7.5 cells stably expressing IFI6.

viral infection. Next, Maikke generated a BiP KO cell line in SCRPSY.IFI6 cells ectopically expressing IFI6. When these cells were infected, the cells were also more permissive to infection than the NT control, which correlates with the result seen when cells were pre-treated with IFN (Figure 7c). Importantly, when Maikke reconstituted BiP in KO cells by expressing a CRISPR-resistant BiP construct, she could restore the cell's IFN-response (Figure 7d). Surprisingly, when Maikke checked for efficient knockout of BiP in the SCRPSY.IFI6 cells by western blot, she observed that in addition to a KO of BiP, IFI6 was also not expressed despite being an ectopically expressed stable cell line (Figure 7e). Because BiP is known to have chaperone activity, Maikke hypothesized that BiP was a chaperone for IFI6.

IFI6 interacts with BiP in a chaperone-dependent manner

To observe an interaction between IFI6 and BiP, I performed a Co-IP (Figure 8a). I generated a SCRPSY.IFI6 3xFLAG cell line stably expressing a 3xFLAG-tagged version of IFI6, with the tag located at the C-terminus of the gene. I initially was unsuccessful in capturing the BiP-IFI6 interaction, until I removed DTT, a reducing agent, from the buffers of the Co-IP. Since BiP is a chaperone in the lumen of the ER and the lumen is an oxidizing environment, the DTT may have disrupted the interactions by breaking disulfide bonds. Additionally, BiP is a chaperone with ATPase-dependent activity (Gaut and Hendershot, 1993). When concentrations of ATP are low, interactions between BiP and its substrate last longer than when ATP concentrations are high. To demonstrate that BiP was interacting with IFI6 in an ATPase dependent manner and therefore as a chaperone, I also added

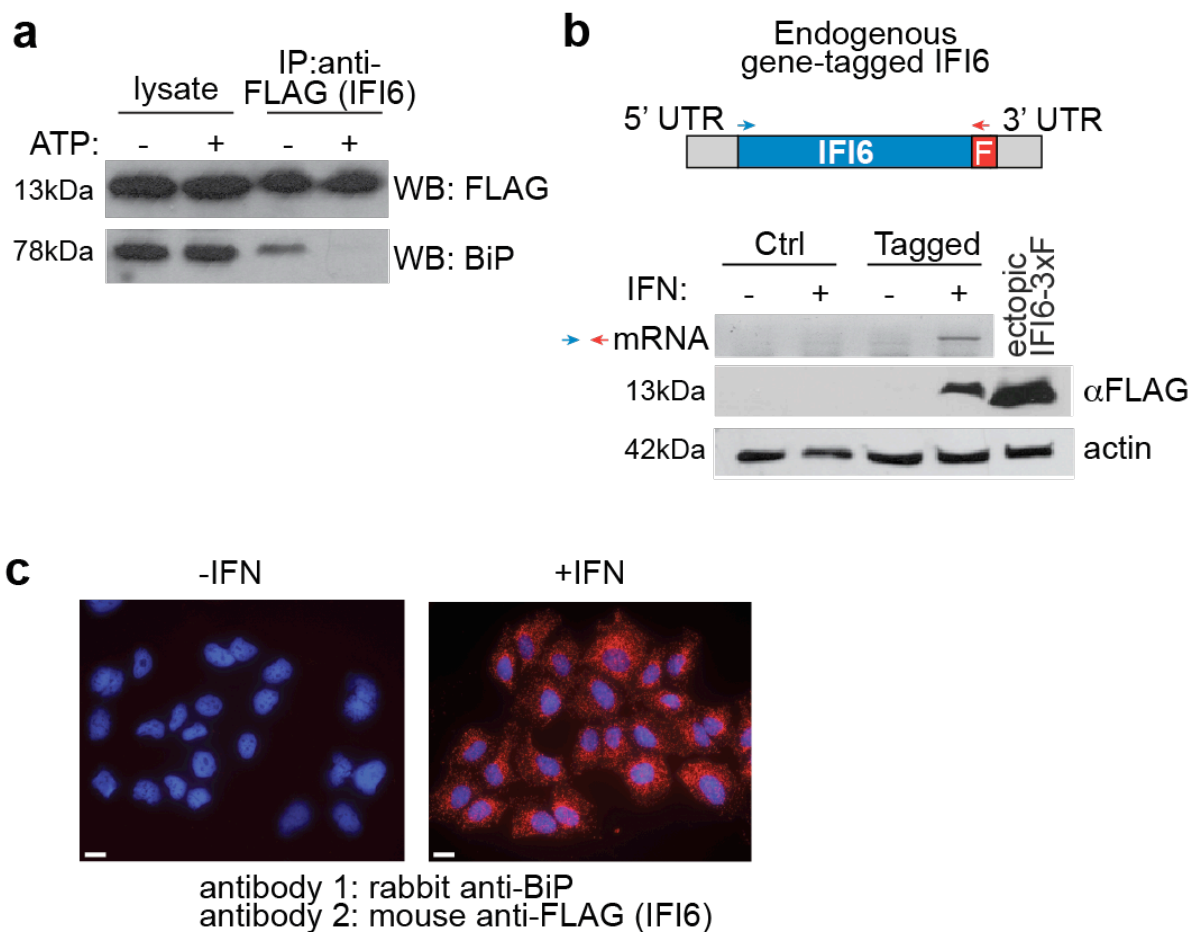


Figure 8: IFI6 binds BiP with overexpression and endogenous expression levels.

a, Co-immunoprecipitation of IFI6 3xFLAG and BiP, with or without the addition of 2mM ATP. **b**, The strategy used to genomically tag IFI6 with a 3xFLAG tag using CRISPR technology. arrows indicate direction and location of primers for RT-PCR. Expression of the endogenous tag was analyzed by mRNA and protein levels in the presence or absence of IFN. **c**, Proximity ligation assay in endogenously tagged U-2 OS cells using BiP and FLAG antibodies in the presence or absence of IFN.

2mM of ATP to one lysis condition to increase the turnover of substrates bound to BiP.

Using FLAG-antibody conjugated beads I immunoprecipitated the IFI6 3xFLAG and looked for BiP expression in the elution of the Co-IP. I observed that a small but consistent band of BiP was present in the elution, and with the addition of ATP this band disappeared. This supports the hypothesis that BiP is interacting with IFI6 as a substrate and therefore is a chaperone for IFI6. Additionally, the small amount of BiP that I observed in the elution suggests that once IFI6 is folded by BiP, an interaction no longer occurs. Since the majority of IFI6 is properly folded, this may explain why the interaction does not appear robust.

As an alternative approach I used a PLA to demonstrate BiP and IFI6 interaction (Figure 8c). A caveat of the Co-IP is that the IFI6-BiP interaction could be artificial due to overexpression. To address this possibility, I wanted to observe an interaction between BiP and IFI6 with endogenous expression levels. Because there are no commercially available antibodies towards IFI6 and the custom antibody I used for western blot experiments gave high background levels, I developed a different strategy. I generated a U-2 OS cell line where IFI6 was genomically tagged using CRISPR technology (Figure 8b). Briefly, the LentiCRISPR V2 vector with a guide sequence to the 3' end of the IFI6 gene was co-transfected with a puC19 vector containing the genomic sequence of IFI6 flanking the 3' end, with a sequence that was both CRISPR resistant and contained a 3xFLAG tag. Cells were selected with antibiotics and sorted into clones and screened for their FLAG expression with IFN treatment. I could detect IFI6 induction at the RNA and protein level using a FLAG antibody and primers that amplified the FLAG sequence. Using this cell line, I used the PLA protocol and recommended control conditions and observed an interaction between BiP and

endogenous IFI6, suggesting this interaction occurs with normal levels of IFI6 expressed with IFN treatment. PLA interactions appear as red punctae, and while I observed a few dim punctae under several control conditions, the punctae were more numerous and brighter when cells were IFN treated and probed with both a BiP and FLAG antibody.

Further support that BiP is required for expression of IFI6 came from CRISPR KO experiments performed by Maikke. Based on the literature, three mutants shown to attenuate the ATPase activity of BiP were overexpressed in the background of Huh7.5 cells lacking endogenous BiP (Gaut and Hendershot, 1993) (Figure 9a). Compared to cells where WT BiP was ectopically expressed to reconstitute endogenous BiP, IFI6 expression was lower, supporting observations made with the BiP-IFI6 Co-IP. Additionally, when cells were depleted of BiP but treated with the proteasome inhibitor MG132, levels of IFI6 remained stable, suggesting that IFI6 degradation is proteasome dependent if BiP chaperone activity is compromised (Figure 9b). Taken together, these data suggest that BiP was a significant hit in the CRISPR screen because its chaperone activity is required for proper expression of IFI6.

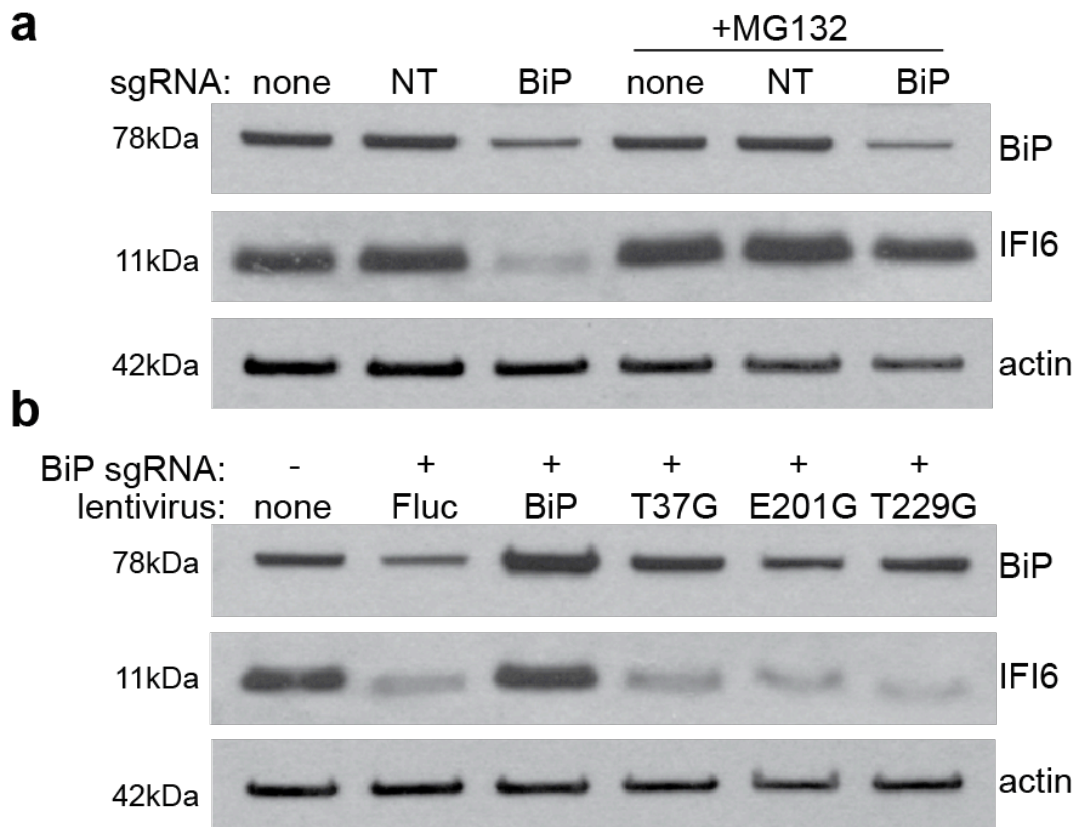


Figure 9: IFI6 is degraded in a proteasome dependent manner, and its expression depends on the ATPase activity of BiP.

a, Western blot illustrating the degradation of IFI6 in BiP depleted cells with or without the treatment of MG132. **b**, Western blot demonstrating the loss of IFI6 expression in endogenous BiP-depleted cells reconstituted with a WT BiP or BiP ATPase mutant.

CHAPTER FOUR

Results

IFI6 IS AN ER LOCALIZED PROTEIN THAT BLOCKS FLAVIVIRUS REPLICATION

Abstract

Since IFI6 was identified as a potent inhibitor of flavivirus infection and interacts with a luminal chaperone, BiP, the localization of IFI6 was investigated. IFI6 is also shown to be an ER-localized integral membrane protein despite reports of mitochondrial localization (Cheriyath et al., 2007; Cheriyath et al., 2018; Tahara et al., 2005). During flavivirus infection, IFI6 inhibits the viral life cycle at the step of replication and blocks the formation of flavivirus replication complexes. IFI6 is most effective when prophylactically expressed, consistent with a role as an ISG. Strikingly, IFI6 has no effect on any other RNA virus genus examined, including hepatitis C virus, a close genetic relative. These data suggest IFI6 functions to block specific membrane rearrangements induced by flaviviruses and represents a novel antiviral mechanism.

IFI6 is an ER-localized protein

Early reports that characterized IFI6 suggested IFI6 was a mitochondrial protein (Cheriyath et al., 2007; Tahara et al., 2005). A recent publication also suggests IFI6 might be expressed on the cell surface (Meyer et al., 2015). Given the potent phenotype towards ER-replicating flaviviruses and an interaction with the luminal chaperone BiP, I sought to confirm the localization of IFI6. Using overexpression of IFI6 3xFLAG in Huh7.5 cells, I

observed a reticular, network-like distribution that overlapped with expression of a luminal ER marker, Sec-61 β -mEmerald (Figure 10a). In an analogous experiment I did not observe colocalization with a mito-GFP marker, suggesting that IFI6 might indeed be ER-localized and not a mitochondrial protein (Figure 10a). Because these experiments used overexpression, I wanted to confirm the localization of endogenous IFI6 was also at the ER. I used the genomically tagged U-2 OS cells previously described to observe localization of IFI6. After IFN treatment, I observed an ER-like distribution and strong overlap of signal with the Sec-61 β -mEmerald marker (Figure 10b). To further demonstrate ER localization, I used immunogold labeling in COS-7 cells with an IFI6-HA overexpression construct (Figure 10c). I chose the HA tag and COS-7 cells since the FLAG tag and Huh7.5 were not suitable for the immunogold protocol. With the assistance of the UTSW Electron Microscopy Core the samples were processed for imaging. A control sample with no primary antibody added to determine background labeling of the gold nanoparticles was also imaged. The majority of the immunogold labeling localized to membranes of the ER and not to the mitochondria. A small number of nanoparticles can be seen adjacent to or very near mitochondria, but these cannot be explicitly defined as mitochondria-localized since the particles often also make contact with ER membranes. In support of this result, IFI6-HA did not colocalize with a mito-GFP marker in COS-7 cells when observed by immunofluorescence (Figure 10d).

Analysis of the IFI6 amino acid sequence predicts a signal peptide at the N-terminus, in the first 23 amino acids (Figure 11a). This is consistent with early sequence analysis of

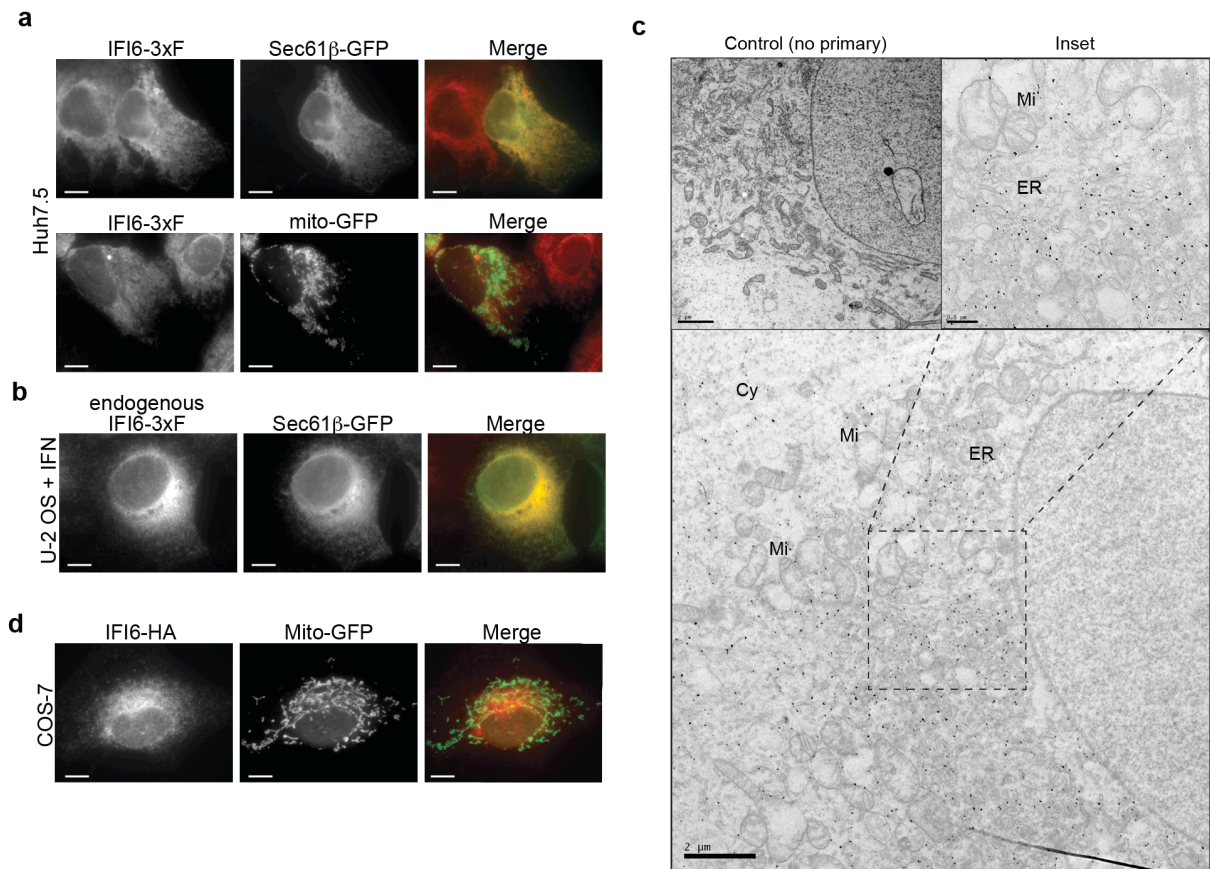


Figure 10: IFI6 is ER-localized in multiple cell lines.

a, Immunofluorescence of Huh7.5 cells ectopically expressing IFI6 3xFLAG transfected with Sec61 β -GFP or mito-GFP organelle markers. **b**, Immunofluorescence of endogenously tagged U-2 OS cells treated with IFN and transfected with the Sec61 β -GFP organelle marker. **c**, Immunogold labeling of COS-7 cells ectopically expressing IFI6-HA without (control) or with a primary HA antibody. **d**, Immunofluorescence of COS-7 cells ectopically expressing IFI6-HA and transfected with a mito-GFP organelle marker.

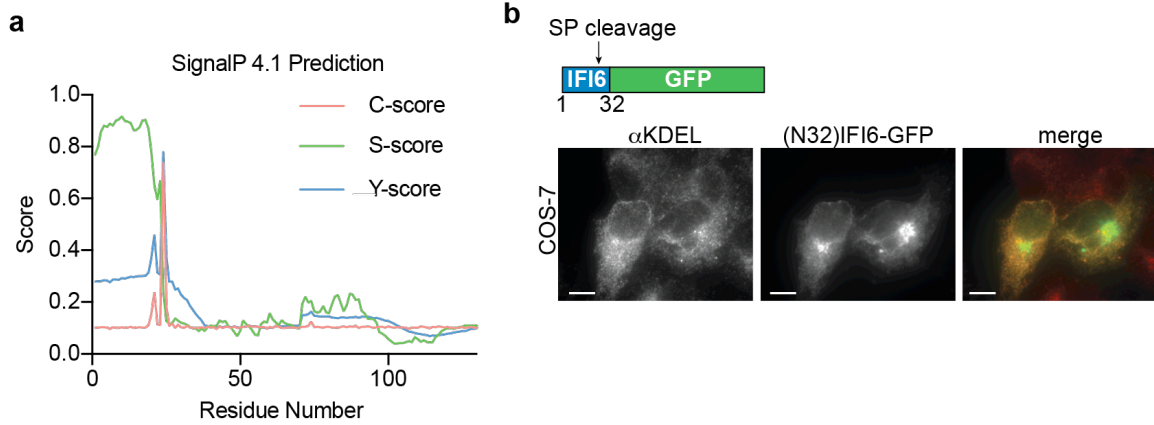


Figure 11: IFI6 contains an N-terminal signal peptide.

a, SignalP prediction of a signal peptide in the N-terminus of IFI6 amino acid sequence. **b**, diagram illustrating the construction of a GFP fused with the first 32 N-terminal amino acids of IFI6 (N32 IFI6-GFP)(top) and immunofluorescence of COS-7 cells transfected with the N32 IFI6-GFP and stained with a KDEL organelle antibody and a GFP antibody (bottom).

IFI6. Sequence analysis also suggests IFI6 is largely hydrophobic (Parker and Porter, 2004). To determine if the N-terminus of IFI6 contains a signal peptide with ER-localizing activity, the first 32 amino acids of the N-terminus of IFI6 was fused to GFP (N32-GFP) (Figure 11b). I expressed this construct in COS-7 cells and observed strong colocalization with the KDEL antibody signal by IF. This suggests that the N-terminus may act as a signal peptide required for localization to ER membranes.

IFI6 localizes to membranes and is a resident protein of the ER

To determine the relationship between IFI6 and membranes I performed a membrane flotation assay (Vogt and Ott, 2015) (Figures 12a, 12b). Briefly, Huh7.5 cells overexpressing IFI6-3xFLAG were gently lysed with PBS and sucrose with a Dounce homogenizer to maintain membrane integrity. These membranes were treated with several physical conditions to discern how IFI6 interacts with membranes. The membranes were then loaded onto an ultracentrifuge gradient in 30% histodenz or iodixanol at the bottom of the tube and layered with 20% and 10% gradient medium, creating three layers of the gradient. The tubes were ultracentrifuged and fractions were collected for analysis by western blot. The membrane flotation assay works by separating membranes based on their lipid content. In the least dense fraction at the top of the gradient, membranes with high lipid content will be present, and represent membranes from lipid droplets and proteins that interact with lipid droplets. In the middle fraction, membranes from endosomes and the ER are present, along with their respective proteins. In the densest fraction, proteins that are either soluble or in an

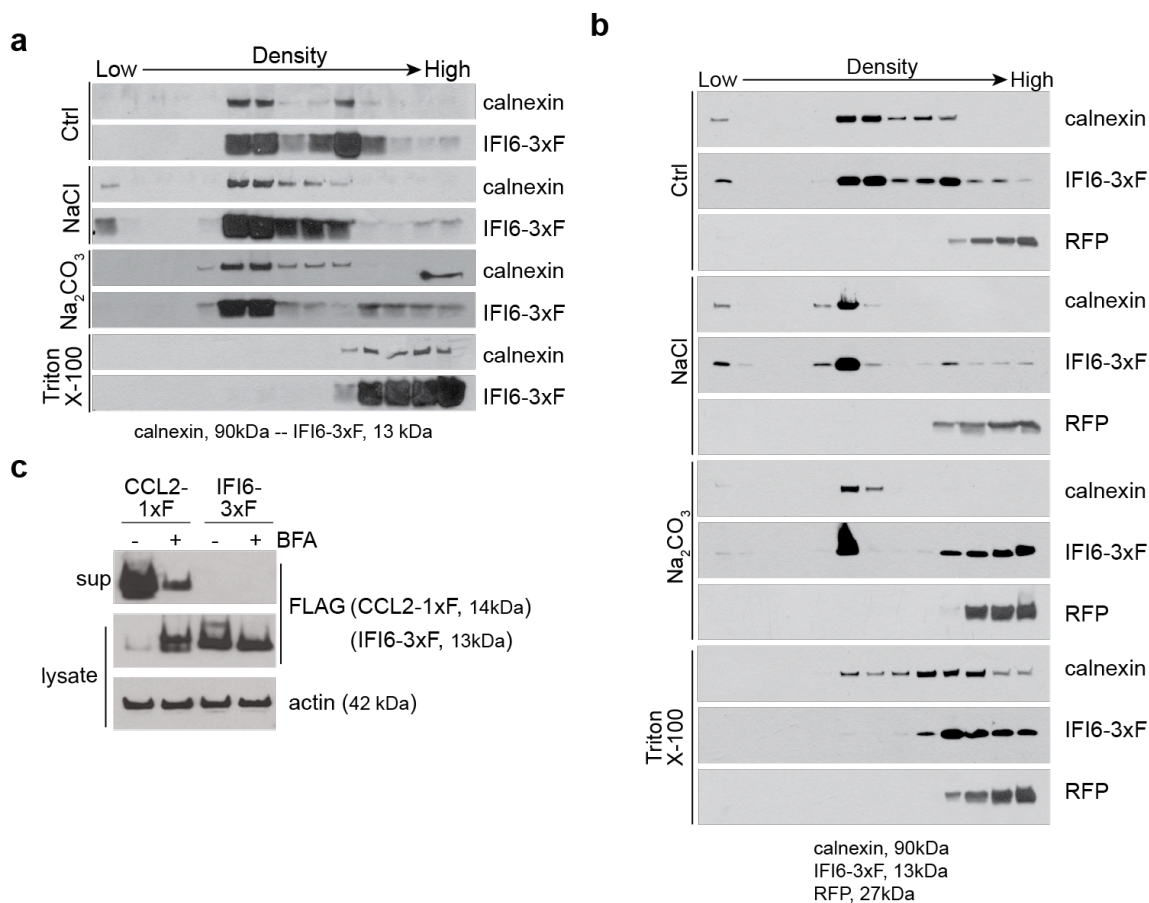


Figure 12: IFI6 is an integral membrane protein and is not secreted.

a, Western blot showing a membrane flotation assay with a Histodenz gradient of Huh7.5 cells ectopically expressing IFI6 3xFLAG, untreated or treated with 1M NaCl, 0.1M Na₂CO₃ pH 11 or 0.5% Triton-X100. Lysates were probed with calnexin or FLAG. **b**, Western blot showing a membrane flotation assay with an iodixanol gradient of Huh7.5 cells ectopically expressing IFI6 3xFLAG, untreated or treated with 1M NaCl, 0.1M Na₂CO₃ pH 11 or 0.5% Triton-X100. Lysates were probed with calnexin, FLAG, or RFP. **c**, Western blot depicting a secretion assay. 293T cells were transfected with CCL2-1xF or IFI6 3xF and left untreated or treated with Brefeldin A. Supernatants and lysates were probed with FLAG antibody or actin.

aggregate will be present, and represent proteins that do not associate with membranes. I used calnexin as a marker for the ER and endosomal membrane fractions.

In conditions with no chemical treatment, I observed that IFI6 co-migrated with calnexin, suggesting IFI6 does interact with membranes. In a separate replicate I also observed that RFP that is co-expressed from the SCRPSY.IFI6 3xFLAG vector did not migrate in this fraction, but remained in the soluble/aggregate fraction, suggesting the proteins migrated in the gradient as predicted (Figure 12b). In addition, I also treated cells with a variety of conditions designed to determine how proteins associate with membranes by causing them to dissociate. I incubated lysate with 1 M NaCl, 0.1 M sodium carbonate pH 11 or with 0.5% Triton-X 100 and loaded the lysate onto the column as previously described. The NaCl treatment should remove proteins from the endosomal/ER fraction if the proteins associate with membranes through ionic interactions with other membrane-associated proteins. Similarly, the carbonate treatment eliminates proteins that associate with the membrane because of interactions with peripheral proteins. Finally, the treatment with Triton-X 100 should solubilize all membrane proteins, including calnexin.

I observed that in the salt and carbonate treatments, most of the IFI6 and calnexin signal remained in the ER/endosomal fraction, suggesting IFI6 does not primarily associate with the membrane because of ionic or peripheral protein interactions. Interestingly, some IFI6 did leave the ER/endosomal fraction with carbonate treatment suggesting that some of the IFI6 membrane interaction depends on pH or interaction with other proteins. Alternatively, the carbonate treatment has also been shown to cause microsomes to flatten into sheets, suggesting that if proteins interact with a membrane because of a high degree of

curvature it may also dissociate from the membrane with this treatment (Fujiki et al., 1982). Lastly, in the Triton-X 100 treatment both IFI6 and calnexin dissociated from the membranes. Because the majority of IFI6 only dissociated from membranes with Triton-X 100 treatment, I conclude that IFI6 is an integral membrane protein.

Because IFI6 showed localization to the ER, I wanted to confirm that IFI6 was not localized to the secretory pathway, since secretory membranes are derived from ER membranes. A secretion assay using a CCL2-1xFLAG expression construct as a positive control or a plasmid expressing IFI6 3xFLAG was transfected into 293T cells. Supernatants and cells were collected and analyzed by western blot. CCL2 was readily detectable in the supernatant, while IFI6 was absent (Figure 12c). With Brefeldin A treatment, which blocks transport of vesicles from the ER to the Golgi, CCL2 was lowly detectable in the supernatant, but more abundant in the lysate, suggesting secretion had been blocked. Regardless of Brefeldin A treatment, IFI6 was only detectable in the lysate, suggesting that IFI6 is not part of the secretory pathway and is a true ER resident protein. Taken together, these data support the idea that IFI6 is an ER-localized protein and may not be predominantly localized to the mitochondria as previously reported.

IFI6 inhibits flavivirus replication

Since I observed a strong inhibitory phenotype against flaviviruses and had confirmed the ER-localization of IFI6, I wanted to determine which step(s) of the viral life cycle was targeted by IFI6. Using a DENV-Fluc reporter virus I observed no inhibition at early timepoints in the viral life cycle that correspond to the translation phase, which occurs

between 2-6 hours post infection (Figure 13a). However, I saw a significant inhibition during the replication phase of the virus, occurring between 24-72 h post infection. This result was supported by a similar experiment with a YFV-RLuc2A replicon (Figure 13a). Because there was no difference in the luciferase activity at timepoints collected during the translation phase, I am inferring, but did not directly test, that early steps in the life cycle were not affected, such as viral attachment and entry.

There are several hallmarks of the replication phase for RNA viruses that can be observed through microscopy. I infected cells with YFV-17D and used a dsRNA antibody to visualize the presence of dsRNA which is only produced during the replication phase (Figure 13c). I could readily detect numerous punctae in the infected control cells, while at the same timepoint in IFI6 cells the dsRNA punctae were nearly absent. If punctae were present, they were dimmer suggesting a lower level of dsRNA present or less efficient replication. Another indication of viral replication is the formation viral replication complexes. These complexes induce dramatic changes of the ER membrane architecture, creating an organelle-like structure where replication machinery and viral RNA are hidden from host cytoplasmic sensors (Paul and Bartenschlager, 2015). The mechanistic details of the formation of these complexes is not known. However, mutation or deletion of non-structural proteins thought to be involved in the formation of the complexes significantly impairs replication (Scaturro et al., 2015). This suggests the formation of these complexes is essential for robust viral replication. I infected Huh7.5 cells stably expressing IFI6 or a control vector with YFV-17D and submitted these cells for processing at the UTSW Electron

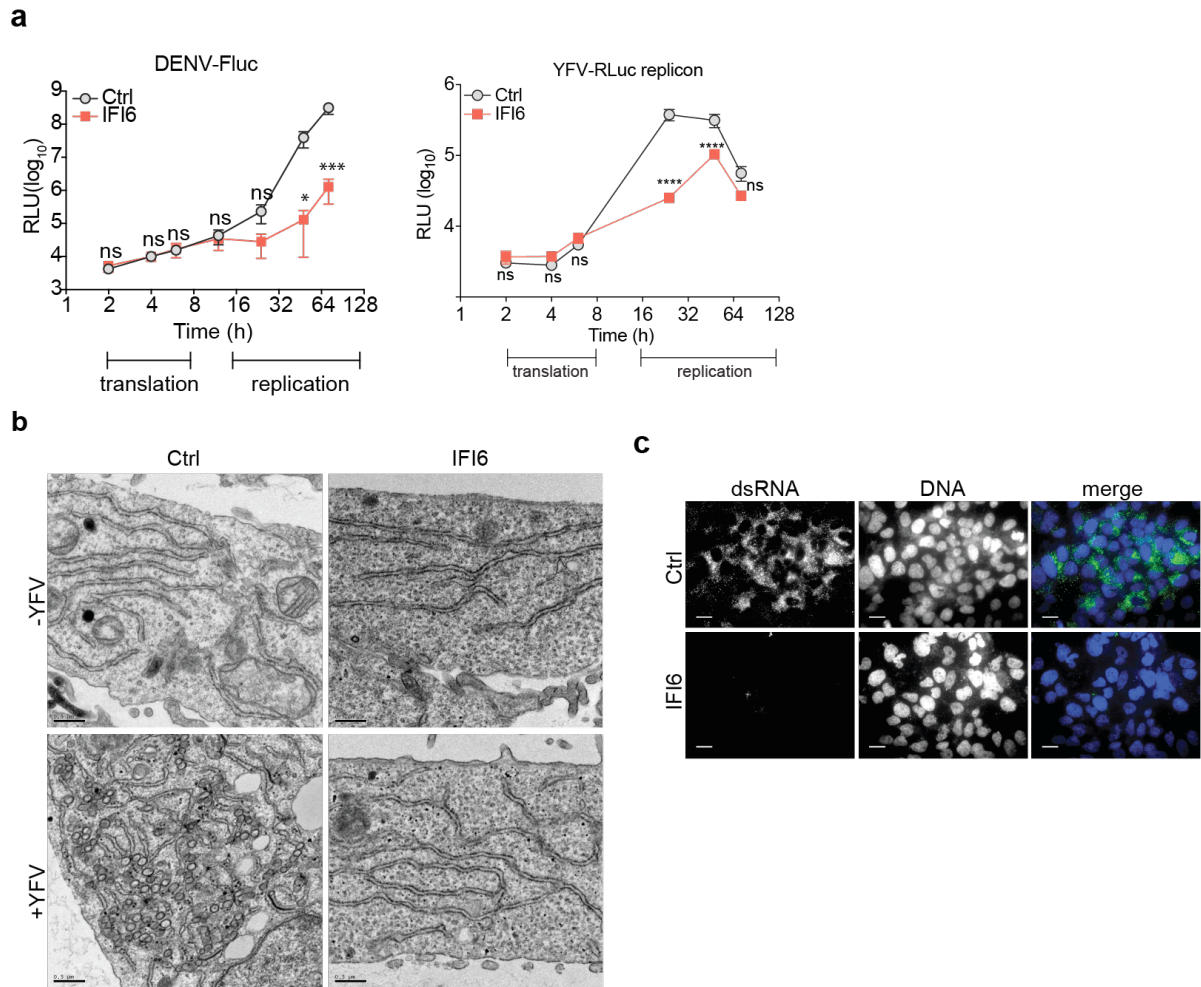


Figure 13: IFI6 inhibits flavivirus replication.

a, Huh7.5 cells stably expressing control or IFI6 were infected with DENV-Fluc virus (left) or transfected with YFV-RLuc (right) and luciferase relative light units were measured. **b**, TEM showing control or IFI6 stable Huh7.5 cells infected or uninfected with YFV-17D. **c**, STAT1^{-/-} fibroblasts expressing Ctrl or IFI6 were infected with YFV-17D and stained with a dsRNA antibody.

Microscopy Core. I observed that control cells readily formed numerous replication complexes, while these complexes were absent in IFI6-expressing cells (Figure 13b). I also examined the ER morphology in these cells to ensure that IFI6 expression was not altering the ultrastructure of the ER. In both cell types, the ER appeared normal.

I also checked steps immediately upstream of the replication phase of the viral life cycle to confirm that those steps were intact. Jennifer Eitson confirmed that the DENV NS2B-NS3 viral protease was also not affected by IFI6 expression, since the WT NS2B-NS3 protease was able to cleave STING in the presence of IFI6 (Figure 14a). As a positive control for inhibition of STING cleavage, a NS2B-NS3(S135A) mutant unable to cleave STING was also tested, and STING was not cleaved in the presence of this viral protease. Similarly, using SPCS1 KO cells generated by the Diamond lab, John Schoggins showed that 293T cells expressing varying amounts of IFI6 had equal levels of DENV infection, suggesting IFI6 does not affect host proteases required for polyprotein processing. John examined cleavage of both DENV 2K-NS4B cleavage and DENV C-pRM cleavage, both shown to be mediated by SPCS1 (Figure 14b, c). Neither of these cleavage events were affected by the presence of IFI6. Together, these data suggest IFI6 does not affect the activity of host and viral proteases required for polyprotein processing, a step in the viral life cycle which occurs immediately before replication begins.

IFI6 must be expressed prior to viral infection and acts prophylactically

A caveat of all the experiments described above is that IFI6 expression occurred before cells encountered a virus. Therefore, it is possible that IFI6 inhibits replication by two

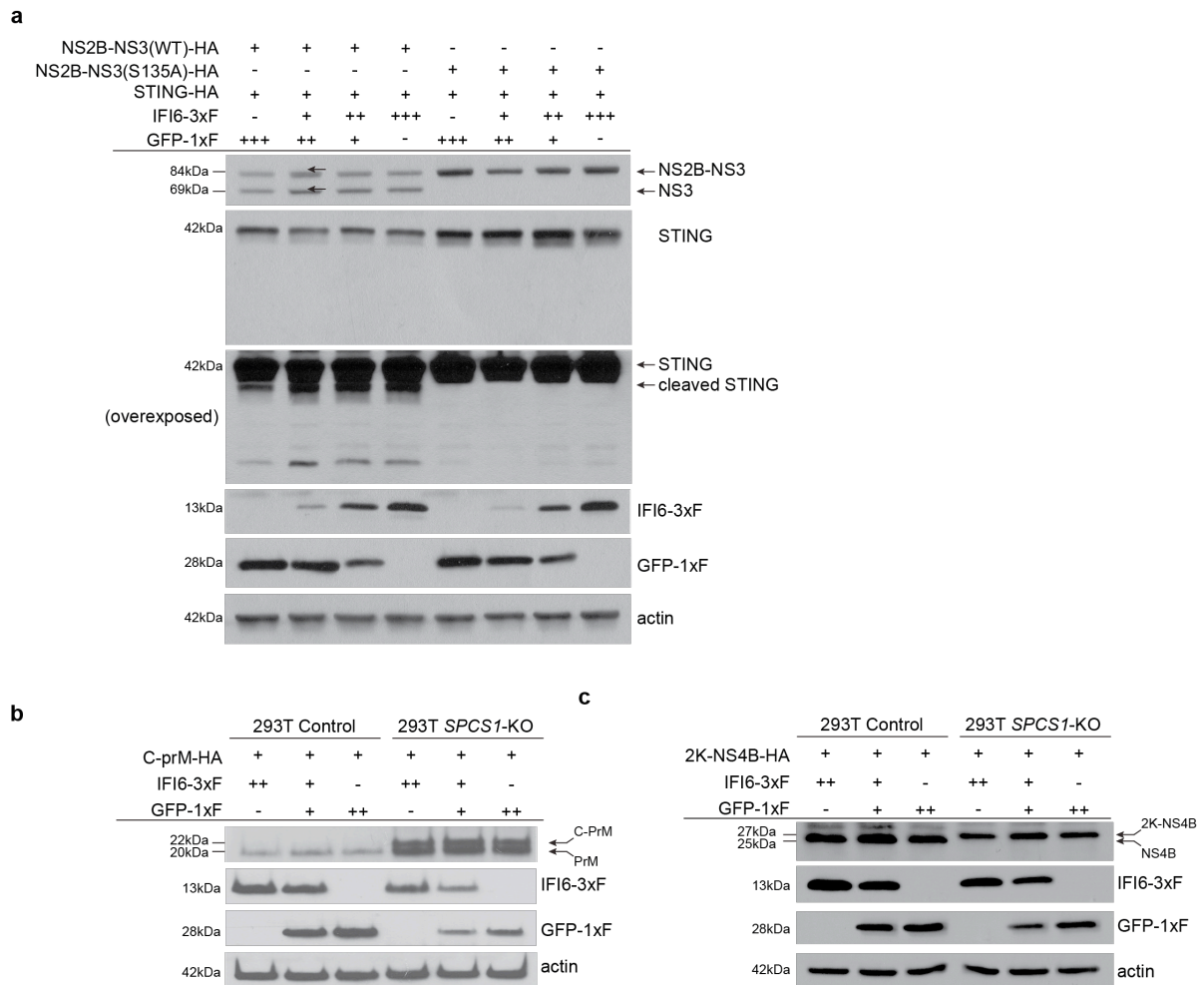


Figure 14: IFI6 does not affect viral or host protease activity.

a, Western blot of 293T cells transfected with a WT or mutant DENV NS2B-NS3-HA protease, STING-HA, and titrating amounts of IFI6 3xF with a GFP 1xF to normalize plasmid amounts. **b,c** 293T control or *SPCS1*-KO cells were transfected with C-prM-HA (b) or 2K-NS4B-HA (c) and titrating amounts of IFI6 3xF with a GFP 1xF to normalize plasmid amounts.

mechanisms. The first possibility is that IFI6 inhibits replication which leads to the loss of formation of replication complexes. Alternatively, IFI6 could be preventing the formation of replication complexes, which leads to a loss of viral replication. One way to test this is to determine if IF6 can block ongoing replication by expressing IFI6 after replication has begun. I developed a strategy to lentivirally transduce IFI6 or control lentivirus into cells 24 h, 8 h, or 4 h before infection, simultaneous with infection, 4 h or 8 h after infection (Figure 15a). I infected cells at time 'zero' relative to transduction, and allowed cells to infect for 48 h. This is longer than a single replication cycle, but I observed that lentivirus transduction attenuated infection even in control cells, so I allowed the infection to spread so that all cells were infected in the control cells at the end of the experiment. I collected cells for flow cytometry and quantified infection (Figure 15b). In a parallel experiment I also collected cells for western blot analysis to measure expression of IFI6 and viral proteins (Figure 15b). I observed that at all timepoints, control cells were infected to approximately the same levels. NS1 expression appears slightly lower in cells transduced earlier in the timecourse, possibly due to the attenuation effects of lentivirus transduction. In IFI6 cells I observed a gradual increase in the amount of infection as I transduced the cells closer to the time of infection. For cells transduced after infection I saw that these cells were nearly all infected. Importantly, at 48 hpi all cells were expressing the same levels of IFI6 despite having differing amounts of infection. This suggests that IFI6 must be present prior to viral infection to be inhibitory, and cannot overcome viral infection once established.

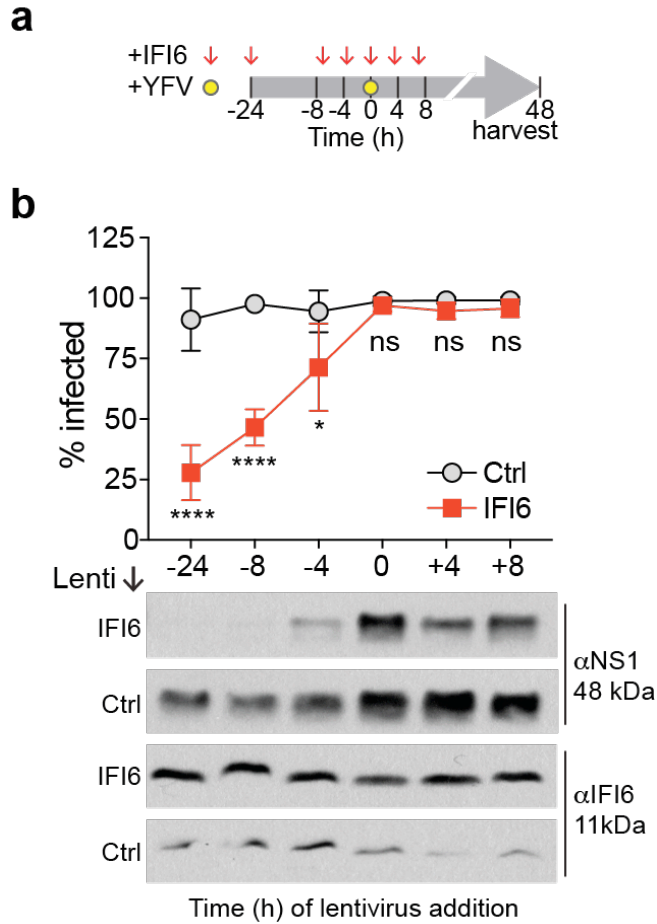


Figure 15: IFI6 prophylactically blocks viral replication.

a, Schematic of time of addition experiment. Red arrows indicate time of IFI6 transduction relative to yellow fever infection shown as a yellow circle. Cells were harvested 48 hours post infection. **b**, (top) Quantification of YFV infectivity in time of addition experiments (bottom) Western blot showing protein levels for YFV NS1 and IFI6 in time of addition experiments at 48 hpi.

IFI6 colocalizes with NS4B but does not bind NS4B

One possibility for explaining how IFI6 inhibits viral replication is viral proteins required for replication are sequestered away from the site of replication. To test this hypothesis, I infected Huh7.5 cells stably expressing IFI6 3xFLAG with a high MOI of DENV. This protocol partially overcomes the inhibitory effects of IFI6, allowing me to observe cells expressing both IFI6 and viral proteins. I, with the assistance of Abhijit Bugde, imaged these cells using confocal microscopy in the UTSW Live Cell Imaging Core. I visualized the localization of IFI6 with an anti-FLAG antibody. I also examined the localization of DENV NS4B, a transmembrane non-structural protein known to be localized to sites of viral replication. In several cells, I observed strong colocalization between the FLAG signal (IFI6) and NS4B signal. (Figure 16a). I analyzed the confocal images using Imaris software to determine a Pearson coefficient for each cell, and found that most cells had a coefficient greater than 0.5, suggesting a good colocalization (Figure 16b). While flavivirus replication occurs at the rough ER, NS4B has been observed in large punctae in the peripheral ER of infected cells. Whether these large punctae are important for replication is unknown. I used these punctae to more easily observe the colocalization between IFI6 and NS4B (Figure 16a, cell 2). These data suggest IFI6 does not inhibit viral replication by relocalizing viral proteins to distal sites where they are unable to generate replication complexes.

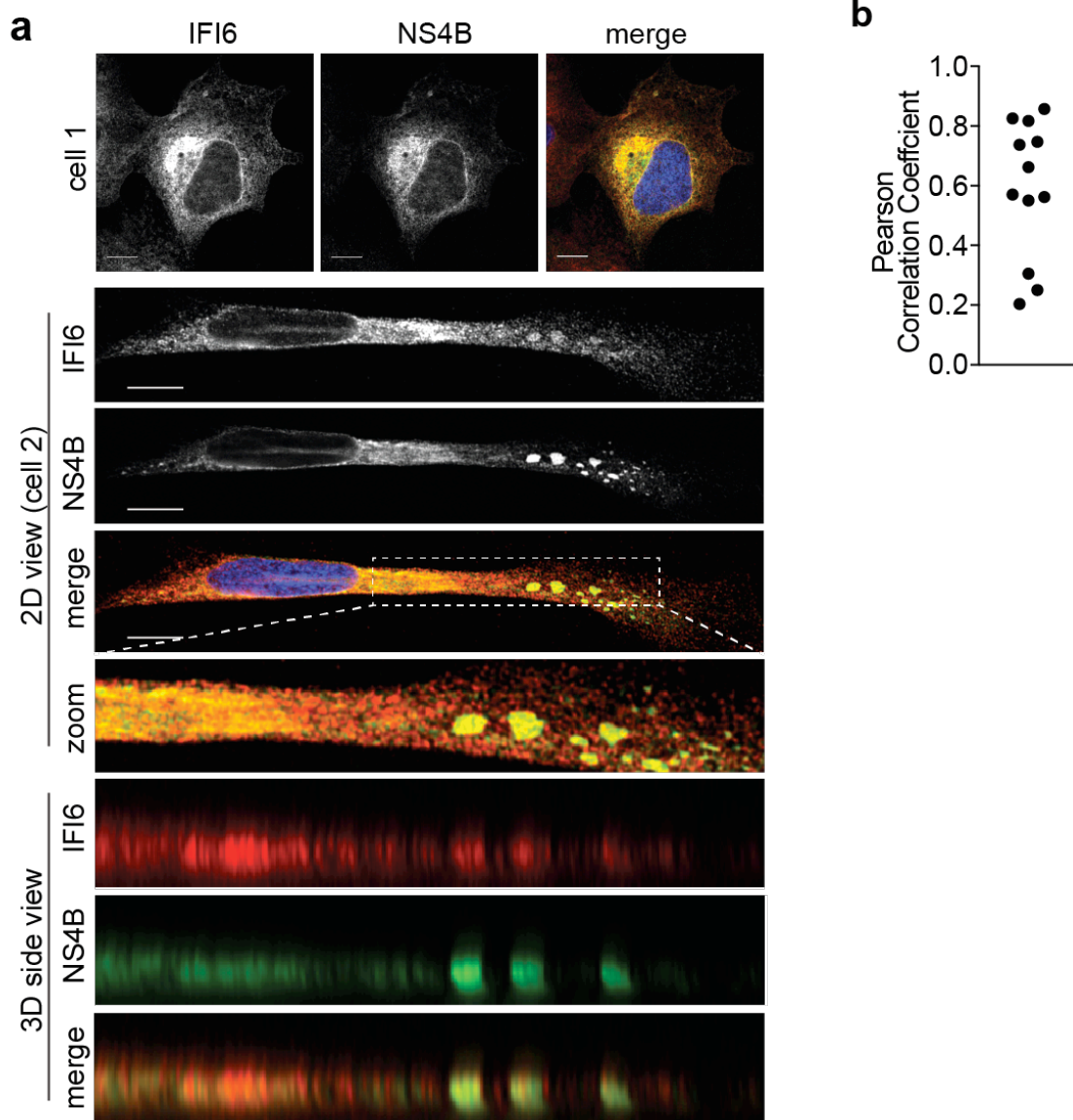


Figure 16: IFI6 colocalizes with DENV NS4B

a, Representative confocal microscopy images of Huh7.5 cells stably expressing IFI6 3xFLAG and infected with DENV. Cells were stained with FLAG antibody and DENV NS4B antibody.

b, Pearson coefficients for NS4B and IFI6 colocalization in 12 cells.

Because IFI6 and NS4B exhibited strong colocalization, I sought to confirm if these proteins interact. I included another non-structural protein known to be required for replication and localized to sites of replication, NS1. I attempted to Co-IP IFI6 3xFLAG with a YFV2K-NS4B-HA or YFV NS1 construct. Alternatively I used a high MOI infection with DENV and a DENV NS4B antibody, however I was unable to confirm an interaction in either of these scenarios (Figures 17a, 17b). I also attempted to chemically crosslink cells expressing 2K-NS4B-HA and was unable to confirm an interaction (Figure 17c).

While I cannot rule out that Co-IP conditions were not suitable to capture this interaction, these data suggest that these proteins, while strongly colocalized, may not physically interact with each other.

IFI6 does not inhibit other RNA viruses

I next wanted to determine if other viruses that utilize the ER for replication were susceptible to the antiviral effects of IFI6. HCV is a close genetic relative to flaviviruses and also utilizes ER membranes for replication. I observed that overexpression of IFI6 did not significantly inhibit HCV replication despite previous literature reports of an inhibitory effect (Figure 18a). I confirmed this phenotype with several HCV viral constructs: a HCV virus expressing a GFP variant (HCV-Ypet), a HCV virus with a Gaussia luciferase reporter (HCV- Gluc), and a HCV replicon expressing Gaussia luciferase (Figures 18c, 18d) . The HCV-Gluc virus and the HCV-Gluc replicon were both susceptible to IRF1, a broadly acting antiviral factor, but not to IFI6. Additionally, Jennifer Eitson generated a secondary knockout line and treated the cells with IFN. She observed that with or without IFN treatment, IFI6 KO cells were equally permissive to HCV infection as NT control cells, suggesting IFI6 does

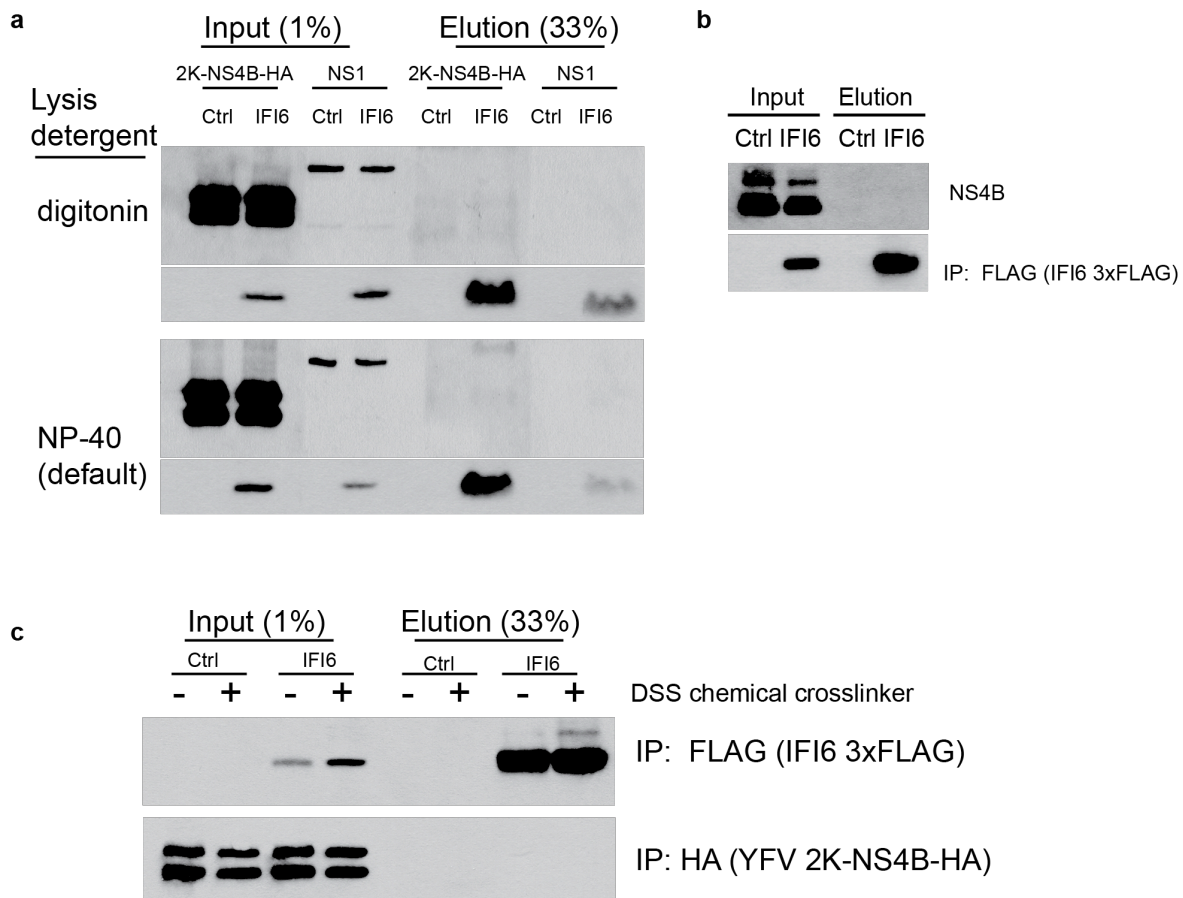


Figure 17: IFI6 does not bind NS4B or NS1.

a, Western blot depicting co-immunoprecipitation of Huh7.5 cells stably expressing IFI6 3xFLAG as bait and YFV 2K-NS4B-HA or YFV NS1. IFI6 3xFLAG was used as bait and lysis conditions used either digitonin (top) or NP-40 (bottom). **b**, Co-immunoprecipitation of Huh7.5 cells stably expressing IFI6 3xFLAG infected with DENV. IFI6 3xFLAG was used as bait and samples were probed with a DENV NS4B antibody. **c**, Western blot depicting co-immunoprecipitation of Huh7.5 cells stably expressing control or IFI6 3xFLAG as bait and YFV 2K-NS4B-HA. Prior to lysis cells were untreated or treated with DSS, a chemical crosslinker.

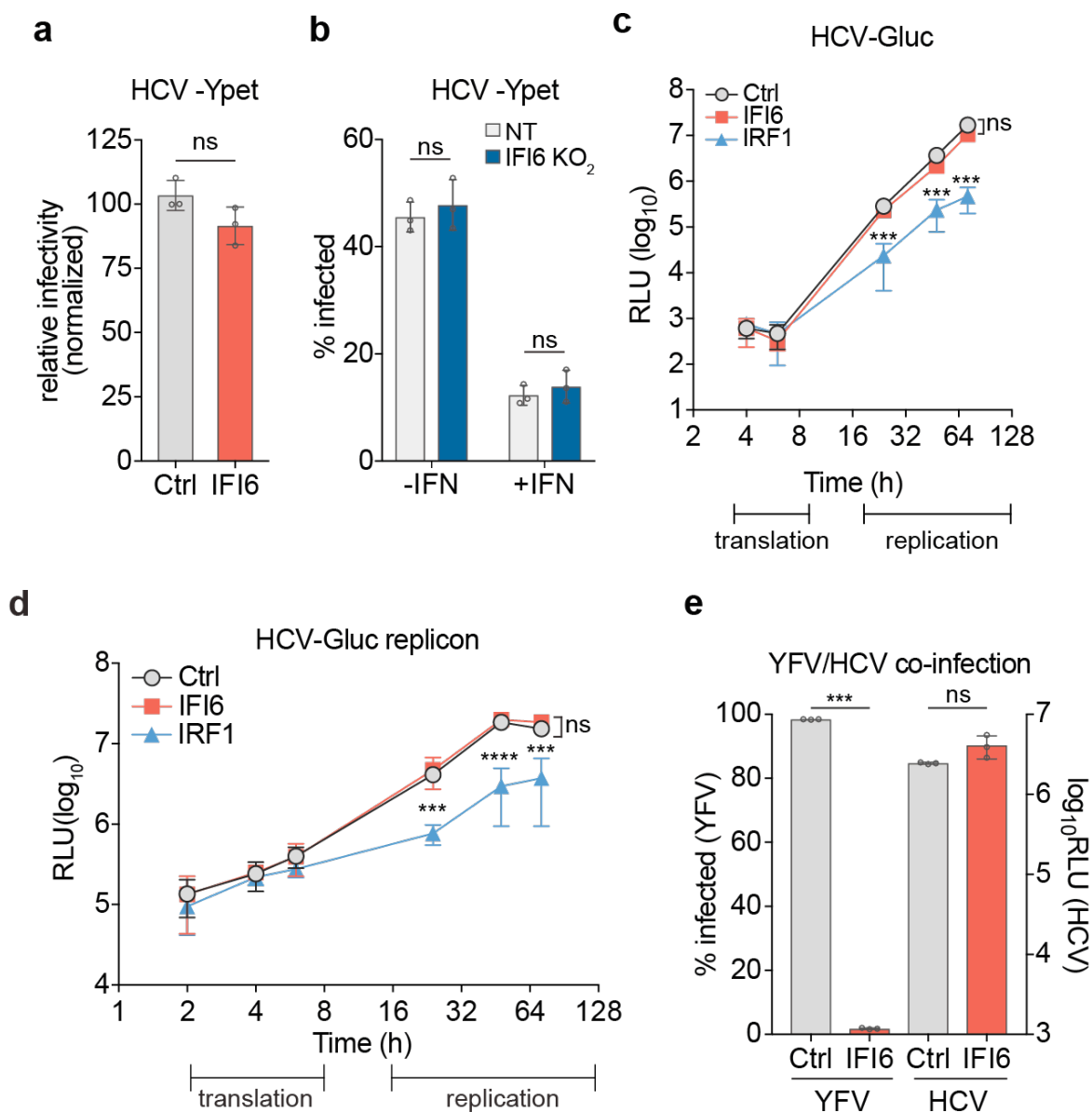


Figure 18: IFI6 does not inhibit HCV replication.

a, b Huh7.5 cells overexpressing (a) or lacking (b) IFI6 were infected with HCV-Ypet. In **b**, cells were either untreated or treated with IFN. **c, d**, Quantification of HCV-Gluc virus infectivity (c) or HCV Gluc replicon activity by relative light units in Huh7.5 cells expressing empty control, IFI6, or positive control for inhibition IRF1. **e**, Quantification of co-infection of YFV-Venus and HCV-Gluc in Huh7.5 cells expressing control or IFI6. YFV infectivity is quantified on the left axis, HCV infectivity is quantified on the right.

not play a role in the IFN response to HCV (Figure 18b). This also suggests that IFI6 has an extremely specific antiviral activity.

Since previous reports showed an inhibitory effect of IFI6 against HCV I wanted to further confirm that IFI6 was not inhibiting HCV. One reason HCV may not be inhibited by IFI6 is because HCV antagonizes the antiviral function of IFI6. If this is true, then a co-infection with a susceptible virus would reveal this activity. To determine the specificity of IFI6, I designed a co-infection experiment using YFV-Venus and HCV Gluc. I infected Huh7.5 cells stably expressing IFI6 or control (Figure 18e). I collected the cells for flow cytometry to quantify YFV infectivity and since Gaussia luciferase is secreted, I collected supernatant to measure HCV infectivity. I observed that YFV was strongly inhibited in cells stably expressing IFI6, but not in control cells. Importantly, HCV replicated to equal levels between control and IFI6-expressing cells. This suggests IFI6 has a very targeted antiviral activity and even viruses that utilize the same membranes for replication complex formation are not inhibited by IFI6.

I also tested another virus known to use ER membranes for replication, human coronavirus (CoV). I found that CoV was not inhibited by IFI6 (Figure 19a). I also tested a dose response against a panel of other diverse RNA viruses, CVB, SINV, and MeV (Figure 19b). CVB and SINV replicate using ER and Golgi-derived membranes while MeV replicates in the cytoplasm. None of the viruses I tested were affected by IFI6, further supporting the specificity of the antiviral activity of IFI6. Taken together, this data supports a model whereby IFI6 inhibits a specific group of flaviviruses, but not other viruses that utilize ER membranes for replication.

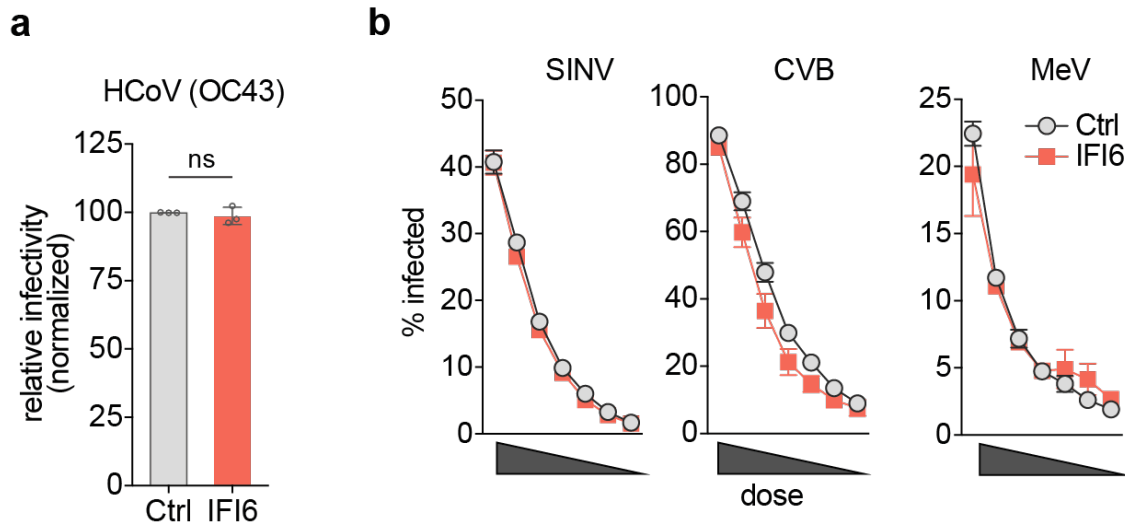


Figure 19: IFI6 does not inhibit replication of other RNA viruses.

a, Huh7.5 cells stably expressing control or IFI6 were infected with HCoV. Cells were antibody stained for the envelope protein and infection was quantified by FACS. **b**, Quantification of infectivity for SINV, CVB, and MeV dose response in Huh7.5 IFI6 stable cells.

Model for IFI6 antiviral activity

The data presented in Chapter 3 and Chapter 4 support a model where IFI6 is potentially antiviral to a specific genus of virus, Flavivirus (Figure 20). IFI6 was identified as a top hit in a CRISPR screen identifying several host factors required for an antiviral response to YFV. The chaperone BiP was another significant hit in the screen. I have demonstrated that these proteins interact, and that BiP is required for expression of IFI6. Importantly, despite previous literature reporting IFI6 to be mitochondria-localized, I have shown IFI6 is an integral membrane protein localized to the ER, the site of flavivirus replication. I have also shown that IFI6 acts during the replication phase of the life cycle to block formation of replication complexes of flaviviruses, but other viruses that replicate using ER membranes, such as HCV are unaffected. This specificity may be due to the differences in the membrane architecture, where flaviviruses bud inwards towards the ER lumen and induce negative curvature; HCV buds outwards into the cytoplasm and induce positive curvature. Finally, IFI6 must act prophylactically in order to be effectively antiviral. Currently, the mechanistic details are not clear, but future ideas for experiments will be discussed in the following chapter.

Inconclusive Data

In other efforts to identify a mechanism for how IFI6 blocks replication, I attempted several experiments which yielded inconclusive results, but felt it was necessary to include the data to allow for discussion of these results. To determine if a mutant virus could overcome the IFI6 block on replication, I performed a serial passaging experiment (Figure

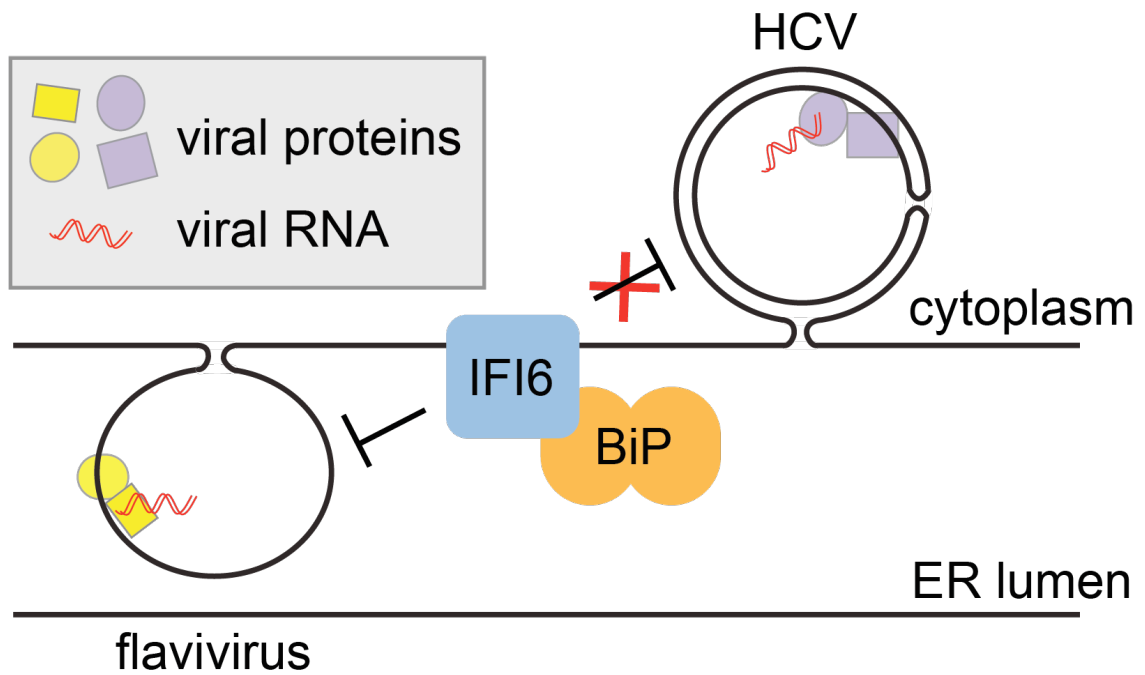


Figure 20: Model of IFI6 specific antiviral activity.

IFI6 is localized to the ER membranes with the help of its chaperone, BiP. Here, it can block the formation of replication complexes formed by flaviviruses which bud inwards into the lumen, but cannot inhibit the formation of other types of replication complexes such as the complexes formed by HCV which bud outwards into the cytoplasm.

21a). I infected IFI6 or control Huh7.5 cells with YFV-17D at a MOI of 1 and allowed the virus to undergo 2 rounds of replication, since I had previously observed this strategy allowed for high titers of virus. I passaged the virus 20 times, and plaqued the virus at every 5th passage. I did not observe a mutant virus emerge from IFI6-expressing cells, suggesting the block in replication could not be overcome. The titers of virus gradually dropped over time, and eventually fell below the limit of detection. Interestingly, in the control cell line, the virus titers dropped slightly over time, to approximately one log of virus lower than in the first passage. Overall, this suggests IFI6 effectively blocks viral replication, and cannot be overcome by a mutant virus under these conditions.

In other attempts at defining a mechanism, I overexpressed a non-structural viral protein, YFV NS1, YFV NS4A, or YFV NS4B together with IFI6 to determine if the antiviral effect of IFI6 could be overcome (Figure 21b). I chose these proteins since they have been previously speculated to be involved in formation of the replication complexes. I overexpressed each protein in cell lines stably expressing IFI6, and infected these or control cells also expressing the non-structural protein with YFV-Venus. I observed that these proteins did enhance infection in the IFI6 stable cells, but also enhanced infection in the control cells. I also did not observe a specific enhancement with a particular non-structural protein, suggesting this enhancement of infection is not specific to IFI6 and may generally enhance infection by increasing protein expression. Interestingly, YFV was able to eventually infect all IFI6 expressing cells, suggesting that the virus can overcome IFI6 if viral protein expression if viral protein levels reach sufficient levels.

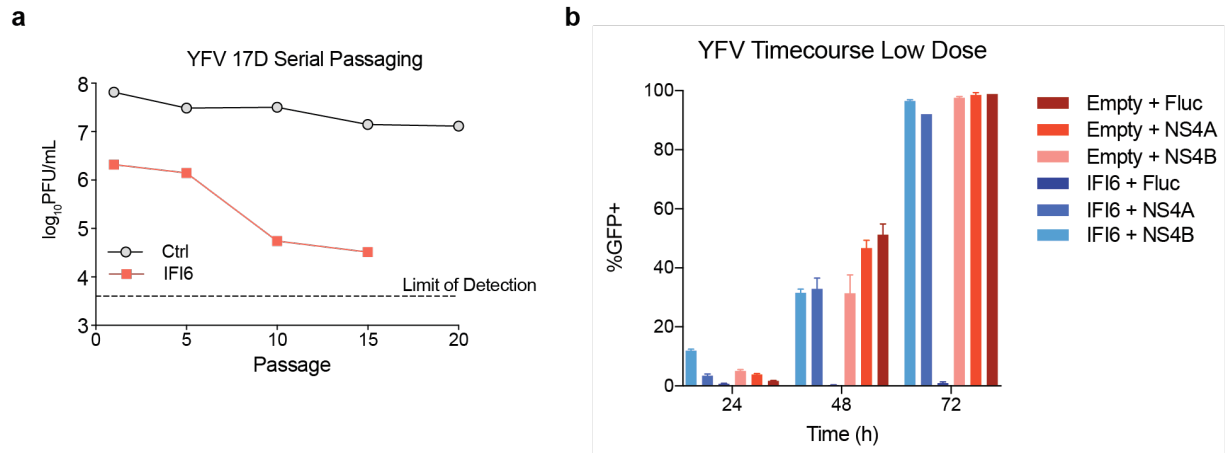


Figure 21: YFV cannot overcome the IFI6 inhibition with a viral mutant, and viral proteins cannot specifically antagonize IFI6.

a, Quantification of plaque assay with YFV serially passaged 20 times in Huh7.5 stable cells expressing control or IFI6. **b**, Huh7.5 stable cells expressing control or IFI6 were transduced with a Fluc control, YFV NS4A or YFV NS4B and infected with YFV-Venus. Cells were collected at indicated timepoints and infection was quantified by FACS.

In addition to manipulating viral proteins, I also attempted several host factor screens that were not successful. I attempted to screen a hORF cDNA library generated by the Alto lab where every gene in the human genome was overexpressed. This screen assumed that the virus needed a specific host pathway that IFI6 was interfering with, and by overexpressing the respective host genes, the virus could overcome the effect of IFI6. Ultimately, the screen gave no positive results.

In a complementary approach to the overexpression screen, I also attempted a genome-wide CRISPR knockout screen. The rationale for the CRISPR screen assumed that IFI6 utilized a host pathway to inhibit viral infection, and by knocking out components of the pathway infection could be restored. The screen used a similar experimental strategy to the screen in Figure 1. Ultimately, I recovered no significant hits from this screen. While these data are not definitive it suggests that IFI6 may not utilize a specific host pathway to block viral replication.

I also attempted several Co-IP/MS experiments to determine if I could capture any protein interactions between IFI6 and other host proteins. I used two cell lines stably expressing IFI6 3xFLAG, and immunoprecipitated using FLAG beads, and then sent the eluted samples for analysis. I obtained several hits that were consistent between the two cell lines, but after validation with Co-IP, I was unable to confirm interaction between IFI6 and these hits. More recently, Wenchun Fan repeated these experiments and used tandem affinity purification to IP IFI6 and purify any contaminating proteins. One of the top hits in the mass spectrometry data was BiP, with several other interesting proteins in the list. Ultimately, Wenchun was unable to validate an interaction between IFI6 with these hits, with the

exception of BiP, which I have also shown interacts with IFI6. Despite several attempts at identifying protein interactions between IFI6 and the host, BiP was the only host factor identified. This suggests IFI6 may have limited interactions with other host proteins.

I also attempted to define a minimal set of flavivirus non-structural proteins required to generate replication complexes. I stably expressed a lentiviral construct expressing DENV NS2B-NS4B. I was primarily interested in the overexpression of NS4A and NS4B, but proper cleavage of these proteins requires both host and viral proteases (NS2B-NS3), so I included those proteins in this construct. I was unsuccessful in observing if these proteins generate replication complexes, making it difficult to further address how IFI6 blocks formation of the complexes.

While these data are inconclusive, they support a model where IFI6 can act independent of host pathways or other proteins in the cell. Additionally, IFI6 may not require an interaction with viral proteins to inhibit replication, suggesting the antiviral mechanism may rely on other properties of IFI6 that have not been characterized.

CHAPTER FIVE

Conclusions and Recommendations

Overview

Through the studies presented, I have demonstrated IFI6 is a potent antiviral ISG. The data presented in previous publications suggests IFI6 is antiviral to HCV and possesses anti-apoptotic properties, two observations I have difficulty reconciling based on the data shown. In addition to data presented above, I have summarized below several experiments from previously formed hypotheses. These include investigations into the role of IFI6 in apoptosis, mitochondrial metabolism, and lipid metabolism. While the mechanistic details are not clear, I propose that IFI6 is not actually interacting with viral or host proteins, but is sensing changes in curvature induced by these viral proteins. However, there are alternative possibilities that should be tested, such as IFI6 interfering with the dimerization of non-structural proteins. I also propose that in future experiments the lncRNA, lncRNA-IFI6, identified to be a negative regulator of IFI6 (Liu et al., 2018) should be confirmed for its regulatory activity, and that the antiviral paralog of the FAM14 family in mice should be identified. Future experiments characterizing the topology of IFI6 are already underway in the lab, with an intriguing model that supports the hypothesis that IFI6 blocks flavivirus replication by sensing perturbations to membrane architecture. Importantly, this mechanism may serve as a template for future antiviral therapies.

PREVIOUS HYPOTHESES

Apoptosis

Because previous literature reported IFI6 to be an antiapoptotic protein, (Cheriyath et al., 2007; Cheriyath et al., 2018; Cheriyath et al., 2012) (Tahara et al., 2005). I sought to confirm this phenotype. I spent a non-trivial amount of time trying to confirm this phenotype, and ultimately was unable to confirm this result. The major difficulty was that in many cells I tested it was difficult to induce apoptosis. I also tested a panel of non-small cell lung carcinoma cell lines to expand the cell types I had been using in lab. I tested a variety of apoptosis inducing drugs for their ability to induce cell death. This group of drugs included cyclohexamide, TNF- α , TRAIL ligand and actinomycin D. Consistently only TRAIL ligand could cause cell death. I did observe a correlation with IFI6 expression and TRAIL sensitivity in these cells, where cells that expressed higher basal levels of IFI6 were more resistant to TRAIL treatment. However, when IFI6 was knocked out of these cells with CRISPR technology the sensitivity of the cells to TRAIL treatment did not change. This suggests that in these particular cells IFI6 may not play a major role in the regulation of apoptosis.

Despite inconclusive evidence from these experiments, in light of the data presented in this thesis, I find it difficult to reconcile an antiviral phenotype with an antiapoptotic phenotype. This is especially difficult since many of the antiapoptotic phenotypes are linked to a mitochondrial localization of IFI6. The observed phenotypes from previously published studies suggest IFI6 plays a role in stabilizing mitochondrial membrane potential and reducing the production of mitochondria reactive oxygen species (mtROS) (Cheriyath et al.,

2007; Cheriya et al., 2018) Since I observed an ER localization for IFI6, one hypothesis that may link IFI6 to apoptosis is that IFI6 may play a role in ER homeostasis. Since IFI6 blocks the formation of viral replication complexes, IFI6 may serve as a regulator of ER homeostasis under other stressful conditions. This alternative function for IFI6 was previously speculated for ancestral IFI6 genes prior to the incorporation into the IFN system (Parker and Porter, 2004). The expression of IFI6 and other ISGs can be elevated in cancer cells (Cheon et al., 2014), so it may be possible for IFI6 to play a regulatory role during cell stress.

Metabolism and Lipidomics

Before I had strong evidence that IFI6 was localized to the ER, I performed a series of experiments under the assumption that IFI6 may be a mitochondrial protein, as claimed in the literature (Cheriya et al., 2007; Cheriya et al., 2018; Tahara et al., 2005). There are several important pathways that connect the ER to the mitochondria, such as production of metabolites and lipid metabolism and transport (Flis and Daum, 2013). It is possible that metabolic pathways in the mitochondria could affect flavivirus replication at the ER. I performed both a metabolomics screen as well as a lipidomics screen with the help of Ben Tu's lab and Jeff McDonald's lab respectively.

In the metabolomics screen I observed differences between control and IFI6 expressing cells with respect to metabolite concentrations. Interestingly, I saw changes in arginine and citrulline levels, as well as polyamine levels. Importantly, several ISGs such as NOS2 and SAT1 are enzymes involved in this metabolic pathway. I speculated IFI6 was

modifying these metabolic pathways because the enzymatic activity of these ISGs was important for the antiviral response. Ultimately, I found that the changes in arginine and citrulline abundance were artifacts linked to the lentiviral system used to express IFI6. When I changed lentiviral systems, I did not observe the changes in arginine and citrulline levels, suggesting these effects were not related to IFI6 antiviral activity. I also attempted to quantify the metabolic activity through experiments with a Seahorse analyzer. This analyzer can measure the oxygen consumption rate as well as the basal metabolic activity of live cells. Ultimately, I obtained similar results to the metabolomics data that appeared specific to the lentivirus system used.

I also performed a lipidomics screen to determine if IFI6 altered concentrations of lipids during viral infection. Cells expressing IFI6 or control were infected and analyzed by mass spectrometry. I observed changes in populations of lipid groups, such as ceramides and sphingolipids. Interestingly, ceramides are known to be important for curvature of membranes. I hypothesized that if membrane concentration of ceramides was important for membrane rearrangement during infection, addition of ceramides would overcome the inhibitory effect of IFI6 by making the membrane more flexible. I attempted to increase concentrations of lipids such as ceramides in cells by adding exogenous ceramide to cells during infection. However, I was unable to rescue infection in IFI6-expressing cells using this approach, suggesting the observed changes in lipid concentrations were not due to the antiviral activity of IFI6.

HCV Phenotype

Several previous publications report an antiviral phenotype against HCV (Fusco et al., 2013; Itsui et al., 2006; Liu et al., 2018; Metz et al., 2012; Meyer et al., 2015; Qi et al., 2017; Zhao et al., 2012) I have demonstrated that IFI6 is not significantly inhibitory to HCV. The major discrepancy is in the order of magnitude of the antiviral activity. Previously published reports observe a two-fold inhibition of HCV replication in the presence of IFI6. The inhibitory effects HCV I observe are smaller in magnitude (Figures 18a-18e). Additionally, the inhibitory effects against flaviviruses is a much stronger phenotype, suggesting that flavivirus replication is the true target of IFI6 (Figure 2, 3, 13). Some of the proposed mechanisms, such as interference of CD81 signaling and antagonism of the p7 protein do not fit with the roles I predict IFI6 has during inhibition of flavivirus replication (Meyer et al., 2015; Qi et al., 2017). Because I have shown IFI6 is ER-localized (Figure 10), it does not seem plausible for IFI6 to interfere with CD81 signaling which occurs on the cell surface, or to be localized to the cell surface (Meyer et al., 2015). Additionally, CD81 signaling occurs early in the viral life cycle, which does not correlate with an effect on viral replication.

The observation that IFI6 antagonizes HCV is linked to a mechanism similar to the apoptosis studies (Qi et al., 2017). The report suggests that IFI6 interacts with p7, but that these proteins have opposing effects on mitochondrial membrane potential. Since I was unable to confirm the antiapoptotic effect of IFI6, the observation that IFI6 affects HCV replication by blocking mitochondrial membrane potential does not seem plausible.

Additionally, there is no precedent for p7 activity in the mitochondria, since p7 is known to be an ion channel in ER membranes (Lin et al., 1994). While it is possible that p7 interacts with IFI6 since they are both ER-localized, I do not think this interaction would affect mitochondrial membrane potential directly. Additionally, the paper claims that there is a discrepancy between the inhibitory effect of IFI6 on HCV replicon systems and infectious clones. I did not observe a difference in the magnitude of inhibition for either the HCV replicon or infectious clone (Figure 18). Finally, several groups performed siRNA screens to identify ISGs important for the restriction of HCV infection (Fusco et al., 2013; Metz et al., 2012; Zhao et al., 2012). IFI6 was not identified in any of these screens as a significant hit.

ANTIVIRAL MECHANISM

The results presented in the previous chapters support a model where IFI6 specifically inhibits a single genus of virus, genus Flavivirus, and not other viruses that replicate on ER membranes. The distinguishing feature of flavivirus replication that makes it unique from the replication strategy of other viruses that replicate with ER-derived membranes lies in the architecture of the replication complex. Flaviviruses are the only known RNA virus in mammals to generate inward-budding spherule replication complexes at the ER, making them unique among mammalian RNA viruses (Paul and Bartenschlager, 2013). More broadly, I am not aware of other host processes that generate the same polarity of curvature (negative curvature) as these replication complexes, further emphasizing the uniqueness of flaviviruses in their site of replication and the structure of their complexes. Therefore, it may be possible IFI6 is not actually sensing a specific viral protein or the activity of a single viral

protein, but rather the perturbation of the membrane as it is rearranged during replication complex formation. Because details of how replication complexes are formed, let alone how this process is initiated are poorly defined, it is difficult to know how the membranes are altered during this step of the life cycle. Only the final product, the spherule morphology of the complexes, is known.

Because I did not observe an interaction with DENV NS1, NS4A or NS4B it is difficult to conclude if IFI6 interacts with any of these proteins or other viral proteins. The major obstacle to addressing these and other questions is that IFI6 blocks replication; therefore it is rare to observe good expression of IFI6 in the same cell as viral proteins. Structurally, the NS4A and NS4B proteins are very similar to the predicted topology of IFI6, since they are small hydrophobic proteins with several transmembrane domains. In data not shown, I very frequently observe a higher molecular weight of FLAG-tagged IFI6 that suggests IFI6 may form dimers, and possibly multimers or oligomers. Since NS4A and NS4B are known to form hetero-oligomers and homo-oligomers, it is possible that IFI6 is interfering with the ability of these proteins to oligomerize, which is presumably required for these proteins to cause membrane rearrangement. However, based on the results of the current experiments, I cannot conclude that IFI6 interacts with these proteins to block RC formation.

While "negative data" presented in the previous chapter are inconclusive, the results do fit with a model where IFI6 does not act through a host pathway to inhibit viral replication. Additionally, it is possible that other hits would have appeared in the IFN CRISPR screen if IFI6 required other host factors for its antiviral activity, since BiP was

identified through this screen. Together this data may support a model where IFI6 does not act through any pathways to block replication and therefore may be a direct effector.

Since flaviviruses are the only known viruses that create inward budding replication complexes on ER membranes, it is still possible IFI6 is not interacting with a particular protein but rather senses changes in membrane curvature. Because there are no other ways to perturb the ER in this manner it is difficult to demonstrate that IFI6 is sensing these changes in the ER membranes, and that other cellular processes that cause a similar type of membrane alteration would also be affected by IFI6 overexpression. While it may not be technically possible, other viruses are known to make spherule replication complexes in other organelles in the cell. Plant viruses such as flock house virus (FHV) and tomato bushy stunt virus (TBSV) both generate spherule replication complexes (Ertel et al., 2017; Nagy et al., 2016). FHV replicates on mitochondria in plants and yeast, while TBSV replicates on peroxisomes in plants and yeast. It is possible the mechanism of their RC formation is similar to that of flaviviruses. If it were possible to relocalize IFI6 to an organelle where other viruses replicate with the same RC architecture, even if the biological scenario is very artificial, it may be useful in determining how IFI6 senses membrane perturbations caused by viral proteins.

FUTURE EXPERIMENTS

Current efforts in the lab are focused on defining the topology of IFI6. IFI6 was previously predicted to have several transmembrane regions and a putative amphipathic alpha helix (Cheriyath et al., 2011). These helices do not span the membrane, but are parallel

to the membrane, typically with a hydrophobic surface buried in the membrane and a hydrophilic surface that faces the cytoplasm. Sequence analysis of the putative amphipathic helix in IFI6 indicates it shares properties with ALPS-like motifs - helices that sense membrane curvature and change conformation with membrane perturbations (Drin et al., 2007). Importantly, the conformational changes of these helices are distinct in that the change occurs because of physical bending of the membranes and not due to changes in charges of residues that contact the membrane. Thus, one explanation for the specific activity of IFI6 is that IFI6 is sensitive to changes in membrane curvature induced by viral proteins, but can stabilize the membrane once a conformational change occurs in the ALPS-like motif. There are a variety of ongoing experiments investigating this hypothesis, including generation of truncations, mutagenesis of the amphipathic helix, localization by microscopy and antiviral studies.

Since I identified a paralog in the murine FAM14 family that appears to be the only antiviral gene in the murine family, I propose future work characterizing this gene, IFI27L2B. Interestingly, this gene has two copies of the ISG12 motif. As I frequently observe higher order bands on my western blot experiments with IFI6, it is interesting to think of this gene as being an 'encoded dimer,' where there is no need for interaction with another protein. In addition to identifying the murine homolog, it may be possible to express human IFI6 in mice to establish more *in vivo* relevance.

While literature reporting IFI6 as antiviral towards HCV is hard to reconcile with my own data, I am intrigued by the identification of a lncRNA, lncRNA-IFI6 in the IFI6 gene. Since members of the FAM14 protein family existed before the IFN system developed in

higher eukaryotes, this may have served as an early way to regulate expression of IFI6-like genes. Additionally, I did not observe high levels of IFI6 basal expression in most cell lines, suggesting this regulatory mechanism could be constitutive. The recent study published where lncRNA-IFI6 was identified used CRISPR to target the lncRNA. I propose that validation of these observations would be a useful tool for determining the regulation of IFI6 expression. Additionally, it would be interesting to determine if IFI6 expression in the absence of the lncRNA would be sufficient for blocking viral replication.

BIBLIOGRAPHY

- Blight, K.J., McKeating, J.A., and Rice, C.M. (2002). Highly permissive cell lines for subgenomic and genomic hepatitis C virus RNA replication. *J Virol* *76*, 13001-13014.
- Chatel-Chaix, L., Cortese, M., Romero-Brey, I., Bender, S., Neufeldt, C.J., Fischl, W., Scaturro, P., Schieber, N., Schwab, Y., Fischer, B., *et al.* (2016). Dengue Virus Perturbs Mitochondrial Morphodynamics to Dampen Innate Immune Responses. *Cell Host Microbe* *20*, 342-356.
- Cheon, H., Borden, E.C., and Stark, G.R. (2014). Interferons and their stimulated genes in the tumor microenvironment. *Semin Oncol* *41*, 156-173.
- Cheriyath, V., Glaser, K.B., Waring, J.F., Baz, R., Hussein, M.A., and Borden, E.C. (2007). G1P3, an IFN-induced survival factor, antagonizes TRAIL-induced apoptosis in human myeloma cells. *J Clinical Invest* *117*, 3107-3117.
- Cheriyath, V., Kaur, J., Davenport, A., Khalel, A., Chowdhury, N., and Gaddipati, L. (2018). G1P3 (IFI6), a mitochondrial localised antiapoptotic protein, promotes metastatic potential of breast cancer cells through mtROS. *Br J Cancer* *119*, 52-64.
- Cheriyath, V., Kuhns, M.A., Jacobs, B.S., Evangelista, P., Elson, P., Downs-Kelly, E., Tubbs, R., and Borden, E.C. (2012). G1P3, an interferon- and estrogen-induced survival protein contributes to hyperplasia, tamoxifen resistance and poor outcomes in breast cancer. *Oncogene* *31*, 2222-2236.
- Cheriyath, V., Leaman, D.W., and Borden, E.C. (2011). Emerging roles of FAM14 family members (G1P3/ISG 6-16 and ISG12/IFI27) in innate immunity and cancer. *J Interferon Cytokine Res* *31*, 173-181.
- Cortese, M., Goellner, S., Acosta, E.G., Neufeldt, C.J., Oleksiuk, O., Lampe, M., Haselmann, U., Funaya, C., Schieber, N., Ronchi, P., *et al.* (2017). Ultrastructural Characterization of Zika Virus Replication Factories. *Cell Rep* *18*, 2113-2123.
- Doench, J.G., Fusi, N., Sullender, M., Hegde, M., Vaimberg, E.W., Donovan, K.F., Smith, I., Tothova, Z., Wilen, C., Orchard, R., *et al.* (2016). Optimized sgRNA design to maximize activity and minimize off-target effects of CRISPR-Cas9. *Nat Biotechnol* *34*, 184-191.
- Drin, G., Casella, J.F., Gautier, R., Boehmer, T., Schwartz, T.U., and Antony, B. (2007). A general amphipathic alpha-helical motif for sensing membrane curvature. *Nat Struct Mol Biol* *14*, 138-146.

- Egger, D., Wolk, B., Gosert, R., Bianchi, L., Blum, H.E., Moradpour, D., and Bienz, K. (2002). Expression of hepatitis C virus proteins induces distinct membrane alterations including a candidate viral replication complex. *J Virol* 76, 5974-5984.
- Emini, E.A., Hughes, J.V., Perlow, D.S., and Boger, J. (1985). Induction of hepatitis A virus-neutralizing antibody by a virus-specific synthetic peptide. *J Virol* 55, 836-839.
- Ertel, K.J., Benefield, D., Castano-Diez, D., Pennington, J.G., Horswill, M., den Boon, J.A., Otegui, M.S., and Ahlquist, P. (2017). Cryo-electron tomography reveals novel features of a viral RNA replication compartment. *Elife* 6.
- Esser-Nobis, K., Romero-Brey, I., Ganten, T.M., Gouttenoire, J., Harak, C., Klein, R., Schemmer, P., Binder, M., Schnitzler, P., Moradpour, D., *et al.* (2013). Analysis of hepatitis C virus resistance to silibinin in vitro and in vivo points to a novel mechanism involving nonstructural protein 4B. *Hepatology* 57, 953-963.
- Flis, V.V., and Daum, G. (2013). Lipid transport between the endoplasmic reticulum and mitochondria. *Cold Spring Harb Perspect Biol* 5.
- Friedman, R.L., Manly, S.P., McMahon, M., Kerr, I.M., and Stark, G.R. (1984). Transcriptional and posttranscriptional regulation of interferon-induced gene expression in human cells. *Cell* 38, 745-755.
- Fujiki, Y., Hubbard, A.L., Fowler, S., and Lazarow, P.B. (1982). Isolation of intracellular membranes by means of sodium carbonate treatment: application to endoplasmic reticulum. *J Cell Biol* 93, 97-102.
- Fusco, D.N., Brisac, C., John, S.P., Huang, Y.W., Chin, C.R., Xie, T., Zhao, H., Jilg, N., Zhang, L., Chevaliez, S., *et al.* (2013). A genetic screen identifies interferon-alpha effector genes required to suppress hepatitis C virus replication. *Gastroenterology* 144, 1438-1449, 1449 e1431-1439.
- Gaut, J.R., and Hendershot, L.M. (1993). Mutations within the nucleotide binding site of immunoglobulin-binding protein inhibit ATPase activity and interfere with release of immunoglobulin heavy chain. *J Biol Chem* 268, 7248-7255.
- Grant, A., Ponia, S.S., Tripathi, S., Balasubramaniam, V., Miorin, L., Sourisseau, M., Schwarz, M.C., Sanchez-Seco, M.P., Evans, M.J., Best, S.M., *et al.* (2016). Zika Virus Targets Human STAT2 to Inhibit Type I Interferon Signaling. *Cell Host Microbe* 19, 882-890.
- Grigorov, B., Rabilloud, J., Lawrence, P., and Gerlier, D. (2011). Rapid titration of measles and other viruses: optimization with determination of replication cycle length. *PLoS One* 6, e24135.

- Hadinegoro, S.R., Arredondo-Garcia, J.L., Capeding, M.R., Deseda, C., Chotpitayasunondh, T., Dietze, R., Muhammad Ismail, H.I., Reynales, H., Limkittikul, K., Rivera-Medina, D.M., *et al.* (2015). Efficacy and Long-Term Safety of a Dengue Vaccine in Regions of Endemic Disease. *N Engl J Med* 373, 1195-1206.
- Hanners, N.W., Eitson, J.L., Usui, N., Richardson, R.B., Wexler, E.M., Konopka, G., and Schoggins, J.W. (2016). Western Zika Virus in Human Fetal Neural Progenitors Persists Long Term with Partial Cytopathic and Limited Immunogenic Effects. *Cell Rep* 15, 2315-2322.
- Itsui, Y., Sakamoto, N., Kurosaki, M., Kanazawa, N., Tanabe, Y., Koyama, T., Takeda, Y., Nakagawa, M., Kakinuma, S., Sekine, Y., *et al.* (2006). Expressional screening of interferon-stimulated genes for antiviral activity against hepatitis C virus replication. *J Viral Hepat* 13, 690-700.
- Itzhaki, J.E., Barnett, M.A., MacCarthy, A.B., Buckle, V.J., Brown, W.R., and Porter, A.C. (1992). Targeted breakage of a human chromosome mediated by cloned human telomeric DNA. *Nat Genet* 2, 283-287.
- Jones, C.T., Patkar, C.G., and Kuhn, R.J. (2005). Construction and applications of yellow fever virus replicons. *Virology* 331, 247-259.
- Junjhon, J., Pennington, J.G., Edwards, T.J., Perera, R., Lanman, J., and Kuhn, R.J. (2014). Ultrastructural characterization and three-dimensional architecture of replication sites in dengue virus-infected mosquito cells. *J Virol* 88, 4687-4697.
- Kelly, J.M., Porter, A.C., Chernajovsky, Y., Gilbert, C.S., Stark, G.R., and Kerr, I.M. (1986). Characterization of a human gene inducible by alpha- and beta-interferons and its expression in mouse cells. *EMBO* 5, 1601-1606.
- Lazear, H.M., Pinto, A.K., Vogt, M.R., Gale, M., Jr., and Diamond, M.S. (2011). Beta interferon controls West Nile virus infection and pathogenesis in mice. *J Virol* 85, 7186-7194.
- Li, J., Ding, S.C., Cho, H., Chung, B.C., Gale, M., Jr., Chanda, S.K., and Diamond, M.S. (2013). A short hairpin RNA screen of interferon-stimulated genes identifies a novel negative regulator of the cellular antiviral response. *MBio* 4, e00385-00313.
- Li, W., Xu, H., Xiao, T., Cong, L., Love, M.I., Zhang, F., Irizarry, R.A., Liu, J.S., Brown, M., and Liu, X.S. (2014). MAGeCK enables robust identification of essential genes from genome-scale CRISPR/Cas9 knockout screens. *Genome Biol* 15, 554.
- Lin, C., Lindenbach, B.D., Pragai, B.M., McCourt, D.W., and Rice, C.M. (1994). Processing in the hepatitis C virus E2-NS2 region: identification of p7 and two distinct E2-specific products with different C termini. *J Virol* 68, 5063-5073.

- Liu, X., Duan, X., Holmes, J.A., Li, W., Lee, S.H., Tu, Z., Zhu, C., Salloum, S., Lidofsky, A., Schaefer, E.A., *et al.* (2018). A novel lncRNA regulates HCV infection through IFI6. *Hepatology*.
- Lucas, T.M., Richner, J.M., and Diamond, M.S. (2015). The Interferon-Stimulated Gene Ifi2712a Restricts West Nile Virus Infection and Pathogenesis in a Cell-Type- and Region-Specific Manner. *J Virol* *90*, 2600-2615.
- Manns, M.P., Buti, M., Gane, E., Pawlotsky, J.M., Razavi, H., Terrault, N., and Younossi, Z. (2017). Hepatitis C virus infection. *Nat Rev Dis Primers* *3*, 17006.
- Manns, M.P., and Rambusch, E.G. (1999). Autoimmunity and extrahepatic manifestations in hepatitis C virus infection. *J Hepatol* *31 Suppl 1*, 39-42.
- Marceau, C.D., Puschnik, A.S., Majzoub, K., Ooi, Y.S., Brewer, S.M., Fuchs, G., Swaminathan, K., Mata, M.A., Elias, J.E., Sarnow, P., *et al.* (2016). Genetic dissection of Flaviviridae host factors through genome-scale CRISPR screens. *Nature* *535*, 159-163.
- Martensen, P.M., and Justesen, J. (2004). Small ISGs coming forward. *J Interferon Cytokine Res* *24*, 1-19.
- Marukian, S., Jones, C.T., Andrus, L., Evans, M.J., Ritola, K.D., Charles, E.D., Rice, C.M., and Dustin, L.B. (2008). Cell culture-produced hepatitis C virus does not infect peripheral blood mononuclear cells. *Hepatology* *48*, 1843-1850.
- Metz, P., Dazert, E., Ruggieri, A., Mazur, J., Kaderali, L., Kaul, A., Zeuge, U., Windisch, M.P., Trippler, M., Lohmann, V., *et al.* (2012). Identification of type I and type II interferon-induced effectors controlling hepatitis C virus replication. *Hepatology* *56*, 2082-2093.
- Meyer, K., Kwon, Y.C., Liu, S., Hagedorn, C.H., Ray, R.B., and Ray, R. (2015). Interferon-alpha inducible protein 6 impairs EGFR activation by CD81 and inhibits hepatitis C virus infection. *Sci Rep* *5*, 9012.
- Miller, S., Kastner, S., Krijnse-Locker, J., Buhler, S., and Bartenschlager, R. (2007). The non-structural protein 4A of dengue virus is an integral membrane protein inducing membrane alterations in a 2K-regulated manner. *J Biol Chem* *282*, 8873-8882.
- Miller, S., Sparacio, S., and Bartenschlager, R. (2006). Subcellular localization and membrane topology of the Dengue virus type 2 Non-structural protein 4B. *J Biol Chem* *281*, 8854-8863.
- Munro, S., and Pelham, H.R. (1986). An Hsp70-like protein in the ER: identity with the 78 kd glucose-regulated protein and immunoglobulin heavy chain binding protein. *Cell* *46*, 291-300.

- Nagy, P.D., Pogany, J., and Xu, K. (2016). Cell-Free and Cell-Based Approaches to Explore the Roles of Host Membranes and Lipids in the Formation of Viral Replication Compartment Induced by Tombusviruses. *Viruses* 8, 68.
- Neufeldt, C.J., Cortese, M., Acosta, E.G., and Bartenschlager, R. (2018). Rewiring cellular networks by members of the Flaviviridae family. *Nat Rev Microbiol* 16, 125-142.
- Parker, N., and Porter, A.C. (2004). Identification of a novel gene family that includes the interferon-inducible human genes 6-16 and ISG12. *BMC Genomics* 5, 8.
- Paul, D., and Bartenschlager, R. (2013). Architecture and biogenesis of plus-strand RNA virus replication factories. *World J Virol* 2, 32-48.
- Paul, D., and Bartenschlager, R. (2015). Flaviviridae Replication Organelles: Oh, What a Tangled Web We Weave. *Annu Rev Virol* 2, 289-310.
- Perelman, S.S., Abrams, M.E., Eitson, J.L., Chen, D., Jimenez, A., Mettlen, M., Schoggins, J.W., and Alto, N.M. (2016). Cell-Based Screen Identifies Human Interferon-Stimulated Regulators of *Listeria monocytogenes* Infection. *PLoS Pathog* 12, e1006102.
- Porter, A.C., Chernajovsky, Y., Dale, T.C., Gilbert, C.S., Stark, G.R., and Kerr, I.M. (1988). Interferon response element of the human gene 6-16. *EMBO* 7, 85-92.
- Qi, H., Chu, V., Wu, N.C., Chen, Z., Truong, S., Brar, G., Su, S.Y., Du, Y., Arumugaswami, V., Olson, C.A., *et al.* (2017). Systematic identification of anti-interferon function on hepatitis C virus genome reveals p7 as an immune evasion protein. *Proc Natl Acad Sci U S A* 114, 2018-2023.
- Romero-Brey, I., Merz, A., Chiramel, A., Lee, J.Y., Chlanda, P., Haselman, U., Santarella-Mellwig, R., Habermann, A., Hoppe, S., Kallis, S., *et al.* (2012). Three-dimensional architecture and biogenesis of membrane structures associated with hepatitis C virus replication. *PLoS Pathog* 8, e1003056.
- Sack, L.M., Davoli, T., Xu, Q., Li, M.Z., and Elledge, S.J. (2016). Sources of Error in Mammalian Genetic Screens. *G3 (Bethesda)* 6, 2781-2790.
- Samuel, M.A., and Diamond, M.S. (2005). Alpha/beta interferon protects against lethal West Nile virus infection by restricting cellular tropism and enhancing neuronal survival. *J Virol* 79, 13350-13361.
- Sanjana, N.E., Shalem, O., and Zhang, F. (2014). Improved vectors and genome-wide libraries for CRISPR screening. *Nat Methods* 11, 783-784.

- Scaturro, P., Cortese, M., Chatel-Chaix, L., Fischl, W., and Bartenschlager, R. (2015). Dengue Virus Non-structural Protein 1 Modulates Infectious Particle Production via Interaction with the Structural Proteins. *PLoS Pathog* *11*, e1005277.
- Schoggins, J.W., Dorner, M., Feulner, M., Imanaka, N., Murphy, M.Y., Ploss, A., and Rice, C.M. (2012). Dengue reporter viruses reveal viral dynamics in interferon receptor-deficient mice and sensitivity to interferon effectors in vitro. *Proc Natl Acad Sci U S A* *109*, 14610-14615.
- Schoggins, J.W., MacDuff, D.A., Imanaka, N., Gainey, M.D., Shrestha, B., Eitson, J.L., Mar, K.B., Richardson, R.B., Ratushny, A.V., Litvak, V., *et al.* (2014). Pan-viral specificity of IFN-induced genes reveals new roles for cGAS in innate immunity. *Nature* *505*, 691-695.
- Schoggins, J.W., Wilson, S.J., Panis, M., Murphy, M.Y., Jones, C.T., Bieniasz, P., and Rice, C.M. (2011). A diverse range of gene products are effectors of the type I interferon antiviral response. *Nature* *472*, 481-485.
- Schwarz, M.C., Sourisseau, M., Espino, M.M., Gray, E.S., Chambers, M.T., Tortorella, D., and Evans, M.J. (2016). Rescue of the 1947 Zika Virus Prototype Strain with a Cytomegalovirus Promoter-Driven cDNA Clone. *mSphere* *1*.
- Shalem, O., Sanjana, N.E., Hartenian, E., Shi, X., Scott, D.A., Mikkelsen, T., Heckl, D., Ebert, B.L., Root, D.E., Doench, J.G., *et al.* (2014). Genome-scale CRISPR-Cas9 knockout screening in human cells. *Science* *343*, 84-87.
- Stanaway, J.D., Shepard, D.S., Undurraga, E.A., Halasa, Y.A., Coffeng, L.E., Brady, O.J., Hay, S.I., Bedi, N., Bensenor, I.M., Castaneda-Orjuela, C.A., *et al.* (2016). The global burden of dengue: an analysis from the Global Burden of Disease Study 2013. *Lancet Infect Dis* *16*, 712-723.
- Szretter, K.J., Brien, J.D., Thackray, L.B., Virgin, H.W., Cresswell, P., and Diamond, M.S. (2011). The interferon-inducible gene viperin restricts West Nile virus pathogenesis. *J Virol* *85*, 11557-11566.
- Tabata, K., Arimoto, M., Arakawa, M., Nara, A., Saito, K., Omori, H., Arai, A., Ishikawa, T., Konishi, E., Suzuki, R., *et al.* (2016). Unique Requirement for ESCRT Factors in Flavivirus Particle Formation on the Endoplasmic Reticulum. *Cell Rep* *16*, 2339-2347.
- Tahara, E., Jr., Tahara, H., Kanno, M., Naka, K., Takeda, Y., Matsuzaki, T., Yamazaki, R., Ishihara, H., Yasui, W., Barrett, J.C., *et al.* (2005). G1P3, an interferon inducible gene 6-16, is expressed in gastric cancers and inhibits mitochondrial-mediated apoptosis in gastric cancer cell line TMK-1 cell. *Cancer Immunol Immunother* *54*, 729-740.

Turri, M.G., Cuin, K.A., and Porter, A.C. (1995). Characterisation of a novel minisatellite that provides multiple splice donor sites in an interferon-induced transcript. *Nucleic Acids Res* 23, 1854-1861.

Vogt, D.A., and Ott, M. (2015). Membrane Flotation Assay. *Bio Protoc* 5.

Wang, J., Lee, J., Liem, D., and Ping, P. (2017). HSPA5 Gene encoding Hsp70 chaperone BiP in the endoplasmic reticulum. *Gene* 618, 14-23.

Welsch, S., Miller, S., Romero-Brey, I., Merz, A., Bleck, C.K., Walther, P., Fuller, S.D., Antony, C., Krijnse-Locker, J., and Bartenschlager, R. (2009). Composition and three-dimensional architecture of the dengue virus replication and assembly sites. *Cell Host Microbe* 5, 365-375.

Wikan, N., and Smith, D.R. (2016). Zika virus: history of a newly emerging arbovirus. *Lancet Infect Dis* 16, e119-e126.

Yanez, R.J., and Porter, A.C. (2002). A chromosomal position effect on gene targeting in human cells. *Nucleic Acids Res* 30, 4892-4901.

Zhang, R., Miner, J.J., Gorman, M.J., Rausch, K., Ramage, H., White, J.P., Zuiani, A., Zhang, P., Fernandez, E., Zhang, Q., *et al.* (2016). A CRISPR screen defines a signal peptide processing pathway required by flaviviruses. *Nature* 535, 164-168.

Zhao, H., Lin, W., Kumthip, K., Cheng, D., Fusco, D.N., Hofmann, O., Jilg, N., Tai, A.W., Goto, K., Zhang, L., *et al.* (2012). A functional genomic screen reveals novel host genes that mediate interferon-alpha's effects against hepatitis C virus. *J Hepatol* 56, 326-333.

Zou, J., Xie, X., Lee le, T., Chandrasekaran, R., Reynaud, A., Yap, L., Wang, Q.Y., Dong, H., Kang, C., Yuan, Z., *et al.* (2014). Dimerization of flavivirus NS4B protein. *J Virol* 88, 3379-3391.

